RECOVERY OF BUTANOL FROM SYNTHETIC FERMENTATION BROTH BY SURFACTANT-AIDED PERSTRACTION USING POLY(ETHER BLOCK AMIDE) MEMBRANE

MR. PHEERAPONG CHANACHOD

A THESIS SUBMITTED IN PARTIAL FULFILLMENT
OF THE REQUIREMENTS FOR
THE DEGREE OF MASTER OF ENGINEERING (CHEMICAL ENGINEERING)
FACULTY OF ENGINEERING
KING MONGKUT'S UNIVERSITY OF TECHNOLOGY THONBURI
2014

Recovery of Butanol from Synthetic Fermentation Broth by Surfactant-aided Perstraction Using Poly(ether block amide) Membrane

Mr. Pheerapong Chanachod B.Sc. (Biotechnology)

A Thesis Submitted in Partial Fulfillment of the Requirements for
the Degree of Master of Engineering (Chemical Engineering)
Faculty of Engineering
King Mongkut's University of Technology Thonburi
2014

Thesis Committee

…… Chairman of Thesis Committee

(Asst. Prof. Chaiwat Prapainainar, Ph.D.)

…… Member and Thesis Adviser

(Assoc. Prof. Anawat Sungpet, Ph.D.)

…… Member

(Prof. Ratana Jiraratananon, Ph.D.)

…… Member

(Assoc. Prof. Somnuk Jarudilokkul, Ph.D.)

…… Member

(Paritta Prayoonyong, Ph.D.)

Thesis Title	Recovery of Butanol from Synthetic Fermentation Broth by Surfactant-aided Perstraction Using Poly(ether block amide) Membrane
Thesis Credits	12
Candidate	Mr. Pheerapong Chanochod
Thesis Advisor	Assoc. Prof. Dr. Anawat Sungpet
Program	Master of Engineering
Field of Study	Chemical Engineering
Department	Chemical Engineering
Faculty	Engineering
Academic Year	2014

Abstract

Poly(ether block amide) or PEBA was used to prepare asymmetric membrane by reverse-phase inversion. Butanol and methanol were used as a solvent and a non-solvent, respectively. PEBA concentrations ranged from 7 to 11 wt. %. A thin dense layer was observed in the film formed by using 7 wt. % PEBA. However, the membrane surface was not defect-free. Therefore, dense PEBA membranes were used in perstraction to recover butanol from synthetic fermentation broth. The membranes were 16.5±1.3 μm thick with an effective area of 5.72 cm^2. The synthetic fermentation broth contained acetone, butanol, and ethanol at the concentrations of 1.0, 19.2, and 1.7 g/L, respectively. Experiments were carried out in a batch mode. Temperatures of the feed and receiving solutions were approximately 37 ^oC, which was above the cloud point of Triton X-114. Butanol fluxes obtained from the experiments using water, 0.7, 0.8, 0.9, 3.5, 7.0 and 10.5 wt. % Triton X-114 as receiving solutions were 273.9, 297.4, 388.6, 352.5, 274.3, 275.1, and 261.2 g/(m^2.h), respectively. After a period of 5 h perstraction, the butanol concentration in the broth was reduced from 19.2 to 16.6 g/L. At the end of perstraction, it was found that butanol was more distributed in the surfactant-rich phase. The mass of butanol in the surfactant-rich phase was between 0.16 and 0.45 g, while the mass in the surfactant-lean phase was between 0.69 and 0.21 g for the receiving phases containing 0.7 to 10.5 wt. % Triton X-114. As the temperature of the receiving solution was reduced to 6 ^oC, which was below the cloud point of Triton X-114, enhancement of butanol flux was observed. The use of 3.5 wt. % Triton X-114 instead of water as the receiving solution resulted in an increase of butanol flux from 11.9 to 95.3 g/(m^2.h). The increase of butanol concentration in the initial receiving solution from 0 to 12 g/L decreased butanol flux from 273.9 to 70.8 g/(m^2.h). The organic fluxes obtained from the perstraction using 0.8 wt. % Triton X-114 were higher than those from pervaporation.

Keywords: Butanol / Perstraction / Poly(ether block amide) Membrane / Triton X-114

หัวข้อวิทยานิพนธ์	การแยกบิวทานอลจากน้ำหมักสังเคราะห์ด้วยสารลดแรงตึงผิวช่วยเพอสแทรกชันที่ใช้พอลิอีเทอร์บล็อกเอไมด์เมมเบรน
หน่วยกิต	12
ผู้เขียน	นายพีระพงศ์ ชนะโชติ
อาจารย์ที่ปรึกษา	รศ. ดร.อนวัช สังข์เพ็ชร
หลักสูตร	วิศวกรรมศาสตรมหาบัณฑิต
สาขาวิชา	วิศวกรรมเคมี
ภาควิชา	วิศวกรรมเคมี
คณะ	วิศวกรรมศาสตร์
ปีการศึกษา	2557

บทคัดย่อ

การเตรียมพอลิอีเทอร์บล็อกเอไมด์เมมเบรนแบบไม่สมมาตร (asymmetric membrane) ใช้วิธีการเปลี่ยนวัฏภาคแบบผันกลับ (reverse-phase inversion) โดยมีบิวทานอลเป็นตัวทำละลายและเมทานอลเป็นตัวไม่ละลาย ความเข้มข้นของสารละลายพอลิอีเทอร์บล็อกเอไมด์ที่ใช้อยู่ในช่วง 7 ถึง 11 เปอร์เซ็นต์โดยน้ำหนัก เมมเบรนที่มีชั้นแน่นบางได้จากการเตรียมโดยใช้สารละลายพอลิอีเทอร์บล็อกเอไมด์ที่มีความเข้มข้น 7 เปอร์เซ็นต์โดยน้ำหนัก แต่ทว่าฟิล์มที่ได้นี้ยังมีรูพรุนอยู่เล็กน้อยบริเวณผิวหน้า ดังนั้น งานวิจัยนี้จึงใช้เมมเบรนแบบแน่นในการทดลองแยกบิวทานอลจากน้ำหมักสังเคราะห์ด้วยเพอสแทรกชัน ความหนาของเมมเบรนที่ใช้คือ 16.5 ± 1.3 ไมโครเมตร และมีพื้นที่หน้าตัดเท่ากับ 5.72 ตารางเซนติเมตร ความเข้มข้นของอะซิโตน, บิวทานอลและเอทานอล ในน้ำหมักสังเคราะห์คือ 1.0, 19.2 และ 1.7 กรัมต่อลิตร ตามลำดับ การทดลองทำในระบบแบบกะ อุณหภูมิของน้ำหมักสังเคราะห์ในด้านป้อนคือ 37 องศาเซลเซียส ซึ่งสูงกว่าอุณหภูมิขุ่นตัวของสารลดแรงตึงผิว Triton X-114 ที่ใช้ในงานวิจัย ค่าฟลักซ์ของบิวทานอลที่ได้จากเพอสแทรกชันที่ใช้น้ำ, 0.7, 0.8, 0.9, 3.5, 7.0 และ 10.5 เปอร์เซ็นต์โดยน้ำหนักของสารลดแรงตึงผิว มีค่าเท่ากับ 273.9, 297.4, 388.6, 352.5, 274.3, 275.1 และ 261.2 กรัมต่อตารางเมตร-ชั่วโมง ตามลำดับ หลังจากเพอสแทรกชันเป็นเวลา 5 ชั่วโมง พบว่าบิวทานอลในด้านป้อนลดลงจาก 19.2 เป็น 16.6 กรัมต่อลิตร และยังพบว่าบิวทานอลกระจายตัวอยู่ในวัฏภาคที่มีความเข้มข้นสารลดแรงตึงผิวสูงมากกว่า ส่วนมวลของบิวทานอลในวัฏภาคที่มีความเข้มข้นสารลดแรงตึงผิวสูงมีค่าอยู่ระหว่าง 0.16 และ 0.45 กรัม ในขณะที่มวลในวัฏภาคที่มีความ

เข้มข้นสารลดแรงตึงผิวต่ำมีค่าอยู่ระหว่าง 0.69 และ 0.21 กรัม สำหรับด้านรับที่มี Triton X-114 อยู่ 0.7 ถึง 10.5 เปอร์เซ็นต์โดยน้ำหนัก เมื่อลดอุณหภูมิด้านรับลงเป็น 6 องศาเซลเซียส ซึ่งต่ำกว่าอุณหภูมิขุ่นตัวของ Triton X-114 ทำให้ฟลักซ์ของบิวทานอลสูงขึ้น การใช้ Triton X-114 ที่ความเข้มข้น 3.5 เปอร์เซ็นต์โดยน้ำหนักแทนน้ำในด้านรับทำให้ฟลักซ์ของบิวทานอลเพิ่มขึ้นจาก 11.9 เป็น 95.3 กรัมต่อตารางเมตร-ชั่วโมง การเพิ่มความเข้มข้นของบิวทานอลในด้านรับจาก 0 เป็น 12 กรัมต่อลิตร ทำให้ฟลักซ์ของบิวทานอลลดลงจาก 273.9 เป็น 70.8 กรัมต่อตารางเมตร-ชั่วโมง ค่าฟลักซ์ของสารอินทรีย์ที่ได้จากเพอสแทรกชันที่ใช้ Triton X-114 ความเข้มข้น 0.8 เปอร์เซ็นต์โดยน้ำหนัก สูงกว่าค่าที่ได้จากเพอแวปพอเรชัน

คำสำคัญ: บิวทานอล / เพอสแทรกชัน / พอลิอีเทอร์บล็อกเอไมด์เมมเบรน / Triton X-114

ACKNOWLEDGMENTS

This research is completed with the help from many people. First of all, I am grateful to Assoc. Prof. Dr. Anawat Sungpet, my advisor, who gave valuable advice, suggestion, encouragement, a great support and his effort in correcting my English writing and proof reading my thesis report throughout the period of this research. Second, I am grateful to Prof. Dr. Ratana Jiraratananon, who supports apparatus and equipment and provides useful advice and recommendations during presentations. I would like to offer my special thanks to Assoc. Prof. Dr. Somnuk Jarudilokkul, Dr. Paritta Prayoonyong, and Asst. Prof. Chaiwat Prapainainar, my committee members, who provide useful advice and recommendations and give their suggestions to fulfill my thesis until it finished. Moreover, I gratefully acknowledge financial support from THE ASAHI GLASS FOUNDATION.

In addition, I would like to thank Mr. Ounsa Nonthphala, Mr. Viwat Simpradit and other scientists at Chemical Engineering department of KMUTT, who taught me how to use equipment and give me many good suggestions. Furthermore, I would like to thank the Department of Chemical Engineer, KMUTT for the best knowledge and many items of essential equipment and convenience. Unforgettably, I would like to thank my sisters, and friends for their morale and many helps. Finally, I am most grateful acknowledge my mother for her morale, suggestion, and a great chance to study for being a chemical engineer.

CONTENTS

PAGE

LIST OF TABLES

TABLE **PAGE**

TABLE **PAGE**

LIST OF FIGURES

FIGURE **PAGE**

FIGURE **PAGE**

FIGURE **PAGE**

LIST OF SYMBOLS

A	= Area, (m^2)
ABE	= Acetone, Butanol and Ethanol
C_i	= Concentration of i species, (g/L)
$C_{i,LP}$	= Concentration of i species in the surfactant-lean phase, (g/L)
$C_{i,RP}$	= Concentration of i species in the surfactant-rich phase, (g/L)
CMC	= Critical micelle concentration
c	= Coagulant
HLB	= Hydrophilic-lipophilic balance
J_i	= Flux of i species, ($g/(m^2.h)$)
M_i	= Mass of i species in a permeate, (g)
$m_{i,RP}$	= Mass of i species in the surfactant-rich phase, (g)
$m_{Triton\ X\text{-}114}$	= Mass of Triton X-114 in the solution, (g)
s	= Solvent
T	= Membrane thickness, (μm)
t	= Time, (h)
x_i	= Mass fraction of i species in a feed
x_j	= Mass fraction of j species in a feed
y_i	= Mass fraction of i species in a permeate
y_j	= Mass fraction of j species in a permeate
α_i	= Separation factor of i species relative to j species
δ_d	= The dispersion solubility parameter
δ_h	= The hydrogen bonding solubility parameter
δ_p	= The polar solubility parameter
δ_i	= Hansen solubility parameter of i species

CHAPTER 1 INTRODUCTION

1.1 Background

Fossil fuel reserves such as those of petroleum crude oil and natural gas are finite and steadily decreasing. The consumption of fossil fuels causes serious environmental issues, particularly global warming, and climate change. Renewable energy is an energy that can be replenished, for example, energy produced from biomass, solar, and wind. Development of renewable energy sources for our society is inevitable. Furthermore, an increase in the world population necessitates a marked shift of the world energy sources to sustainable alternatives, i.e. the energy sources that do not have a negative impact on the global food production. Biofuels are expected to grow rapidly in the next decade, especially in the automotive fuel market because of its environmental merits [1]. Furthermore, biofuels provide energy security and socioeconomic development.

Bio-butanol is a renewable and sustainable fuel. It can be produced by using strains that can utilize lignocellulosic hydrolysate sugars such as pentose and hexose sugars without organism modification [2]. The use of these economic carbohydrates adds an advantage to butanol and increases the chance of butanol to be produced cost-competitively. Butanol can be blended in large quantities with conventional diesel fuel [3]. It can also be blended with gasoline and utilized in existing gasoline engines because the air/fuel ratio of butanol is comparable to that of gasoline. Compared with ethanol, butanol has the higher net heat of combustion, less readily contaminated with water, and less corrosive [4].

Although butanol possesses many advantages, there are several issues that prevent bio-butanol from being industrially produced. The toxicity of butanol to the culture is the root of the problems. A high butanol concentration in fermentation broth cause damages to the cell membrane, leading to the permeability of ADP (adenosine diphosphate) and some ions. The leakage consequentially leads to cell lysis. The low productivity, ranging from 0.1 to 0.6 g/(L.h), and the consequential dilute product concentration of less than 2 wt. % in fermentation broth give rise to energy-intensive product recovery. This has been a long-standing problem that the production of bio-butanol has encountered for years. The reduction in the separation energy and cost can make it possible for butanol to compete with fossil fuels, and, therefore, a breakthrough in the butanol separation is essential. A recovery technology that requires less than 4 MJ per kilogram of butanol, approximately 10 % of the internal combustion energy of butanol (36.2 MJ/kg), for butanol recovery can be considered as an energy efficient process [5].

Besides the genetic improvement of butanol-producing strains, considerable research effort has been put into the recovery of butanol from fermentation broth while it is being produced. The integration of fermentation and continuous recovery offers several advantages over traditional batch culture, for example, reduction in process volume and time, increases in reactor productivity, substrate utilization, and product concentration [6].

There are various promising techniques such as adsorption, gas stripping, liquid-liquid extraction, and membrane based-separations that can reduce the limitations imposed by butanol toxicities. Among these techniques, pervaporation and perstraction are very promising by virtue of their energy utilization efficiency [4].

Perstraction is the transport of different liquid species through a dense membrane from a feed side to a receiving side containing an extracting liquid. Due to a very low butanol concentration in the fermentation broth and a consequential small concentration gradient in the membrane, a thin membrane with high affinity to butanol is a necessity. The membranes in this work were prepared from a thermoplastic elastomer, poly (ether block amide).

The thermoplastic elastomer contains polyamide blocks interconnected to polyether blocks by ester linkages. The two blocks are separated into two microphase-domains because of their thermodynamic incompatibility. The polyamide crystalline domains provide mechanical strength, while the polyether amorphous domains offer dynamic properties because of the high chain mobility of the ether linkage. In this work, commercially available poly(ether block amide), PEBAX® 2533, is chosen as the membrane material because it has a considerably high affinity to butanol [7]. Oleyl alcohols are commonly used as extractants in the receiving phase [8]. They are however difficult to be separated from the products. A large amount of solvent is needed in the product recovery [9]. An extractant that can efficiently remove butanol from the fermentation broth can reduce the energy requirement for the product recovery. Triton X-114, a surfactant, possessed many properties as an excellent medium for butanol extraction. It exhibited the highest butanol capturing capacity among the surfactants used in [10]. Its cloud point temperature of 25 ^{o}C was also low. Therefore, the surfactant-rich phase containing butanol could be formed by slightly heating the aqueous solution. Given that boiling point of butanol, 117.7 ^{o}C, was significantly lower than that of Triton X-114, 177 ^{o}C, separation of butanol from the surfactant-rich phase can easily be done. Nevertheless, Triton X-114 was not biocompatible with the butanol producing strain. By using an aqueous solution of Triton X-114 in a receiving side of perstraction, the surfactant is separated from the culture by a membrane. It can no longer do any harm to the butanol-producing strain. As a result, its suitability as a butanol extractant can be effectively utilized. The aim of this work is to evaluate the potential of Triton X-114 as an extractant for butanol recovery by perstraction.

1.2 Objective

To develop a perstraction membrane process that can efficiently remove butanol from acetone-butanol-ethanol (ABE) aqueous solution facilitated by surfactant, Triton X-114

1.3 Scope of Work

1. Integrally skinned asymmetric poly(ether block amide) or PEBA membranes were prepared by phase inversion. Commercially available PEBA, PEBAX® 2533, kindly supplied by ArkemaPte Ltd, Singapore, was used. The membranes were characterized by SEM.
2. Perstraction of acetone, butanol, and ethanol and the mixture (1:19.2:1.7 (g/L) ABE) of these compounds was studied.
3. The aqueous solution of Triton X-114 was used as the receiving phase.
   The effect of Triton X-114 concentrations in the receiving side was investigated.

1.4 Expected Benefits

The development of integrally-skinned PEBA membrane can enhance the organic fluxes in the separation process because the membrane has a low resistance. The use of Triton X-114 in the receiving solution enhances the butanol flux because of the increase of solubility in the receiving phase. Triton X-114 and entrapped butanol can be easily separated from the receiving solution because Triton X-114 has a low could point temperature. In addition, butanol and Triton X-114 do not form azeotropic mixture. Therefore, butanol can be further purified by conventional distillation.

CHAPTER 2 THEORY AND LITERATURE REVIEW

Theories of chemical structure, poly(ether block amide) membranes, membranes process and perstraction process are presented in this chapter providing the necessary understanding. In addition, research work related to membrane synthesis and permeation through inorganic membrane as poly(ether block amide) membranes are reviewed.

2.1 Poly(ether block amide) Membrane

The linear chains of rigid polyamide segments are alternately linked to flexible polyether (PE) (i.e., polytetramethylene oxide) segments through ester groups, as shown in Figure 2.1 [11]. It has a micro-phase separated morphology [12]. PEBA has an oranophilic property, and therefore has attracted much attention as a good membrane material for butanol separation. According to Boddeker et al. [13], they studied effect of butanol though a PEBA compared PDMS and polyether-based polyurethane membrane in pervaporation unit. The permeation flux of PEBA membrane was higher than those of the other membranes.

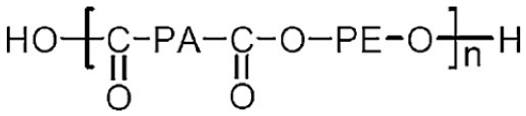

Figure 2.1 Structure of poly(ether-block-amide). PA and PE represent hard polyamide (i.e. Nylon 12) segments and soft polyether (i.e., polytetramethylene oxide) segment [11]

2.2 Wet Phase Inversion [14]

Phase inversion is a common preparation method for integrally-skinned asymmetric membrane. First, the polymer solution is cast on the glass plate to form a thin film. An evaporation of solvent is introduced before the film is immersed into a coagulation bath, where solvent is replaced by non solvent, and the precipitation of polymer then occurs.

The precipitation step is important in determining the membrane structure [15]. In Figure 2.2, the flux of solvent flowing out of casting solution is represented by J_2. The flux of non-solvent inflow is represented by J_1. For the composition path in a ternary phase diagram shown in Figure 2.3, when the ratio of solvent flux to non-solvent flux is large, the change in the composition of casting solution reaches the one-phase gel region and a dense structure is formed. When the ratio is small, the composition enters the two-phase region and a porous structure is formed.

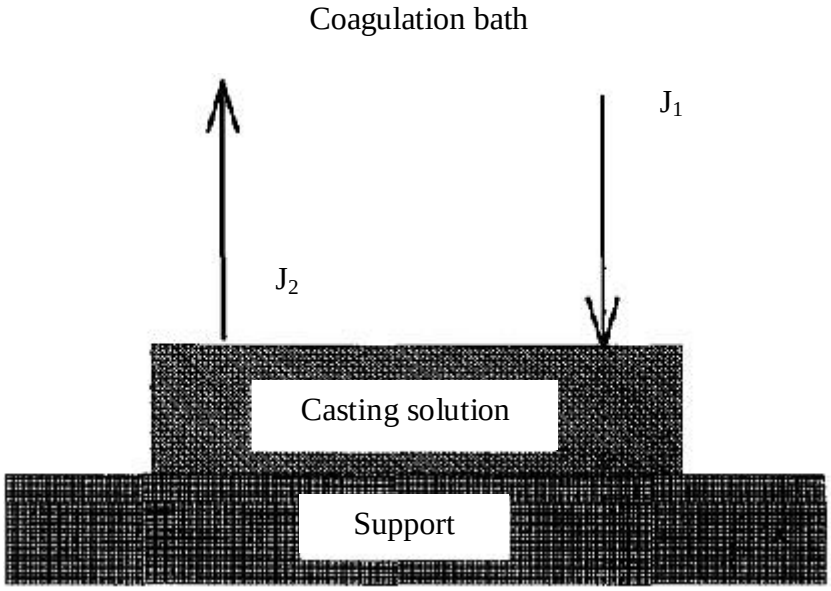

Figure 2.2 Fluxes of non-solvent (J_1) and solvent (J_2) at the interface between casting solution and the coagulation bath (non-solvent) [15]

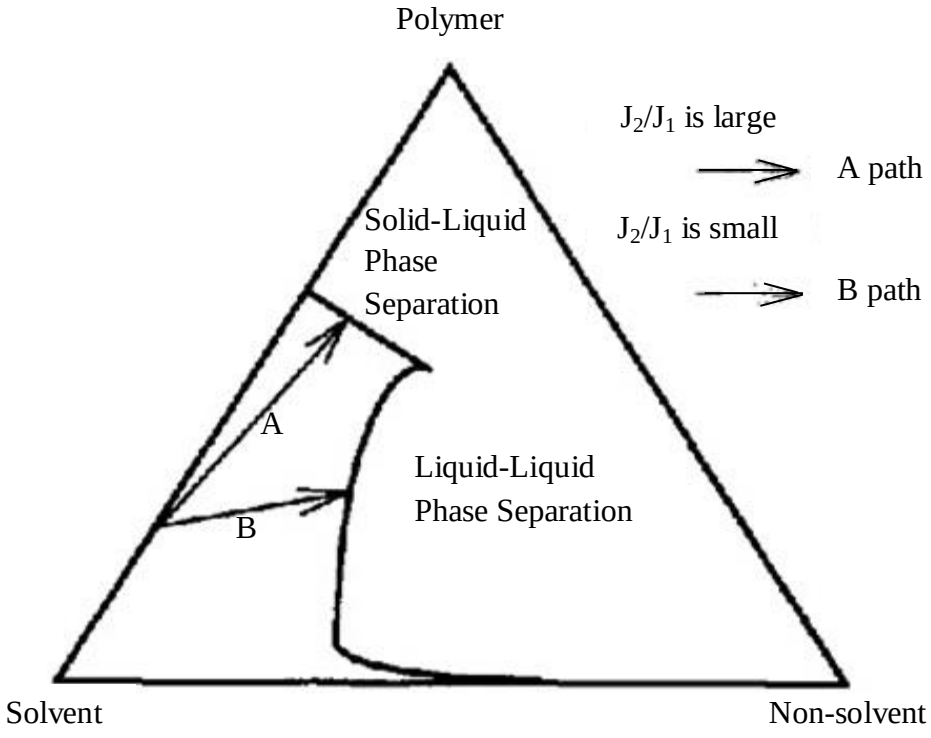

Figure 2.3 Ternary phase diagram of non-solvent/ solvent/ polymer. A, B: coagulation path [15]

In the polymer-solvent-precipitation medium phase diagram, a membrane is formed by the change in the composition of casting solution. The initial composition of casting solution represents an initial point. The final composition of casting solution or the membrane composition is reached by losing a solvent and gaining a non-solvent.

Figure 2.4 represents an isothermal phase diagram of polymer, solvent, and non-solvent. Points at boundary lines between any two corners represent mixtures of two components, and any point inside the triangle represents a mixture of all three components. The diagrams have two main regions. The first region has one-phase. This one-phase region can be divided into three regions, i.e., a fluid polymer solution region, a polymer gel region, and a glassy solid polymer region. All components in one-phase region form a homogeneous solution. The second region has two phases. The immiscible solution can be separated into a solid (polymer-rich) phase and a liquid (polymer-poor) phase. During precipitation of the membrane casting solution, the casting solution moves from a composition in the one-phase region to a composition in the two-phase or metastable region by crossing the binodal boundary. Polymer solution compositions in this region are not normally precipitate unless well nucleated. Besides, polymer solutions spontaneously separate into two phases with compositions linked by tie lines. The boundary between the metastable and unstable regions is the spinodal boundary.

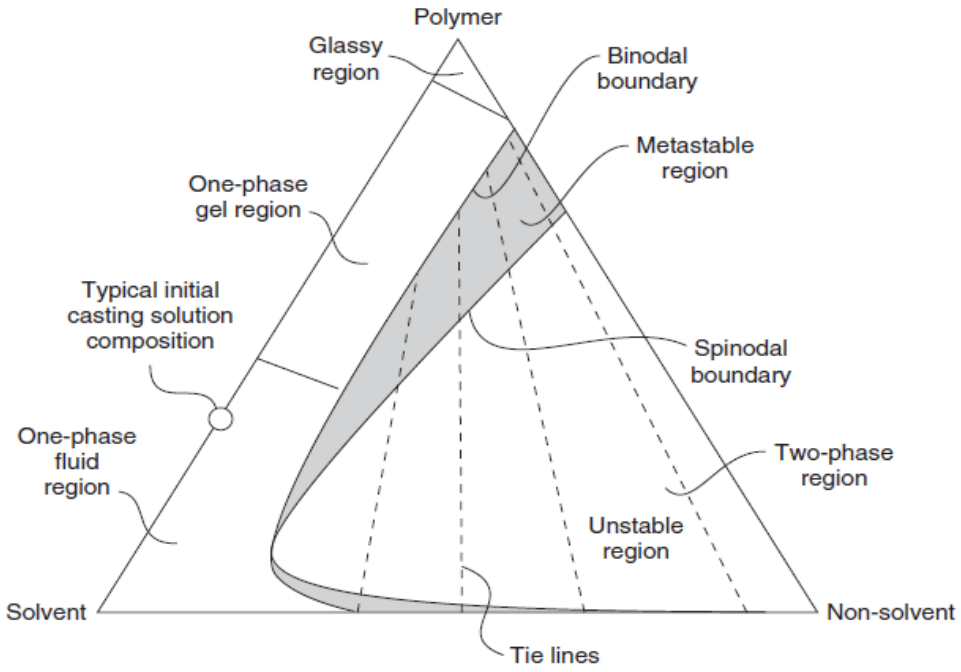

Figure 2.4 Schematic of the three-component phase diagram often used to rationalize the formation of non-solvent-precipitation phase separation membranes. In the two-phase region of the diagram, tie lines link the precipitated polymer-rich phase with its equilibrium polymer-poor phase [14]

For the membrane precipitation process, polymer precipitation occurred when the composition of casting solution enters the two-phase region. In this region, the casting solution is separated into a solid (polymer-rich) phase and a liquid (polymer-poor) phase. In the first step of precipitation process, the polymer-rich phase precipitates and then becomes a semi-solid gel. After that, the solvent in the polymer-rich phase is depleted because it diffuses into a coagulation solution. The depletion of solvent in the polymer-rich phase changes the polymer phase to a solid gel phase whereas the structure of membrane does not change. In the final step of membrane formation, the solid gel phase or a solid (polymer-rich phase) forms the membrane matrix and the solvent-non-solvent phase or a liquid (polymer-poor) phase forms the pores.

Strathmann et al. [16] described the process of membrane formation by using a line from point A (composition of initial casting solution) to point D (final membrane composition) as shown in Figure 2.5. The A to D path is the overall precipitation process. Point A is the initial casting solution, which is a two-component mixture. At point D, when the composition of membrane reaches the equilibrium, the compositions of solid (polymer-rich) phase and liquid (polymer-poor) phase are presented by points S and L, respectively. The solid (polymer-rich) phase forms the matrix of the final membrane. The liquid (polymer-poor) phase consists of membrane pores filled with precipitant. In the system of three-component phase diagram for membrane formation, when the solvent of casting solution diffuses out of the casting solution and the non-solvent penetrates into the casting solution, the composition of casting solution changes from points A to point B, C and D, respectively. At point B, the polymer solution initially precipitates. During the precipitation process, the solvent in the polymer solution is decreased because of the solvent-precipitant exchange. At point C, the viscosity of polymer solution is increased, leading to solidification.

A single line in Figure 2.5 is the average composition of the whole membrane. This line links an initial casting solution or a polymer-solvent mixture to a final membrane composition or a polymer-non-solvent mixture. When the phase inversion occurs, the rate of precipitation and the precipitation path through the phase diagram differs at different points of the membrane. The top surface of the casting solution begins to precipitate first after the casting solution is immersed into the precipitation medium. This polymer solution in the surface layer rapidly precipitates. Microporous structure is formed because the two phases created on precipitation have no time to agglomerate. The microporous surface layer acts as a barrier, which reduces the exchange rate between solvent and non-solvent. Therefore, the rate of precipitation slowly decreases from the top surface to the bottom surface. The slow precipitation allows more time for the two-phase formed to separate, resulting in the larger average pore size. As each pace in the casting solution precipitates at different rates and different pathways, the precipitation process can be described by the transition of one point to another point.

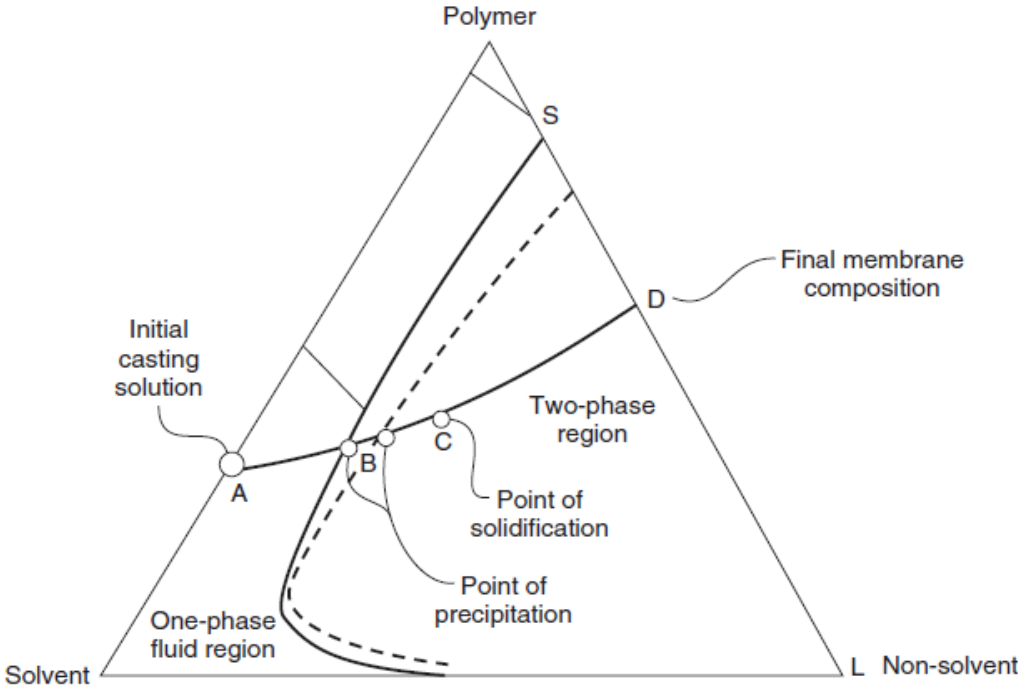

Figure 2.5 Membrane formation in non-solvent-precipitation membranes was first rationalized as a path through the three-component phase diagram from the initial polymer casting solution (A) to the final membrane (D) [17]

The transition is presented in Figure 2.6. For example, at time t_2, the top surface of casting solution completely precipitates after the precipitation process starts for a few seconds. The composition of this surface layer is at point A in the Figure, which is near the polymer non-solvent axis. At the bottom surface of the film, the composition is near the initial composition of casting solution because the precipitation has only just begun. In Figure 2.6, the precipitation pathway goes through the two-phase region of the phase diagram over the critical point, where the binodal and spinodal lines intersect. The change of composition above the critical point is important because it means that precipitation will take place as a liquid droplet in a continuous polymer-rich phase. When the dilute casting solution is used, the precipitation pathway goes through the two-phase region of the phase diagram below the critical point. The polymer gel particles in a continuous liquid phase are produced by precipitation, resulting in weak and powdery membrane.

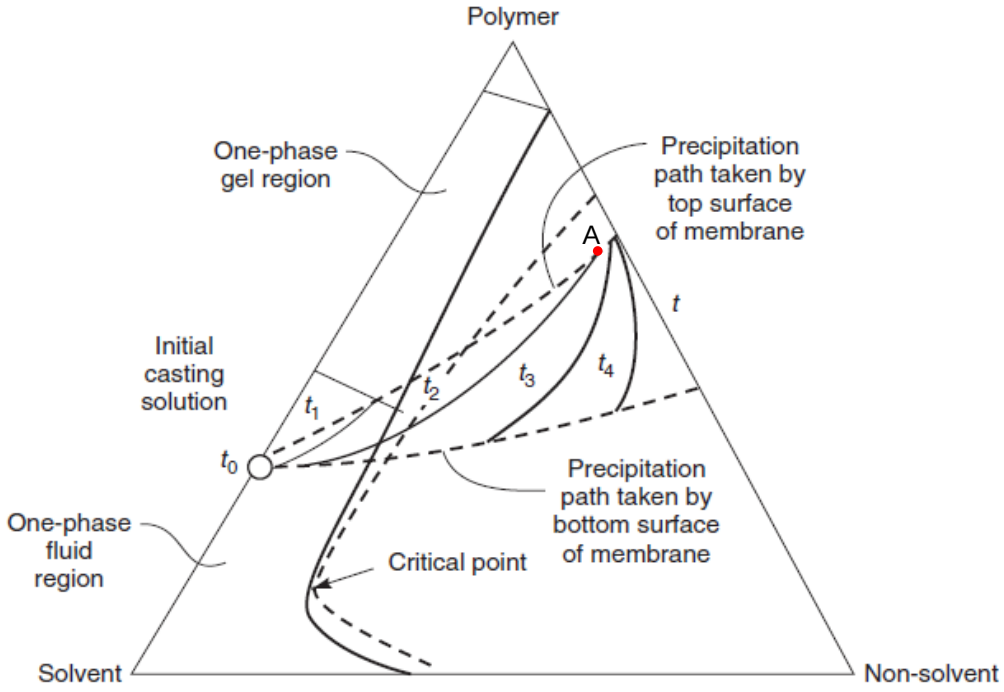

Figure 2.6 The surface layer of non-solvent-prcipitationmembranes precipitates faster than the underlying substrate. The precipitation pathway is best represented by the movement of a line through the three-component phase diagram [18]

2.3 Perstraction Process

Perstraction, define as the extraction and transport through membrane that is the transport of a solute, through a membrane, from a higher concentration, [C_1], feed side to the lower concentration, [C_2], receiving side as shown in Figure 2.7. In such a system, butanol diffuses preferentially through the membrane, while other components are retained in the feed side. Because of the fact that the operational costs of a recovery system mainly attributes to the energy consumption in the recovery system, perstraction becomes an attractive technology. The energy requirement of butanol recovery by perstraction, 9 MJ/kg, is less than those of most techniques [5]. The main advantage of the perstraction is process intensification by integrating the fermentation and recovery of butanol into one single step. This results in less process time because of the reduced number of unit operations. The integration of perstraction with a bioreactor is schematically presented in Figure 2.8.

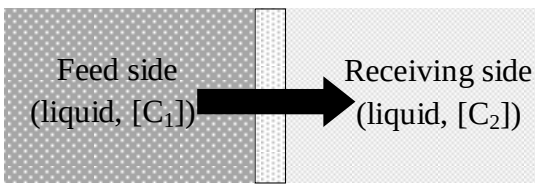

Figure 2.7 Pertraction:([C_1] > [C_2]) [19]

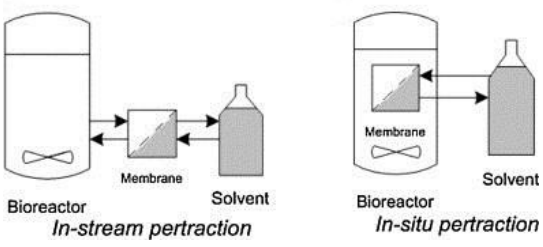

Figure 2.8 Integration of pertraction with a bioreactor [19]

2.4 Solution-Diffusion Mechanism [20]

The solution-diffusion mechanism consists of three steps. Firstly, molecules are absorbed at the upstream boundary or feed-membrane interface and dissolved into the dense film. Secondly, the dissolved molecules diffuse through the membrane, and, lastly, they desorbs on the other side of the membrane. In a perstraction process, the molecules are absorbed or extracted into the extractant. In general, the rates of absorption and desorption at the membrane interface are much higher than the rate of diffusion through the membrane. As the model assumes that the pressure within a membrane is constant, the driving force of the permeation across the membrane or the chemical potential gradient is therefore a concentration gradient. Molecules are separated by their differences in solubility into and mobility through the membrane. The latter one depends on interacting forces between the molecules of the membrane material and permeates molecules.

2.5 Non-ionic surfactant

Micelles of non-ionic surfactant are formed when the concentration of surfactant reaches a critical micelle concentration. The location of solubilization in the micelles is not clearly understood. Some authors have proposed that the core of non-ionic surfactant is surrounded by a mantle of aqueous hydrophilic chains. Solubilization may occur in both the core and the mantle. This hypothesis is represented in Figure 2.9 [21].

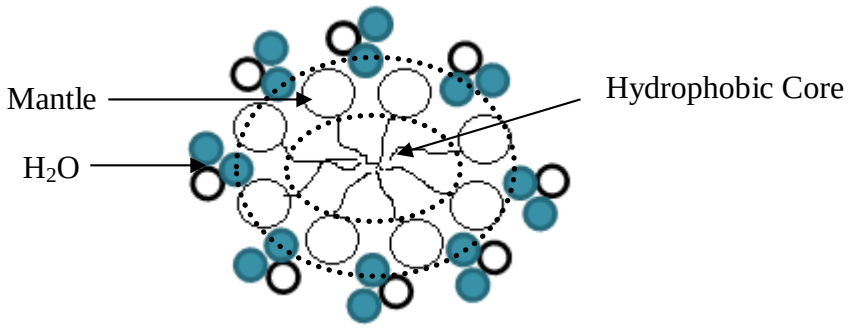

Figure 2.9 Schematic of micelle formation consisting of a mantle and a hydrophobic core

When a temperature of non-ionic surfactant is below a cloud point, surfactant can be dissolved in water, yielding the homogeneous phase. As the temperature is raised to above a cloud point, the surfactant solution separates into a surfactant-lean and surfactant-rich phase as shown in Figure 2.10. Nonionic surfactant in a surfactant-rich phase form micelle. Micelle consist a two beneficial characteristic as polar head and hydrophobic tail, then polar head is contacted with aqueous and hydrophobic tail is contacted with organic solute [10].

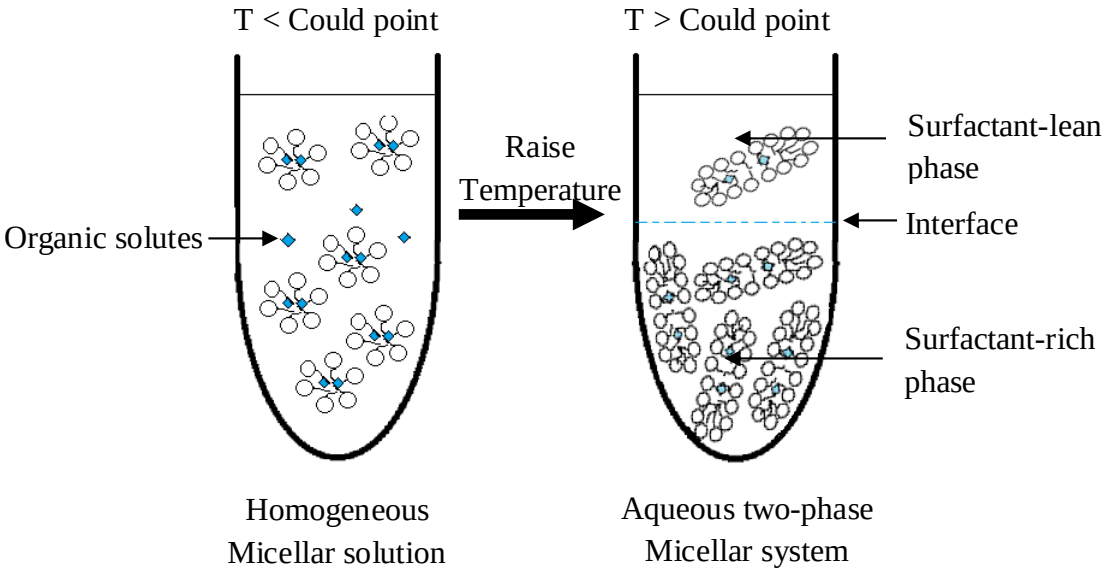

Figure 2.10 The effect of temperature on the micellar structure

Triton X-114, a non-ionic surfactant is used in this work. The synonym is polyethylene glycol *tert*-octylphenyl ether. The surfactant has a critical micelle concentration and could point temperature of ~0.2 mM or 0.009 % (w/w water) and 25 ^{o}C, respectively [22]. The chemical structure of Triton X-114 consists of a polyoxyethylene group as a polar head and hydrocarbon groups as a hydrophobic tail as shown in Figure 2.9.

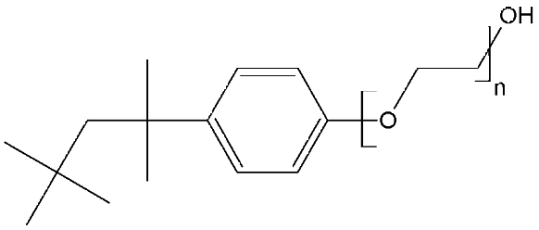

Figure 2.11 Structure of polyethylene glycol *tert*-octylphenyl ether [22]

Other physical properties of the surfactant are average molecular weight of 537 g/mol, a density at 25 ^{o}C of 1.058 gmol/cm^{3} and HLB value of 12.4 [10, 22].

2.6 Production of butanol

Butanol is the main product of ABE fermentation, and has some attractive properties. The advantages of butanol include 30 % higher energy content (29.2 MJ/L) over ethanol (19.6 MJ/L), lower vapor pressure, less volatile, less flammable, and mixable with gasoline [23]. However, since the discovery of ABE fermentation a century ago, biobutanol production has faced numerous difficulties, preventing it from becoming a commercially viable process. There are two interrelated outstanding challenges facing the commercialization of biobutanol today. The first is the end-product toxicity to the fermenting microorganisms. Butanol at low product concentrations (normally < 20 g/L) causes cell growth inhibition and premature termination of ABE fermentation [24]. The toxicity of butanol has been ascribed to passive proton flux by butanol causing

membrane leaking [25], disruption of the lipid structure in cell membranes that alters membrane-bound enzyme activity [26], and membrane fluidity in the presence of butanol [27].

2.7 Membrane Performance Evaluation

The parameters for membrane performance evaluation are explained in the terms of permeated flux.

2.7.1 Permeate Flux (J)

Flux is the amount of substance that permeates through the membrane per unit area and time. For the perstraction experiment, a high flux indicates that organic permeate is highly solubilized into a receiving solution. Permeate flux (J) (g/(m^2.h)) is calculated by

$$J_i = \frac{M_i}{A \cdot t} \times \frac{16.5\ \mu m}{T} \quad (1)$$

where M_i is the mass of i species in a permeate, (g)
A is the membrane area, (m^2)
t is the time of the experiment, (h)
T is the membrane thickness, (μm)
16.5 is the average of membrane thickness, (μm)

2.7.2 Separation Factor (α) for pervaporation

Separation factor is a ratio of concentration of organic i in a permeate to concentration of organic i in a feed. A high separation factor indicates that organic permeate is effectively separated by pervaporation. Separation factor (α) is defined as

$$\alpha = \frac{(y_i/y_j)}{(x_i/x_j)} \quad (2)$$

where y_i is the mass fraction of i species in a permeate
y_j is the mass fraction of j species in a permeate
x_i is the mass fraction of i species in a feed
x_j is the mass fraction of j species in a feed

2.8 Triton X-114 Performance Evaluation

Parameters for Triton X-114 performance evaluation are explained in terms of distribution coefficient and capturing capacity.

2.8.1 Distribution Coefficient

A distribution coefficient of component i is a ratio of concentration of i in the surfactant-rich phase to concentration of i in the surfactant-lean phase at extraction equilibrium. A high distribution coefficient indicates that an organic solute is more dissolved in a surfactant-rich phase than a surfactant-lean phase. A distribution coefficient is defined as

$$\text{Distribution coefficient of component i} = \frac{C_{i,RP}}{C_{i,LP}} \tag{3}$$

where $C_{i,RP}$ is the concentration of i species in the surfactant-rich phase (g/ L)
$C_{i,LP}$ is the concentration of i species in the surfactant-lean phase (g/ L)

2.8.2 Capturing Capacity

A capturing capacity of component i is a ratio of mass of i in the surfactant-rich phase to mass of Triton X-114 at extraction equilibrium. It indicates the ability of Triton X-114 to entrap an organic solute. A high capturing capacity means the surfactant efficiently captures an organic solute. Capturing capacity is defined as

$$\text{Capturing capacity of i} = \frac{m_{i.RP}}{m_{\text{Triton X}-114}} \tag{4}$$

where $m_{i,RP}$ is the mass of i species in the surfactant-rich phase, (g)
$m_{\text{Triton X-114}}$ is the mass of Triton X-114 in the solution, (g)

2.9 Literature Review

Liu et al. [7] used poly(ether block amide) (PEBA) membrane for acetone-butanol-ethanol separation by pervaporation. They found that PEBAX® 2533 was dissolved by n-butanol but it was not dissolved in acetone and ethanol at an elevated temperature. The result of sorption experiment using a temperature of 23 ^{o}C showed that the polymer could uptake butanol, acetone, and ethanol for 6.83, 0.71 and 0.56 (in g solvent/g polymer) respectively. The result of pervaporation experiment using a relatively thick (100 µm) dense membrane demonstrated the permselecivity in the order of n-butanol > acetone > ethanol. In addition, n-butanol had the highest permeating flux because of its high solubility in the membrane.

Fouad and Feng [11] used poly(ether block amide) (PEBAX® 2533) membrane for butanol separation from dilute aqueous solution by pervaporation. They studied about the effects of feed concentration, temperature, and membrane thickness on the separation performance. They found that the flux of butanol was increased when the concentration of butanol in the feed was increased, while the flux of water was not changed. The flux of butanol and water were increased when the temperature of feed

was increased. The separation factor was increased with feed temperature. This was because butanol had the higher activation energy for permeation (35.6–58.6 kJ/mol) than the activation energy for water permeation (23.1–25.8 kJ/mol). The organic flux was decreased when the membrane was thicker. They suggested that the resistance of the membrane was a rate-controlled process. The decrease of membrane thickness leaded an increase of permeating flux.

Qureshi and Maddox [8] used oleyl alcohol as the perstraction solvent for butanol separation by perstraction. They showed that the removal of ABE by perstraction was faster than the production rate in the reactor. The maximum concentration of ABE in the oleyl alcohol was 9.75 g/L, It is viewed that recovery of ABE from oleyl alcohol (at this concentration) would be more economical than recovery from the fermentation broth.

Dhamole et al. [10] studied effect of non-ionic surfactant to enhance butanol production by extractive fermentation. The results from that work were the primary motivation behind the concept of this work. Several non-ionic surfactants, Triton X-114, L64, L62LF, L61, and L62, were tested to extract and separate butanol from the fermentation broth, and to enhance the acetone-butanol production. Triton X-114 possessed many properties as an excellent medium for butanol extraction. It exhibited the highest butanol capturing capacity among the surfactants used in that work. Its cloud point temperature was also lowest, 25 ^{o}C. Therefore, the surfactant-rich phase containing butanol could be formed by slightly heating the aqueous solution. Given that boiling point of butanol, 117.7^{o}C, was significantly lower than that of Triton X-114, 177^{o}C, separation of butanol from the surfactant-rich phase can easily be done. Nevertheless, Triton X-114 unfortunately was not biocompatible with the butanol producing strain.

Darcovich and Kutowy [28] investigated surface tension of three systems. The systems were solvent-additive systems, solvent-polymer systems, and casting solutions. Polymers were cellulose acetate, polyamidehydrazide, and polysulfone. Solvents were acetone, DMA, NMP, and DMSO. In a solvent-additive system, an additive such as H_2O or salt or other minor components was added into a solvent. In solvent-polymer systems, a system consisted of only a polymer and a solvent. They investigated an effect of increase of polymer concentration on the surface tension of system. In casting solutions, different amounts of additive were added into polymer solutions. For a solvent-polymer system consisting of cellulose acetate as a polymer and either acetone or DMSO as a solvent, they found that the system using acetone as the solvent had a surface tension of approximately 24 dynes/cm. However, the system using DMSO as a solvent had a surface tension of approximately 47 dynes/cm. In accordance with the surface tension data of this work, in case of acetone as a solvent, a film formed by Tanny [29] had a dense layer at solvent/ non-solvent interface or gelation bath. However, by using DMSO as a solvent, the structure of membrane consisted of a dense layer at the solid surface, which was supported by open pores. This structure was reverse skinned.

Bloch and Frommer [30] studied the mechanism for formation of skinned membranes. The skinned membranes consisted of a dense layer which was supported by a porous structure. They found that the dense layer was formed at the support surface by using dimethyl sulfoxide (DMSO) as the solvent and water as the coagulation solution. When the cellulose acetate membrane was prepared by acetic acid as the solvent, the dense skin formed at the solvent/non-solvent interface.

Form previous research, poly(ether block amid) or PEBA membrane exhibited high performance for butanol separation by pervaporation. The membrane had high affinity to butanol. The polymer will be used to prepare integrally-skinned asymmetric membranes in this work. In addition, Triton X-114, a non-ionic surfactant, showed that it had very high butanol capturing capacity although it was quite toxic to the butanol producing culture. It will be used in the receiving phase of the perstraction in this work, which can prevent its harmful effects when applied to the actual fermentation broth.

CHAPTER 3 EXPERIMENT

The PEBAX® 2533, poly(ether block amide), was used to prepare dense and integrally-skinned asymmetric membranes. Asymmetric membranes were synthesized by Loeb-Sourirajan method. The perstraction of acetone (A), butanol (B), ethanol (E) aqueous solutions and the mixture of ABE in water through the membranes was done. Aqueous solutions of Triton X-114, a non-ionic surfactant, were used as receiving solutions. The effects of perstraction conditions, i.e., feed composition, surfactant concentration, receiving phase temperature, initial butanol concentration in receiving solution, were studied. In addition, pervaporation of ABE using a dense membrane was tested. The experimental procedures are described in this chapter.

3.1 Materials and Equipment

3.1.1 Chemicals and Materials

1. PEBAX® 2533, kindly given by ARKEMA, Singapore
2. Triton X-114
3. Butanol 99.89 % (v/v)
4. Ethanol 99.89 % (v/v)
5. Acetone 99.89 % (v/v)
6. Mixture of Acetone: Butanol: Ethanol 1: 19.2: 1.7 g/L

3.1.2 Experimental apparatus

1. Gas Chromatograph equipped with FID detector (Agilent 6890)
2. 10 μL Syringe
3. Stopwatch (Casio HS-5)
4. Perstraction apparatus as shown in Figure 3.1
5. Pervaporation apparatus as shown in Figure 3.3
6. Glassware such as graduated cylinder, beaker, pipettes, volumetric flask etc.
7. Washing bottle
8. Scanning Electron Microscope (SEM)

3.2 Experimental Procedure

3.2.1 PEBA asymmetric membrane preparation

PEBAX® 2533 was dissolved in a solvent at 80 ˚C under vigorous stirring to form a homogenous polymer solution consisting of 7 to 11 wt. % polymer. The solvents were pure butanol, mixtures of methanol and butanol. After the polymer solution was kept at room temperature without disturbance for one day to remove the air bubbles entrapped. The casting solution was heated to 40 ^{o}C so that the polymer was completely dissolved, yielding the homogeneous solution. The solution would form a film of uniform thickness. A glass plate was also heated to a temperature of 40 ^{o}C. About 3 mL of the casting solution was poured onto the plate and allowed to disperse. The glass plate was

tilted so that the solution was evenly distributed. This pouring and dispersion of polymer consumed approximately 2 min. The solution was immersed into methanol, a non-solvent, where it remained for a predetermined period of time, ranging from 30 min to 3 d. The gel-like film was removed from the coagulation bath and allowed to dry in the ambient air. It was subsequently immersed into DI water so that it could be removed from the glass plate. After the film was peeled off the glass, it was then dried in an ambient air for at least 48 h. The ultimate aim was to obtain the integrally-skinned asymmetric membrane having sponge-like structure.

Table 3.1 Conditions for asymmetric PEBA membrane preparation

Film code	**PEBA (wt. %)**	**Solvent (wt. %)**	**Coagulation time (h)**
7-0-0.5(37.4 μm)	7%	93% BuOH	0.5
7-0-1(49.6 μm)	7%	93%BuOH	1
7-0-1.5(42.4 μm)	7%	93% BuOH	1.5
7-0-24(44.6 μm)	7%	93% BuOH	24
7-0-72(34.6 μm)	7%	93% BuOH	72
8-0-0.75(56.4 μm)	8%	92% BuOH	0.75
8-0-24(43.1 μm)	8%	92% BuOH	24
9-0-0.75(51.5 μm)	9%	91% BuOH	0.75
9-0-1(57.1 μm)	9%	91% BuOH	1
9-0-1.5(62.4 μm)	9%	91% BuOH	1.5
9-0-5(50.5 μm)	9%	91% BuOH	5
9-0-24(48.7 μm)	9%	91% BuOH	24
11-0-72(44.5 μm)	11%	89% BuOH	72
7-20-24(40.0 μm)	7%	20%MeOH -73%BuOH	24
8-20-24(38.9 μm)	8%	20%MeOH -72%BuOH	24
9-10-0.5(56.4 μm)	9%	10%MeOH -81%BuOH	0.5
9-10-1(60.6 μm)	9%	10%MeOH -81%BuOH	1
9-20-0.5(47.6 μm)	9%	20%MeOH -71%BuOH	0.5
9-20-1(57.8 μm)	9%	20%MeOH -71%BuOH	1
9-20-2(54.7 μm)	9%	20%MeOH -71%BuOH	2
9-20-3(54.1 μm)	9%	20%MeOH -71%BuOH	3

Table 3.1 Conditions for asymmetric PEBA membrane preparation (Continued)

Film code	PEBA (wt. %)	Solvent (wt. %)	Coagulation time (h)
9-20-5(44.8 μm)	9%	20%MeOH -71%BuOH	5
9-20-72(41.5 μm)	9%	20%MeOH -71%BuOH	72
11-20-72(45.6 μm)	11%	20%MeOH -69%BuOH	72

*Numbers in a film code denote PEBA weight percent - methanol weight percent in a casting solution - coagulation time(film thickness in microns)

3.2.2 PEBA dense membrane preparation

PEBAX® 2533 was dissolved in butanol at 80 ˚C under vigorous stirring to form a homogenous polymer solution containing 7 wt. % of the polymer. After the polymer solution was kept at room temperature without disturbance for one day to remove air bubbles entrapped, about 1.8 mL of the solution was poured onto a glass plate at ambient temperature. Then, the solvent was allowed to evaporate until a clear dense film with a uniform thickness was formed. After the evaporation, the film was dried in a hot air oven at 50 ^{o}C where it remained for at least 24 h to ensure that residual butanol was completely evaporated. To remove the film from the glass plate, the plate was subsequently immersed into DI water. After the film was peeled off the glass, it was then dried at ambient air temperature. Thickness of the membrane was 16.5±1.3 μm. There were 25 membranes used in this work. The result of membrane preparations were tabulated in appendices D.

3.2.3 SEM analysis of poly(ether block amide) membrane

After the membrane preparation**,** the morphology of poly(ether block amide) membrane was investigated by using Scanning Electron Microscope.

3.2.4 Perstraction experiment

The apparatus for perstraction experiments is shown in Figure 3.1. Concentration of acetone, butanol, and ethanol in feed container were 1, 19.2, and 1.7 g/L, respectively. These were the corresponding fermentation broth final concentrations produced by *Clostridium acetobutylicum* [4]. The experiments were carried out with the receiving side at a 37 ^{o}C, which was the optimum temperature for *Clostridium acetobutylicum* growth [4]. The working volume of the feed was 300 cm^3. The dense poly(ether block amide) membrane was used in the perstraction cell. The area and thickness of the membrane in contact with the feed solution were 5.72 cm^2 and 16.5 ± 1.3 μm. The receiving side of the cell was an aqueous solution of Triton X-114.Volume of the receiving compartment was 157 cm^3. Based on the work done by Galera-Gomez and Gu [31], the cloud point of the solution was about 25^{o}C. The receiving chamber was immersed in warm water, approximately 37±2 ^{o}C. In an experiment with a receiving

temperature of 6 ^{o}C, which was below the cloud point of Triton X-114, the receiving compartment was immersed in an ice bath. After the permeation cell was assembled, the experiment was allowed to proceed for 5 h. An aliquot, 5μL, of the receiving solution was collected every 30 min with a syringe. 2 μL of the solution was injected into a gas chromatograph to analyze for the concentrations of acetone, ethanol and butanol. A graph plotted between mass of the solute appearing in the receiving solution and time was used to calculate a flux. A solute flux was obtained by dividing the slope of straight line of the graph by the effective membrane area. To verify that the concentration of the feed remained unchanged during the experiment, the feed was also analyzed for the concentrations.

After end of 5 hours perstraction experiment, the receiving solution containing acetone, butanol, ethanol, and surfactant was allowed to settle at temperature of 37 ^{o}C for 24 hours. A clear phase separation between surfactant lean-phase and surfactant rich-phase was observed. Concentrations of acetone, butanol, and ethanol in a surfactant-lean phase were analyzed by injecting 2 μL of the solution into a gas chromatograph. Mass of each organic solute present in the solution was obtained by multiplying the volumes of surfactant-lean phases. Mass of each organic solute in the surfactant-rich phase was calculated by using the mass balance.

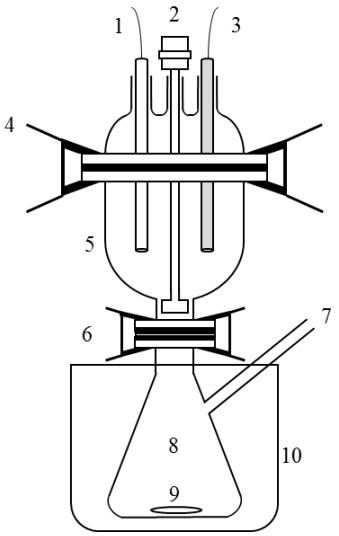

Figure 3.1 Perstraction cell: 1 = Thermostat, 2 = Stirrer, 3 = Heater, 4 = Clip, 5 = Feed container, 6 = Membrane in between 2 O-rings, 7 = Sampling port, 8 = Receiving container, 9 = Magnetic stir bar, 10 = Heating/Cooling bath

Table 3.2 Conditions for perstraction

Experimental number	Feed solution	Receiving solution	Temperature of receiving solution (^{o}C)	Data in Appendix
1	A:B:E: 1: 19.2: 1.7 (g/L)	Pure water	37	D.1.1
2	A:B:E: 1: 19.2: 1.7 (g/L)	Pure water	37	D.1.2
3	A:B:E: 1: 19.2: 1.7 (g/L)	Pure water	37	D.1.3
4	A:B:E: 1: 19.2: 1.7 (g/L)	0.7 wt. % Triton X-114	37	D.2
5	A:B:E: 1: 19.2: 1.7 (g/L)	0.8 wt. % Triton X-114	37	D.3
6	A:B:E: 1: 19.2: 1.7 (g/L)	0.9 wt. % Triton X-114	37	D.4
7	A:B:E: 1: 19.2: 1.7 (g/L)	3.5 wt. % Triton X-114	37	D.5
8	A:B:E: 1: 19.2: 1.7 (g/L)	7.0 wt. % Triton X-114	37	D.6
9	A:B:E: 1: 19.2: 1.7 (g/L)	10.5 wt. % Triton X-114	37	D.7
10	Acetone: 1 (g/L)	3.5 wt. % Triton X-114	37	D.8
11	Ethanol: 1.7 (g/L)	3.5 wt. % Triton X-114	37	D.9
12	Butanol: 19.2 (g/L)	3.5 wt. % Triton X-114	37	D.10
13	A:B:E: 1: 19.2: 1.7 (g/L)	Pure water	6	D.11.1
14	A:B:E: 1: 19.2: 1.7 (g/L)	3.5 wt. % Triton X-114	6	D.11.2
15	A:B:E: 1: 19.2: 1.7 (g/L)	6 g/L Butanol solution	37	D.12.1
16	A:B:E: 1: 19.2: 1.7 (g/L)	6 g/L Butanol solution	37	D.12.2
17	A:B:E: 1: 19.2: 1.7 (g/L)	6 g/L Butanol solution	37	D.12.3
18	A:B:E: 1: 19.2: 1.7 (g/L)	12 g/L Butanol solution	37	D.13.1
19	A:B:E: 1: 19.2: 1.7 (g/L)	12 g/L Butanol solution	37	D.13.2

Table 3.3 Conditions of distribution coefficient determination after five hours of perstraction

Experimental Number	Composition in the receiving solution		Data in Appendix
	Organic solute	Triton X-114 (wt. %)	
1	A:B:E: 0.079: 5.4: 0.085 (g/L)	0.7	D.16
2	A:B:E: 0.11: 6.7: 0.11 (g/L)	0.8	
3	A:B:E: 0.12: 6.4: 0.12 (g/L)	0.9	
4	A:B:E: 0.061: 4.0: 0.066 (g/L)	3.5	
5	A:B:E: 0.088: 5.4: 0.089 (g/L)	3.5	
6	A:B:E: 0.071: 4.2: 0.066 (g/L)	7.0	
7	A:B:E: 0.077: 4.6: 0.076 (g/L)	7.0	
8	A:B:E: 0.065: 4.2: 0.063 (g/L)	10.5	

3.2.5 Distribution coefficient experiment

A distribution coefficient is the ratio of a solute concentration in the surfactant-rich phase to that of the surfactant-lean phase. Distribution coefficients were determined by using the ABE concentrations at the fifth hour of perstraction that used pure water as a receiving phase. The concentrations of acetone, butanol, and ethanol were 0.079, 4.8, and 0.078 g/L respectively. The concentrations of Triton X-114 were varied from 0.5 to 7.0 wt. %. The total volume of ABE and the surfactant was 157 mL. The mixture was immersed in a water bath at 37 ^{o}C for 30 min, while shaken at all time. After that, the mixture was allowed to settle for 24 h at 37 ^{o}C, which resulted in a phase separation as shown in Figure 3.2. The volumes of surfactant-rich and surfactant-lean phases were noted. Concentrations of acetone, butanol, and ethanol in a surfactant-lean phase were analyzed by gas chromatography. The concentrations of ABE were determined by the material balance calculations. The distribution coefficient, mass, and capturing capacity were subsequently calculated.

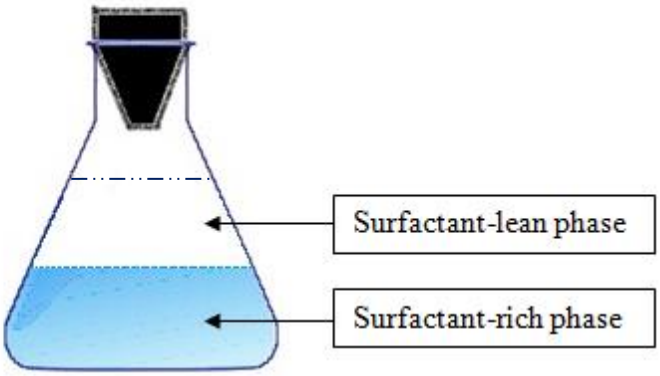

Figure 3.2 Schematic of phase separation from settled surfactant solution at 37 ^{o}C for 24 h

Table 3.4 Concentrations of Triton X-114 in distribution coefficient experiments using concentrations of acetone, butanol, and ethanol of 0.079, 4.8, and 0.078 g/L, respectively

Experimental Number	Triton X-114 (wt. %)	Data in Appendix
1	0.5	D.14
2	0.6	
3	0.7	
4	0.8	
5	0.9	
6	1.0	
7	1.1	
8	1.2	
9	1.3	
10	1.4	
11	1.5	
12	0.5	D.15
13	0.6	
14	0.7	
15	0.8	
16	0.9	
17	1.0	
18	1.3	
19	1.5	
20	3.5	
21	7	

3.2.6 Pervaporation experiment

The apparatus for pervaporation experiments is shown in Figure 3.3. The working volume of feed was 300 cm^3. A feed consisted of acetone, butanol, and ethanol at the concentrations of 1, 19.2, and 1.7 g/L, respectively. The feed temperature was the same as that used in perstraction, 37±2 ˚C. The dense poly(ether block amide) membrane was used in the perstraction cell. The area and thickness of the membrane in contact with the feed solution were 5.72 cm^2 and 16.5 ± 1.3 μm. The permeates were swept by dried air at a flow rate of 120 mL/min. After the permeation cell was assembled, the experiment was allowed to proceed for a predetermined period of time. Permeate was condensed by condensers, which were surrounded with ice/rock-salt mixture at -8 ±1 ^oC. The total mass was analyzed by an analytical balance (3 point). 2 μL of permeate was injected into a gas chromatograph to analyze for the concentrations of acetone, ethanol and butanol. A graph plotted between mass of the solute appearing in permeate and time was used to calculate a flux. A solute flux was obtained by dividing the slope of straight line of the graph by the effective membrane area. To verify that the concentration of the feed remained unchanged during the experiment, the feed was also analyzed for the concentrations. The feed was refreshed every hour.

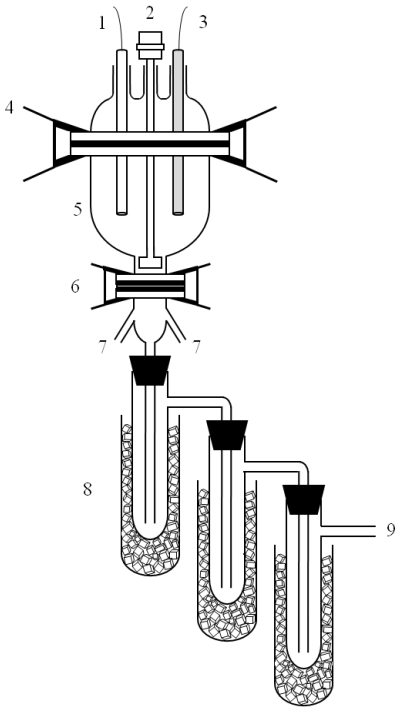

Figure 3.3 Pervaporation cell: 1 = Thermostat, 2 = Stirrer, 3 = Heater, 4 = Clip, 5 = Feed container, 6 = Membrane in between 2 O-rings, 7 = Air inlet, 8 = Condenser, 9 = Air outlet

Table 3.5 Conditions for pervaporation

Experimental number	**Feed solution**	**Pervaporation period (h)**	**Data in Appendix**
1	A:B:E: 1: 19.2: 1.7 (g/L)	5	D.17.1
2	A:B:E: 1: 19.2: 1.7 (g/L)	6	D.17.1
3	A:B:E: 1: 19.2: 1.7 (g/L)	7	D.17.1
4	A:B:E: 1: 19.2: 1.7 (g/L)	8	D.17.1
5	A:B:E: 1: 19.2: 1.7 (g/L)	9	D.17.1
6	Pure water	5	D.17.2
7	Pure water	6	D.17.2
8	Pure water	7	D.17.2

CHAPTER 4 RESULTS AND DISCUSTION

In this section, discussion of research is divided into two parts: poly(ether block amide) or PEBA asymmetric membrane preparation and perstraction of acetone-butanol-ethanol (ABE) using dense poly(ether block amide) membranes. Triton X-114, a non-ionic surfactant, was used in the receiving phase of perstraction. Effects of Triton X-114 concentration, temperature of the receiving solution, and initial butanol concentration in receiving solution were studied. Distribution coefficients of acetone, butanol, and ethanol between surfactant-rich and surfactant-lean phases were determined. In addition, pervaporation of ABE solution was investigated. Performance of the membranes was evaluated based on permeation flux.

4.1 PEBA Asymmetric Membrane Preparation

Butanol was used as a solvent for PEBA because it was reported to have strong affinity with the polymer [7].

Interactions between solvent and non-solvent were very important to the phase inversion. Water, methanol, and ethanol were investigated to determine their potential as a non-solvent. They were chosen based on Hansen solubility parameters presented Table 4.1.

Table 4.1 Hansen solubility of butanol, ethanol, methanol, and water [32]

Component	**Hansen Solubility Parameters** $(\boldsymbol{MPa})^{\frac{1}{2}}$**, at 25 °C**				**Difference from coagulant**
	$\boldsymbol{\delta_i}$	$\boldsymbol{\delta_d}$	$\boldsymbol{\delta_p}$	$\boldsymbol{\delta_h}$	$\boldsymbol{\Delta\delta_{s-c}}$
Butanol	23.2	16	5.7	15.8	-
Ethanol	26.5	15.8	8.8	19.4	4.8
Methanol	29.6	15.1	12.3	22.3	9.4
Water	47.8	15.5	16	42.3	28.4

$$*\delta_i = \sqrt{\delta_{d,i}^2 + \delta_{p,i}^2 + \delta_{h,i}^2}$$

$$*\Delta\delta_{s-c} = \sqrt{4(\delta_{d,s} - \delta_{d,c})^2 + (\delta_{p,s} - \delta_{p,c})^2 + (\delta_{h,s} - \delta_{h,c})^2}$$

Among the selected non-solvents, water had the weakest affinity with butanol. An asymmetric membrane prepared by using water as non-solvent was unsuccessful because PEBA solution was dispersed in water after the casting solution was immersed into water. This was likely because of a large difference between solubility parameters ($\Delta\delta_{s-c}$) of butanol and water, leading to weak interaction between the solvent and non-solvent. To prevent the dispersion of 3 wt. % PEBA solution in water, the solution must be allowed to stand in the ambient air for at least 70 minutes prior to the immersion in water. However, this procedure resulted in a dense film as shown in Figure 4.1.

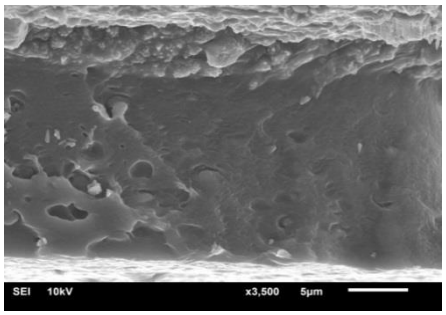

Figure 4.1 A cross section of 3 wt. % PEBA by scanning electron microscope

Despite smaller difference in solubility parameters ($\Delta\delta_{s-c}$) between butanol and ethanol, ethanol could not be used as a non-solvent. A PEBA film cast by using butanol as a solvent was dissolved by ethanol. Interactions between butanol and methanol were strong as implied by $\Delta\delta_{s-c}$. The rate of solvent and non-solvent exchange was possibly rapid as described in section 2.2 of Chapter two. Therefore, the system of methanol/butanol/PEBA could reach liquid–liquid phase separation and, with appropriate PEBA concentration and coagulation time, resulted in membranes with porous structure.

Even though methanol was used as a coagulant, a high concentration of PEBA in a casting solution could lead to the formation of a dense film. Structures of the membranes obtained from the casting solutions containing 7 to 11 wt. % PEBA are shown in Figure 4.2 (7-0-72(34.6µm) and 11-0-72(44.5µm). A porous structure was obtained from the 7 wt. % casting solution while a dense structure was obtained from 11 wt. % casting solution. This result could be discussed based on three-component phase diagram presented in section 2.2 of Chapter two. Casting solution of 7 wt. % PEBA had a low polymer concentration, causing liquid-liquid demixing in the two-phase region. The increase of polymer concentration 11 wt. % was high enough to trigger solid-liquid demixing in one-phase gel region. At the lower PEBA concentration, which corresponded to the higher butanol concentration, the solubility of methanol in butanol/PEBA mixture was higher and the ratio of solvent to non-solvent diffusion rate was lower. The relatively higher coagulant inflow rate resulted in the porous structure. By contrast, the higher PEBA concentration was responsible for the lower solubility of methanol. As a consequence, the ratio of solvent to non-solvent exchange was higher and induced the dense film structure.

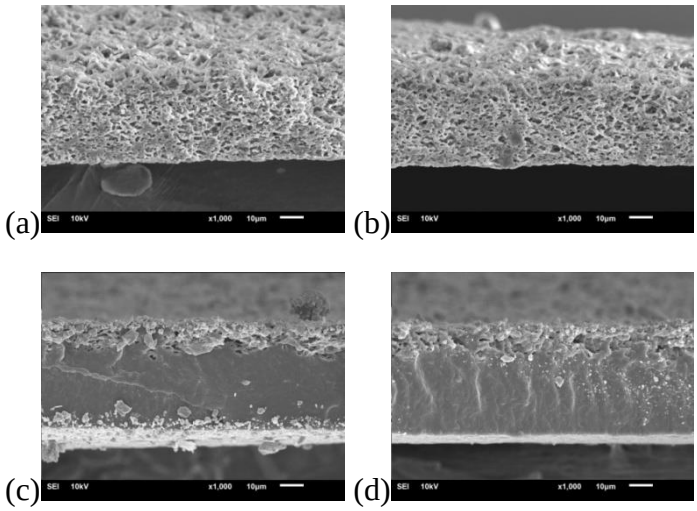

Figure 4.2 Effects of casting composition on membrane structures:
(a) 7-0-72(34.6μm) zone 1, (b) 7-0-72(34.6μm) zone 2,
(c) 11-0-72(44.5μm) zone 1, and (d) 11-0-72(44.5μm) zone 2

Effects of immersion time on membrane structure are depicted by Figure 4.3 to 4.5. The porosity of film was increased from the increase of immersion time. As the casting solution was immersed in the coagulation bath, the phase inversion continued until the composition reached the solvent-free state. However, the phase inversion could be stopped by the removal of casting solution from the coagulation bath. For the coagulation time of 30 min (7-0-0.5(37.4μm) in Figure 4.3), the membrane prepared from 7 wt. % PEBA solution had the dense layer at solution/glass interface. This was because the non-solvent did not penetrate into the deep portion of the casting solution. By contrast, the structure of membrane formed by using a 7 wt. % PEBA solution was completely porous when the coagulation time was longer than 30 min.

Moreover, a dense skin layer of the membrane could be observed at a solution/glass interface (7-0-0.5(37.4μm)). The low polymer concentration could produce porous membrane with high porosity. Although a membrane prepared by using 7 wt. % PEBA solution could produce a thin dense layer at the bottom surface, few pores were found the on the surface.

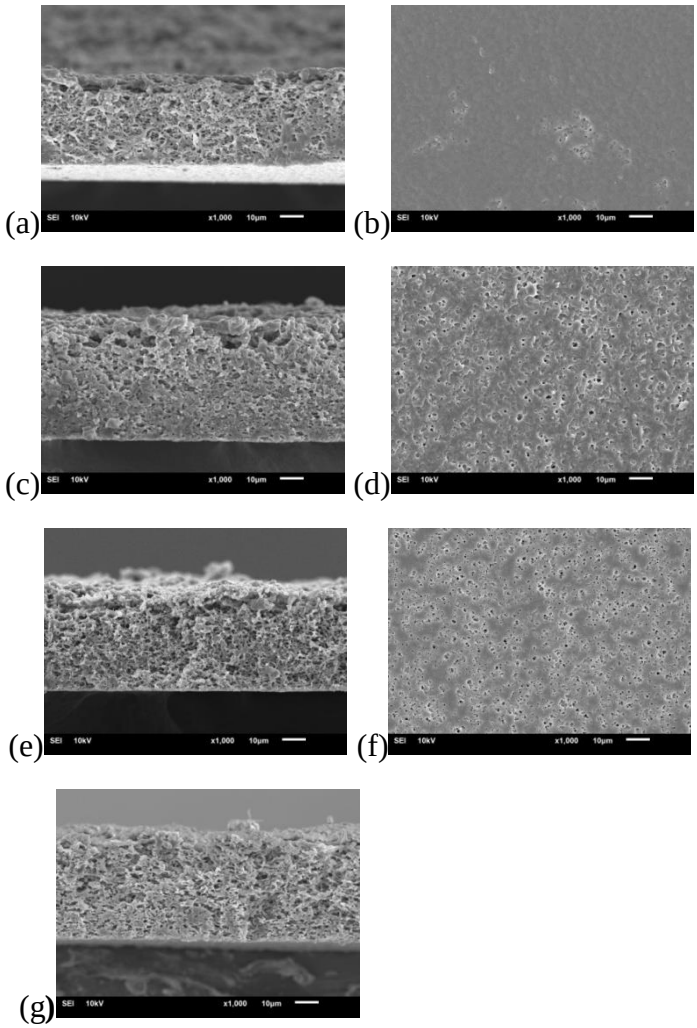

Figure 4.3 Effects of coagulation time on membrane structures:
(a) 7-0-0.5(37.4μm) cross section, (b) 7-0-0.5(37.4μm) bottom surface,
(c) 7-0-1(49.6μm) cross section, (d) 7-0-1(49.6μm) bottom surface,
(e) 7-0-1.5(42.4μm) cross section, (f) 7-0-1.5(42.4μm) bottom surface,
and (g) 7-0-24(44.6μm) cross section

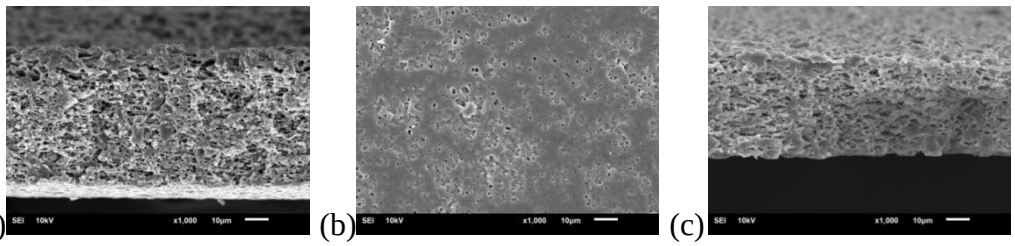

Figure 4.4 Effects of coagulation time on membrane structures:
(a) 8-0-0.75(56.4μm) cross section,
(b) 8-0-0.75(56.4μm) bottom surface,
and (c) 8-0-24(43.1μm) cross section

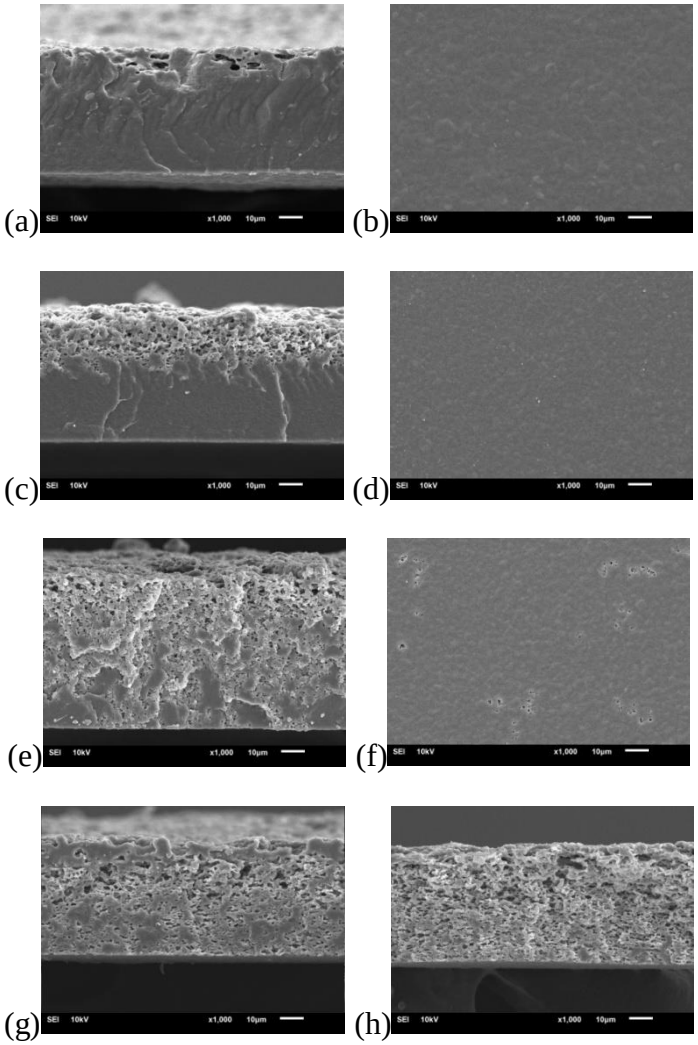

Figure 4.5 Effects of coagulation time on membrane structures:
(a) 9-0-0.75(51.5μm) cross section, (b) 9-0-0.75(51.5μm) bottom surface,
(c) 9-0-1(57.1μm) cross section, (d) 9-0-1(57.1μm) bottom surface,
(e) 9-0-1.5(62.4μm) cross section, (f) 9-0-1.5(62.4μm) bottom surface,
(g) 9-0-5(50.5μm) cross section and (h) 9-0-24(48.7μm) cross section

Similarly, the increase of coagulation time resulted in the increase in porosity of the membranes prepared by using 8 and 9 wt. % PEBA solutions. However, for the membrane prepared from 9 wt. % PEBA solution, the removal of the film from the coagulation bath after 45 min of immersion time gave a dense membrane (9-0-0.75(51.5µm) in Figure 4.6). A plausible explanation was that methanol penetration rate was reduced by the higher PEBA concentration. However, the increase of coagulation time to 24 h produced a film with a porous structure because the solvent/non-solvent time was long enough for liquid-liquid demixing to occur.

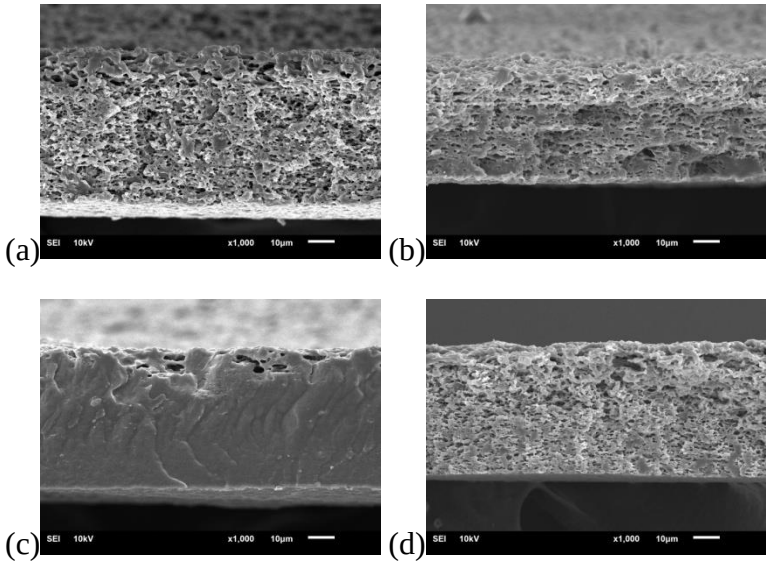

Figure 4.6 Effects of composition and coagulation time on membrane structures: (a) 8-0-0.75(56.4µm) cross section, (b) 8-0-24(43.1µm) cross section, (c) 9-0-0.75(51.5µm) cross section, and (d) 9-0-24(48.7µm) cross section

Addition of methanol, a non-solvent, into 7 and 8 wt. % PEBA casting solutions decreased the porosity of membranes. Concentration of methanol added into the casting solution was 20 wt. %. The structures of resulting films are shown in Figure 4.7 (7-20-24(40.0µm) and 8-20-24(38.9µm)). Compared with the structures of the membranes prepared from the casting solutions without the addition of methanol (7-0-24(44.6µm) and 8-0-24(43.1µm) in Figure 4.7), the presence of methanol in the casting solution enlarged the pore size of membrane, while the porosity was reduced. The presence of methanol in the initial casting solution reduced the time required for liquid-liquid demixing. At the same period of immersion time, methanol concentration in the liquid (polymer-poor) phase was higher when methanol was added into the initial casting solution. As a consequence, the pore size was larger because the pores were created by the disappearance of methanol from the solution. By contrast, the solid (polymer-rich) phases were aggregated as a result of the growing in pore size. Therefore, the pore wall thickness was thicker than that obtained from the casting solution without added methanol.

The effect of methanol addition into the casting solution was pronounced as the PEBA concentration was increased to 9 wt. %. The addition influenced the formation of the membrane in a unique way. Unlike the porous structure of the film prepared from the casting solution without the addition of methanol (9-0-5(50.5µm) in Table 4.8), a dense layer was observed at the solution/glass interface as shown in Table 4.8 (9-20-5(44.8µm)). Due to the high polymer concentration, it was hypothesized that the casting solution was divided into two domains, which were not clearly distinguishable. After the casting solution was immersed into a coagulation bath, the domain containing a higher polymer concentration was in the one phase fluid region because the concentration of non-solvent could not sufficiently produce liquid-liquid demixing. The primary cause of the inadequate methanol concentration was because the casting solution was removed from the coagulation bath before methanol and butanol exchange could take place. Therefore, the domain containing a higher polymer concentration entered the one phase gel region. Based on the hypothesis, the dense layer formed after the casting solution had been removed from the coagulation bath. This was because if the casting solution was allowed to remain in the coagulation bath for an enough period of time, a porous structure was observed in the same way as discussed in the previous paragraph. The upper layer of the film was formed by the domain containing a lower polymer concentration. The porous structure was produced by liquid-liquid demixing because the polymer concentration was lower than that at the solution/glass interface.

A similar result was reported by Fujita and co-workers [33]. They found a formation of dense layer at solution/glass interface. A porous/asymmetric membrane was prepared from poly(styrene-co-di-vinylbenzene) using glycerol as a non-solvent. Due to a slower penetration rate of the non-solvent compared with the diffusion rate of solvent, NMP, out of the solution, a dense layer was formed at the bottom portion of film. The formation of dense layer was the result of polymer precipitation. Another similar finding was reported by Young and Chen [34]. They found a dense layer at the bottom

layer of ethylene-vinyl alcohol membrane. As they described, most solvent at bottom layer was depleted, leading to the solidification.

For a very high concentration of PEBA in a casting solution, addition of the non-solvent had negligible effect on membrane structure. As shown in Figure 4.8 (11-0-72(44.5µm) and 11-20-72(45.6µm)), mostly dense structures were obtained whether methanol was added into the casting solution or not. The high concentration of PEBA, 11 wt. %, caused the majority of the solution to enter the one-phase gel region. The upper layer was still porous because the composition of the casting solution at the solution/non-solvent interface allowed the entering into the liquid-liquid demixing region.

The effect of coagulation time on the structure of membrane formed by adding methanol into the initial casting solution was also studied. As the coagulation time increased, the porosity of film was increased. The structures of the films prepared from the casting solutions containing 20 wt. % methanol and 9 wt. % PEBA are shown in Figure 4.9 (9-20-0.5(47.6µm) to 9-20-72(41.5µm)). As mentioned earlier, the addition of methanol into casting solution possibly caused the formation of dense layer due to the solid-liquid demixing. By increasing the coagulation time, the solid-liquid demixing was reduced because there was more time for methanol to diffuse into the casting solution. The extent of solvent/non-solvent exchange and the corresponding liquid-liquid demixing were increased. The dense layer became thinner as coagulation time was increased from 30 min to 3 days.

The effect of methanol concentration in the initial concentration was also studied. As shown in Figure 4.10 (9-10-0.5(56.4µm) and 9-10-1(60.6µm)), the porosity of the membrane increased when the methanol concentration was decreased from 20 to 10 wt. %. The miscibility of the solution was increased when the methanol concentration decreased. The domain containing a higher polymer concentration was reduced and the dense layer became thinner. Correspondingly, more casting solution proceeded into the two phase region.

Although PEBA membrane preparation using methanol as a non-solvent produced a dense skin layer at the bottom surface, the membrane surface was not defect-free. Therefore, dense PEBA membranes were used in the perstraction experiments.

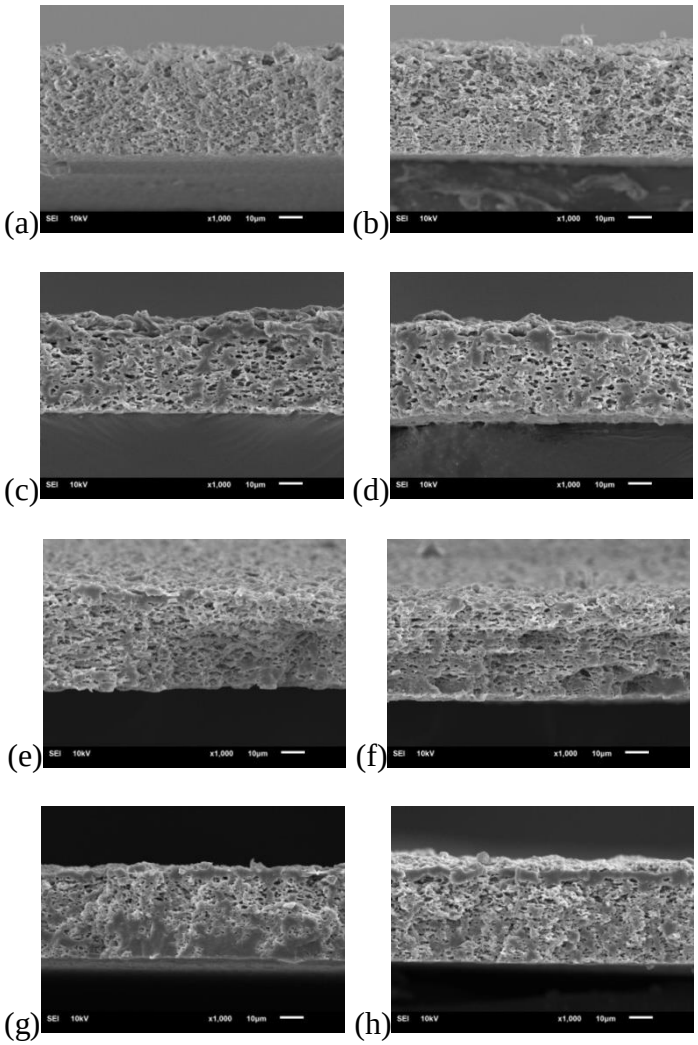

Figure 4.7 Effects of added methanol on membrane structures: the cross sections of membranes (a) 7-0-24(44.6μm) zone 1, (b) 7-0-24(44.6μm) zone 2, (c) 7-20-24(40.0μm) zone 1, (d) 7-20-24(40.0μm) zone 2, (e) 8-0-24(43.1μm) zone 1, (f) 8-0-24(43.1μm) zone 2, (g) 8-20-24(38.9μm) zone 1, and (h) 8-20-24(38.9μm) zone 2

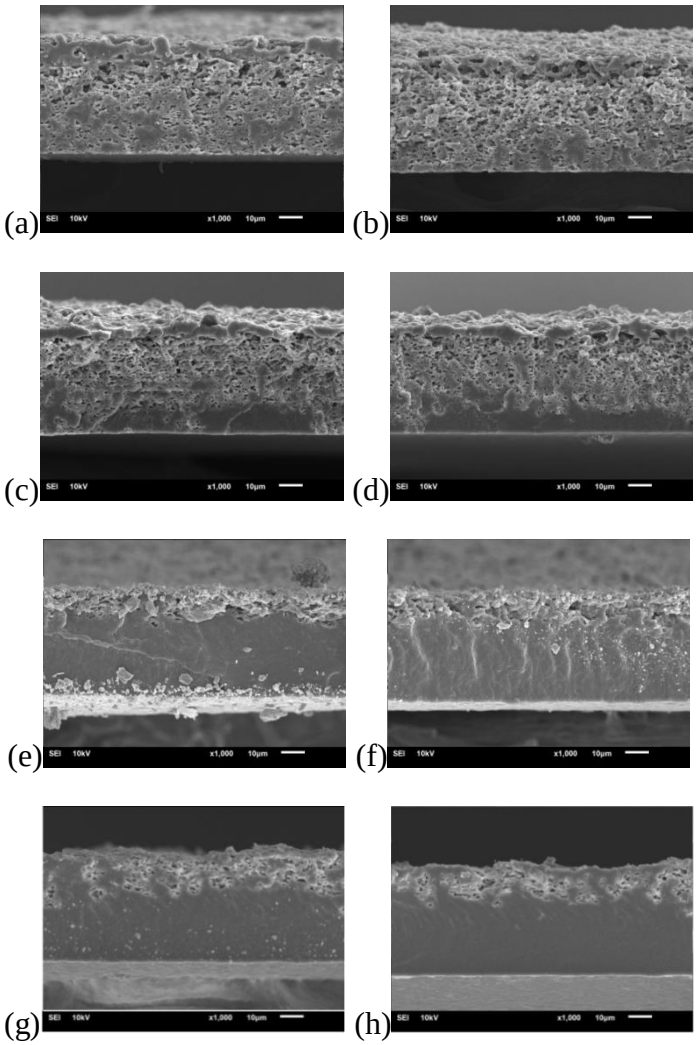

Figure 4.8 Effects of added methanol on membrane structures: the cross sections of membranes (a) 9-0-5(50.5µm) zone 1, (b) 9-0-5(50.5µm) zone 2, (c) 9-20-5(44.8µm) zone 1, (d) 9-20-5(44.8µm) zone 2, (e) 11-0-72(44.5µm) zone 1, (f) 11-0-72(44.5µm) zone 2, (g) 11-20-72(45.6µm) zone 1, and (h) 11-20-72(45.6µm) zone 2

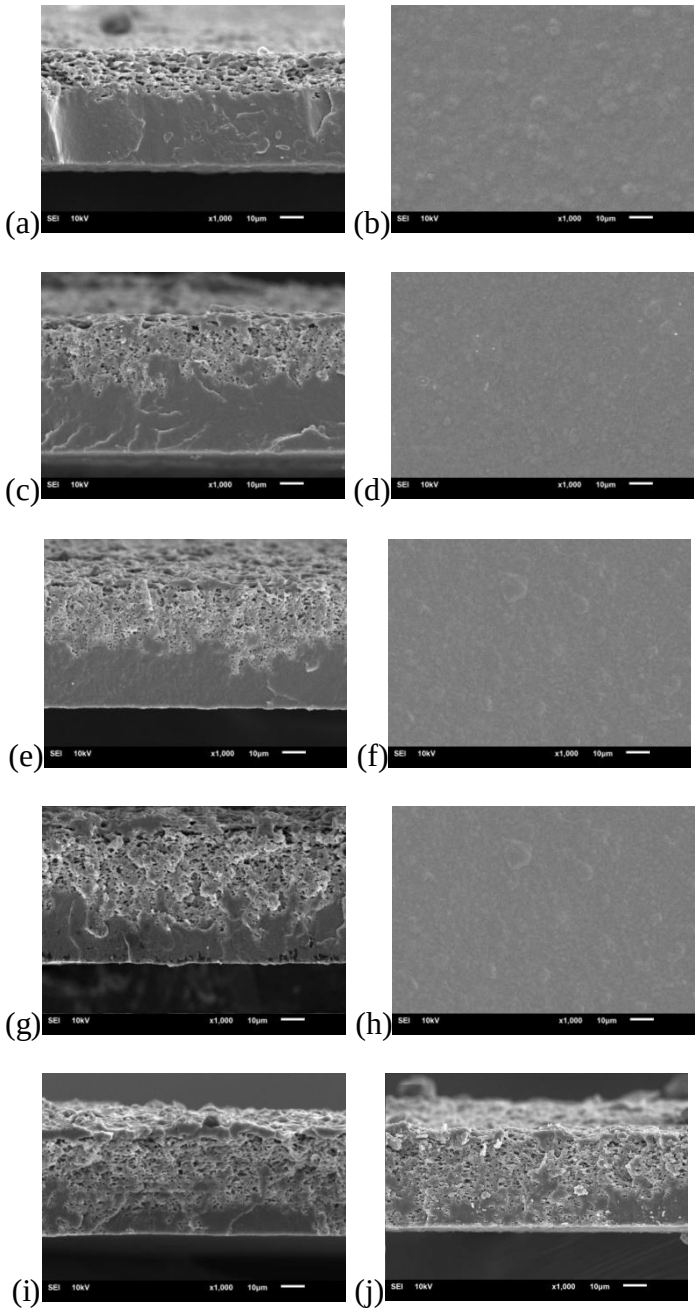

Figure 4.9 Effects of coagulation time on the structures of membranes prepared by 20 wt. % methanol: (a) 9-20-0.5(47.6μm) cross section, (b) 9-20-0.5(47.6μm) bottom surface, (c) 9-20-1(57.8μm) cross section, (d) 9-20-1(57.8μm) bottom surface, (e) 9-20-2(54.7μm) cross section, (f) 9-20-2(54.7μm) bottom surface, (g) 9-20-3(54.1μm) cross section, (h) 9-20-3(54.1μm) bottom surface, (i) 9-20-5(44.8μm) cross section, and (j) 9-20-72(41.5μm) cross section

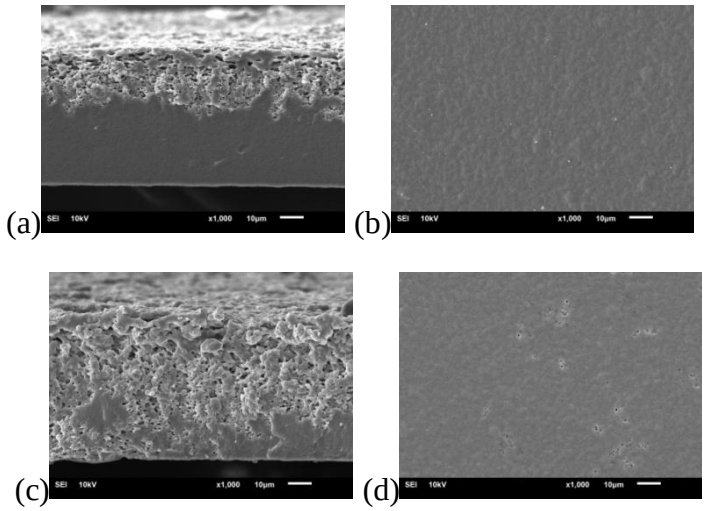

Figure 4.10 Effects of coagulation time on the structures of membranes prepared by 10 wt. % methanol: (a) 9-10-0.5(56.4µm) cross section, (b) 9-10-0.5(56.4µm) bottom surface, (c) 9-10-1(60.6µm) cross section and (d) 9-10-1(60.6µm) bottom surface

4.2 Distribution Coefficients of Acetone, Butanol, and Ethanol

Distribution coefficient of butanol as a function of Triton X-114 is presented in Figure 4.11. The highest distribution coefficient of butanol was 5.9, which was obtained from the Triton X-114 concentration of 0.8 wt. %. At lower concentrations, less micelles were available with a consequential reduction in the distribution coefficient. The decrease in distribution coefficient at higher surfactant concentrations was probably because the micelle structure became less suitable for the solvent extraction. It has long been known that an increase in a concentration of Triton X-114 results in an increase of the micelle-micelle interactions [35]. Diffusion of a solvent into a micelle could be more difficult when the micelles aggregated in the cluster. An increase of Triton X-114 concentration, therefore, lessened the ability of the surfactant in extracting butanol. Similarly, the distribution coefficients of acetone and ethanol decreased when a concentration of Triton X-114 was higher than the optimum value.

Intriguingly, the distribution coefficient of butanol was lower than those of acetone and ethanol at each surfactant concentration. This was because butanol was more hydrophobic than acetone and ethanol, which had comparable distribution coefficients. Therefore, butanol experienced repulsive forces from polar heads because micelles contacted with water by using their polar heads.

A similar phenomenon was also found in the utilization of Triton X-114 to extract mercury [36]. At a concentration of 0.12 % (w/v), the mercury extraction efficiency was highest. A lower concentration of the surfactant led to a lower extraction efficiency due to the inadequacy of the surfactant to quantitatively entrap mercury. Nevertheless, the extraction efficiency was also reduced when the surfactant concentration was higher than 0.12 % (w/v).

Capturing capacity of butanol as a function of Triton X-114 concentration is presented in Figure 4.14. The highest butanol capturing capacity was 0.106 g butanol/g Triton X-114, which was observed when the receiving solution contained 0.8 wt. % Triton X-114. The capturing capacity decreased although higher Triton X-114 concentrations were employed. An excessive amount of the surfactant, which led to larger micelle, was probably responsible for the decrease in butanol capturing capacity. Similarly, capturing capacities of acetone and ethanol also decreased when the concentration of Triton X-114 increased as shown in Figures 4.15 and 4.16.

By considering mass of butanol captured by Triton X-114 shown in Figure 4.17, it was clear that the reduction in butanol capturing capacity was not because the surfactant could trap less butanol. Despite more butanol in the surfactant-rich phase as the higher concentrations were used, an amount of trapped butanol was not significantly increased.

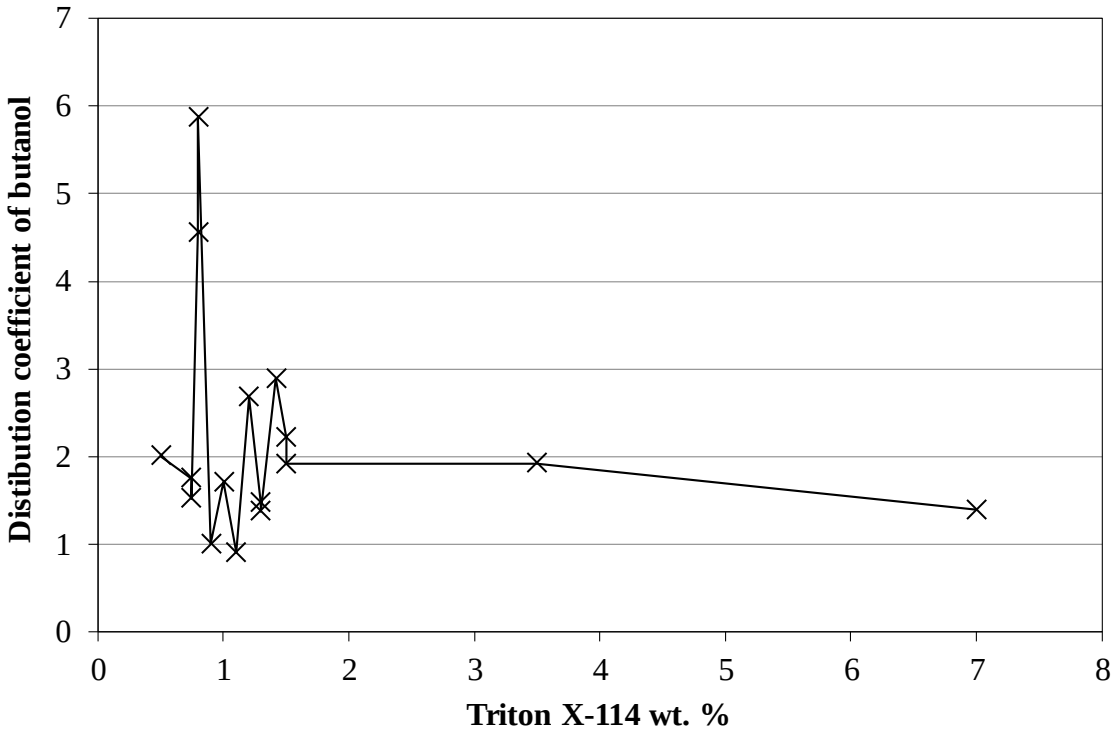

Figure 4.11 Distribution coefficients of butanol as a function of Triton X-114 wt. % at a temperature of 37 ^{o}C

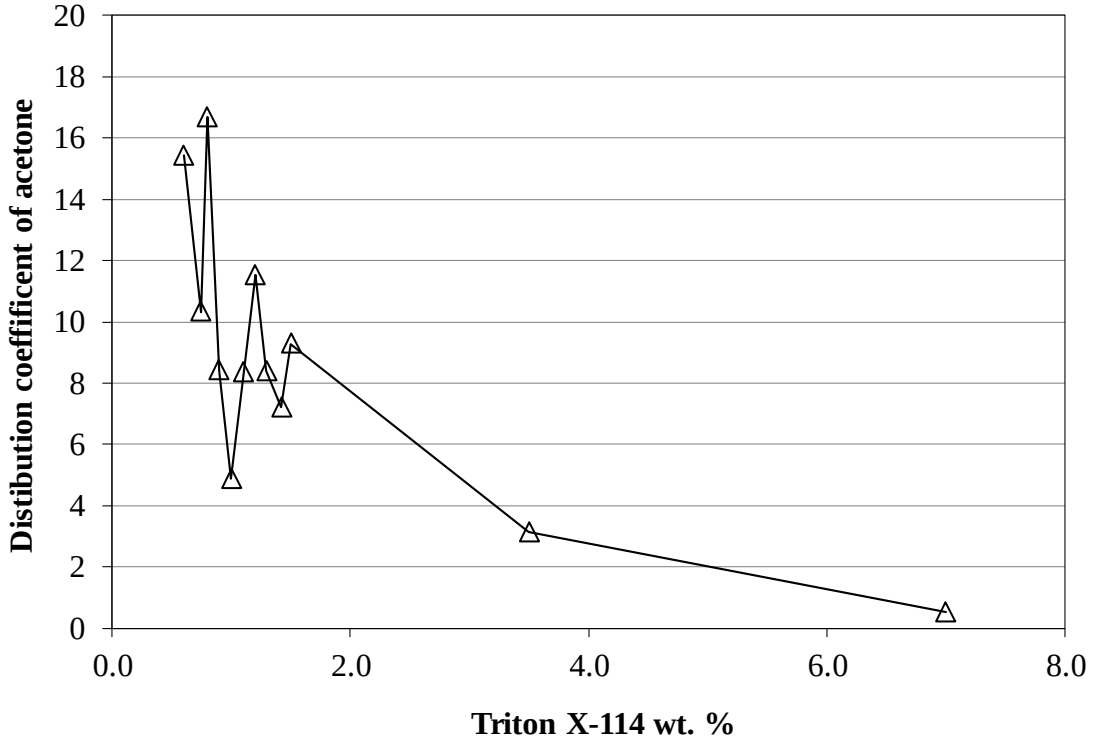

Figure 4.12 Distribution coefficients of acetone as a function of Triton X-114 wt. % at a temperature of 37 ^{o}C

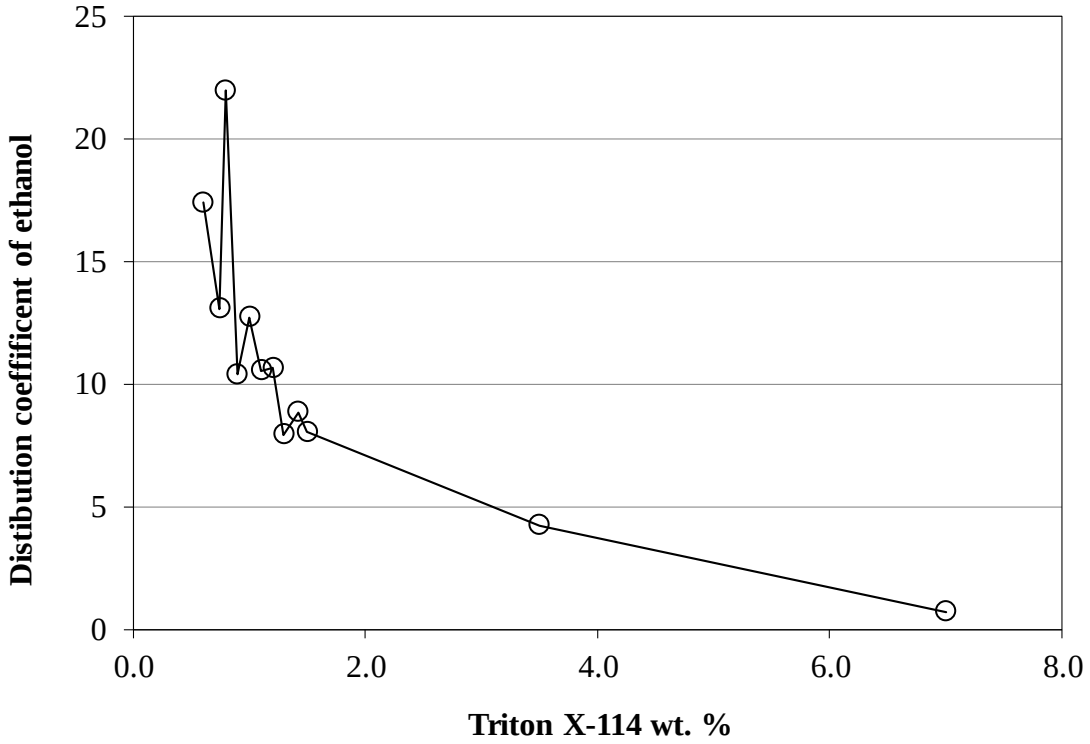

Figure 4.13 Distribution coefficients of ethanol as a function of Triton X-114 wt. % at a temperature of 37 ^{o}C

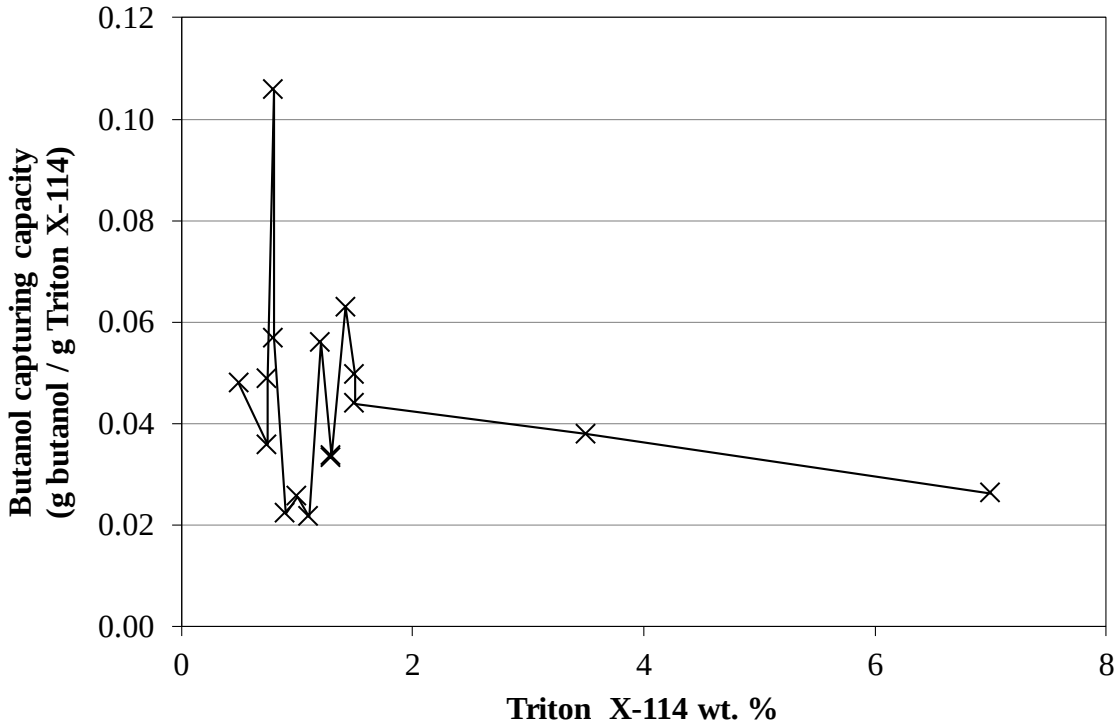

Figure 4.14 Capturing capacity of butanol as a function of Triton X – 114 wt. % at a temperature of 37 ^{o}C

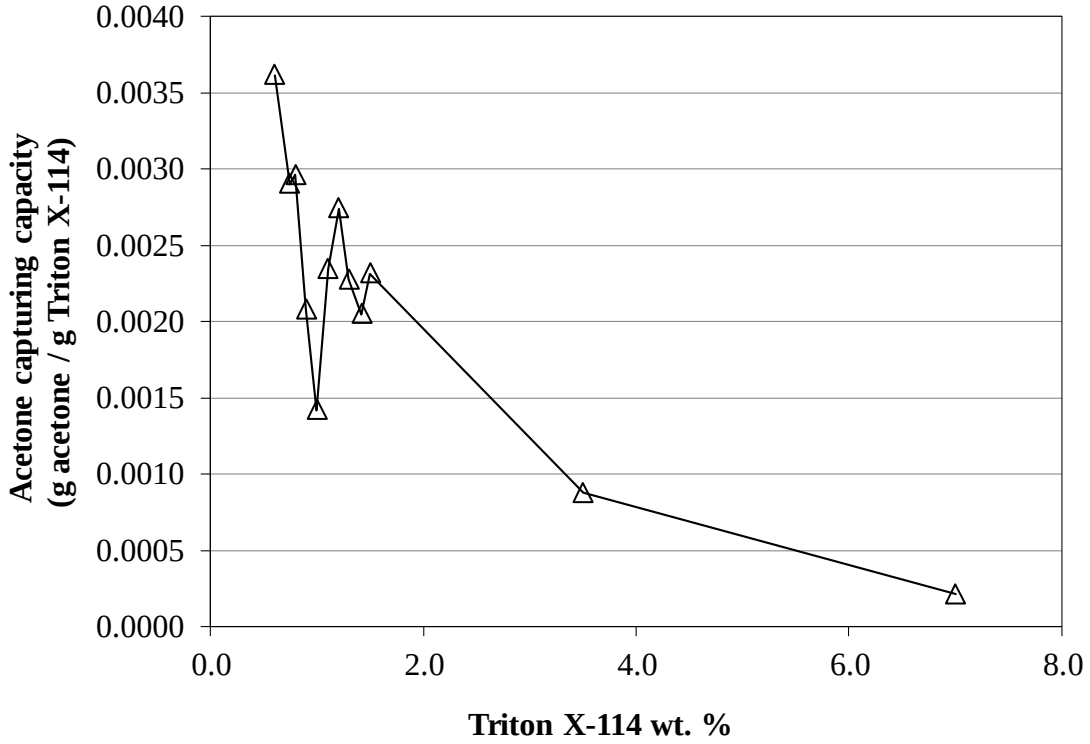

Figure 4.15 Capturing capacity of acetone as a function of Triton X – 114 wt. % at a temperature of 37 ^{o}C

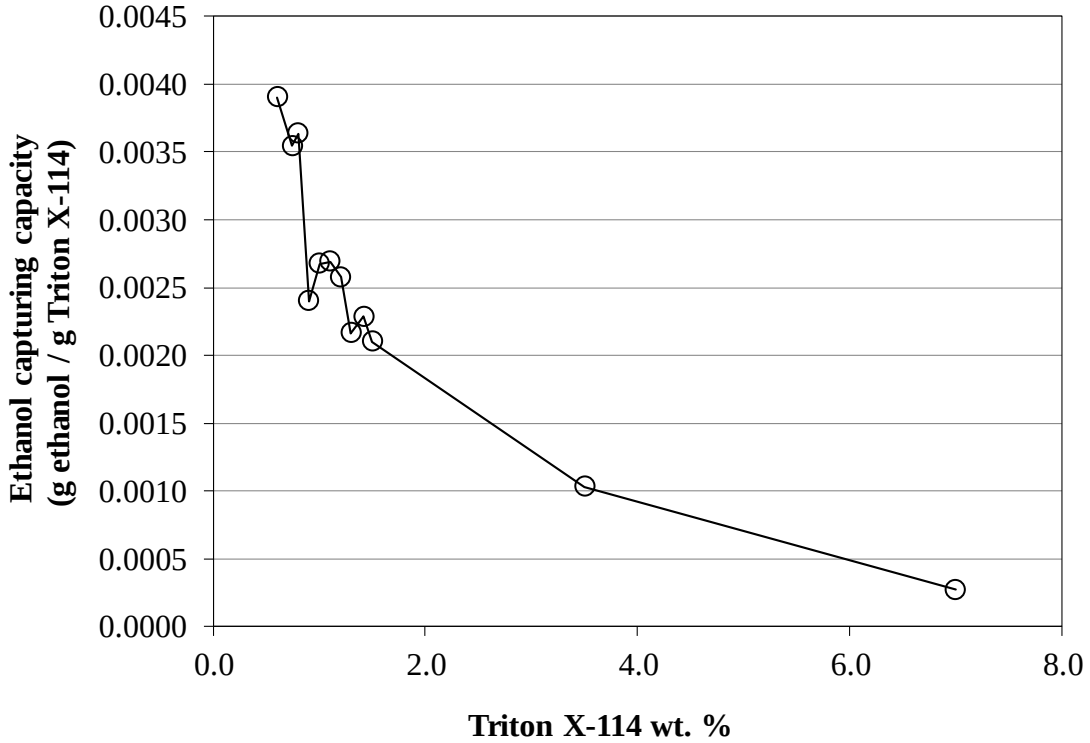

Figure 4.16 Capturing capacity of ethanol as a function of Triton X – 114 wt. % at temperature of 37 ^{o}C

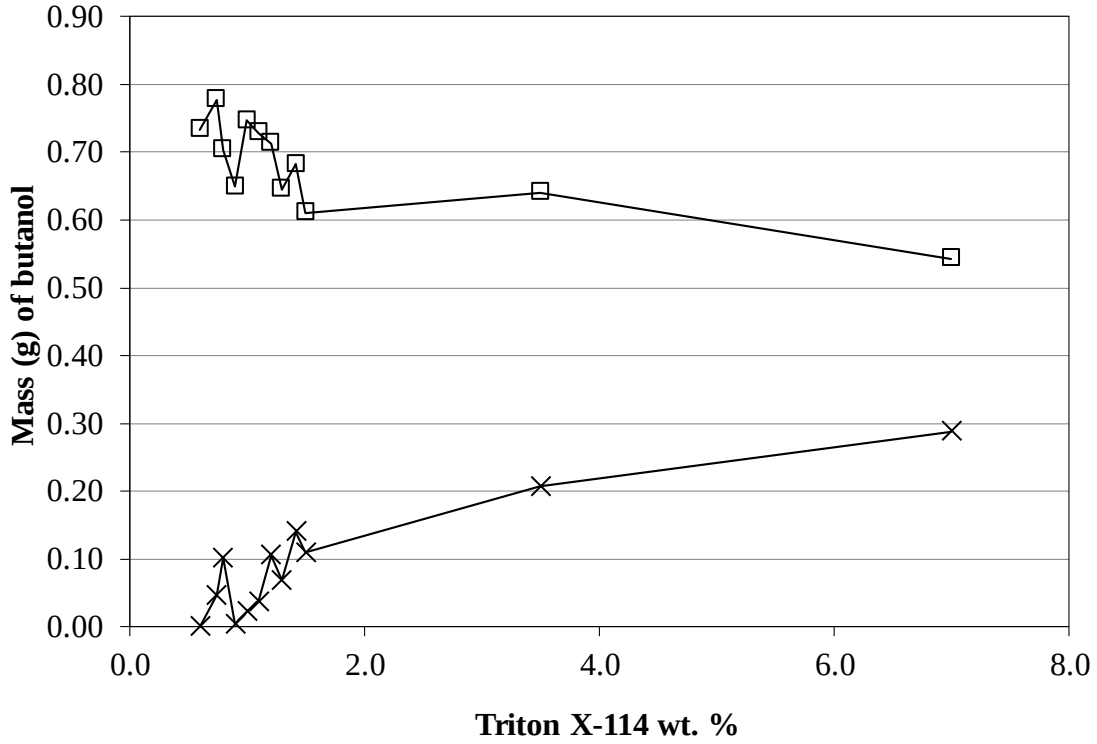

Figure 4.17 Mass of butanol as a function of Triton X-114 wt. %: Butanol (×) in surfactant-rich phaseand Butanol (□) in surfactant-lean phase at a temperature of 37 ^{o}C

4.3 Effect of Triton X-114 Concentration

Effects of Triton X-114 concentrations on fluxes of acetone, butanol, and ethanol were studied. Water and aqueous solutions of 0.7, 0.8, 0.9, 3.5, 7.0, and 10.5 wt. % of Triton X-114 were used as the receiving phase. The experiments were carried out with the receiving side at 37 ^{o}C, which was above the cloud point of the surfactant. Perstraction employing the receiving solution at a temperature below the cloud point of Triton X-114 solution was also done.

The mass of butanol in receiving solution as a function of time at various concentrations of Triton X-114 are shown in Figure 4.18. Although the butanol concentration in the feed container was reduced from 19.2 g/L to 16.6 g/L after 300 min, the mass in the receiving side linearly increased. Swelling and stretching of the membrane was the main reason as the membrane thickness was reduced by about 15 %. The solute flux was obtained by dividing the slope of straight line of the graph by the effective membrane area. Butanol fluxes calculated from the plots are presented in Figure 4.19. The highest butanol flux was obtained from the experiment using 0.8 wt. % Triton X-114 as the receiving solution. It was 388.6 g/(m^2.h). The relationship between butanol flux and Triton X-114 concentration was corresponding to that of distribution coefficient and Triton X-114 concentration reported in the previous section. There was an optimum surfactant concentration of 0.8 wt. %.

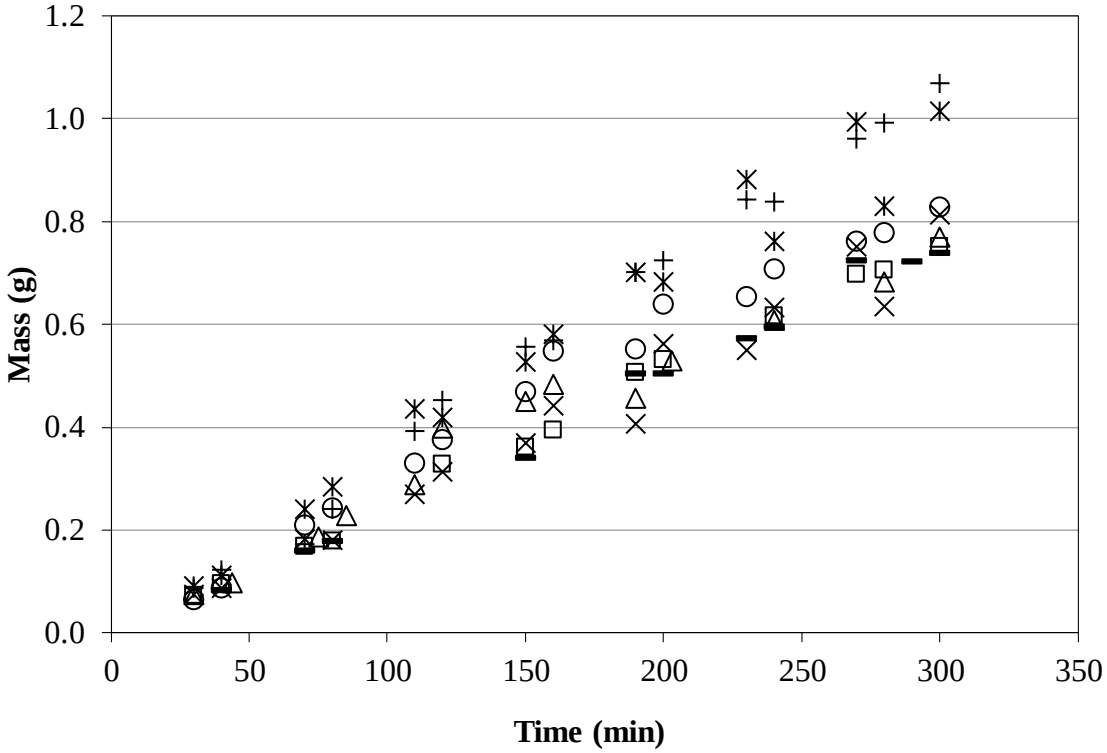

Figure 4.18 Mass of butanol in receiving solutions at various time: Water as the receiving solution (□), 0.7 wt. % Triton X-114 as the receiving solution (○), 0.8 wt. % Triton X-114 as the receiving solution (+), 0.9 wt. % Triton X-114 as the receiving solution (∗), 3.5 wt. % Triton X-114 as the receiving solution (×), 7 wt. % Triton X-114 as the receiving solution (—), 10.5 wt. % Triton X 114 as the receiving solution (Δ)

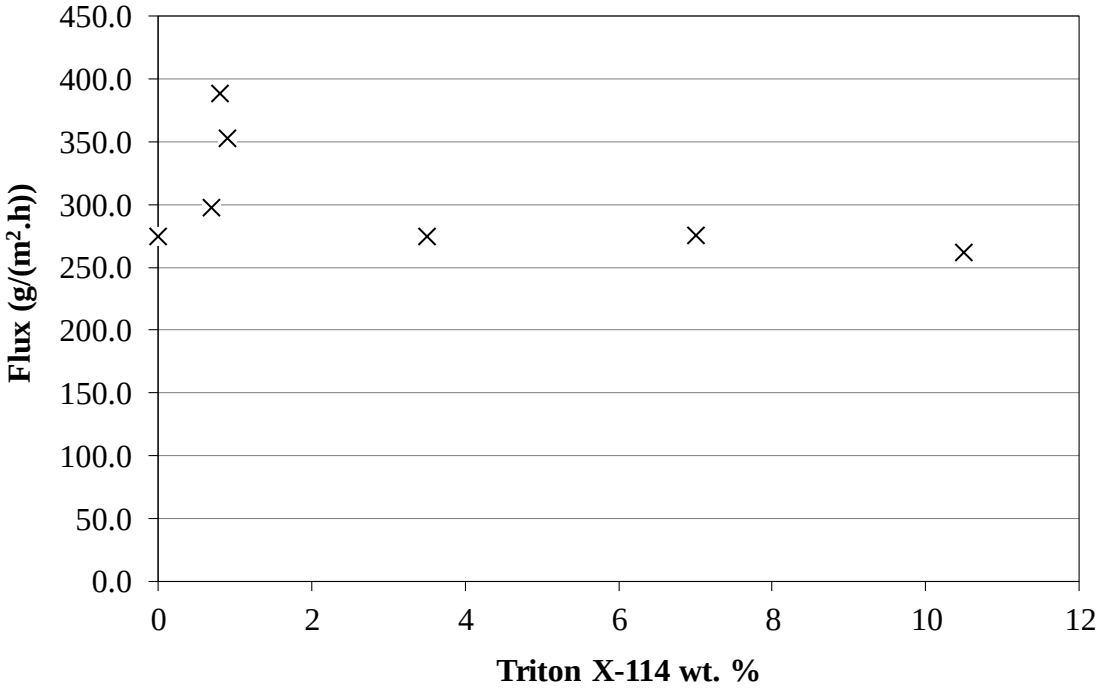

Figure 4.19 Flux of butanol as a function of Triton X-114 wt. % from perstraction using ABE solution as a feed

It was highly probable that micelle-micelle interactions played an important role in the perstraction. The flux enhancement was observed when the concentrations of Triton X-114 were lower than 1 wt. %. At a low concentration of Triton X-114, the solubility of surfactant in water was high because micelles attached some water molecules by their oxyethylene groups. High miscibility of the surfactant in water because of low micelle-micelle interactions and small micelle clusters allowed butanol to be easily dissolved into the surfactant-rich phase. Therefore, the solubilization of butanol in a receiving solution was increased. By contrast, when Triton X-114 concentrations were increased to 3.5 wt. % and higher, fluxes of butanol were approximately the same as those without the presence of the surfactant in the receiving phase. As pointed out by Arunagiri et al. [35], the micelle-micelle interactions increased with the surfactant concentration. This was because, at a high concentration of the surfactant, the micelles were dehydrated, forming larger clusters, and less miscible in water. These clusters imposed high resistance to the solubilization of butanol. Nevertheless, the butanol flux obtained from using 0.7 wt. % Triton X-114 was lower when compared with that obtained from 0.8 wt. % Triton X-114 because of the inadequacy of micelles.

The effect of Triton X-114 concentration on the micellar structure is hypothesized and demonstrated in Figure 4.20. At a low surfactant concentration, the organic solutes were easily dissolved and mixed in the surfactant solution because micelle-micelle interactions were small. Micelles could be distributed in water. However, at a high surfactant concentration, micelle-micelle interactions were strong. Therefore, organic solutes were negligibly transferred into micelles because micelles form large clusters and their solubility in water was reduced.

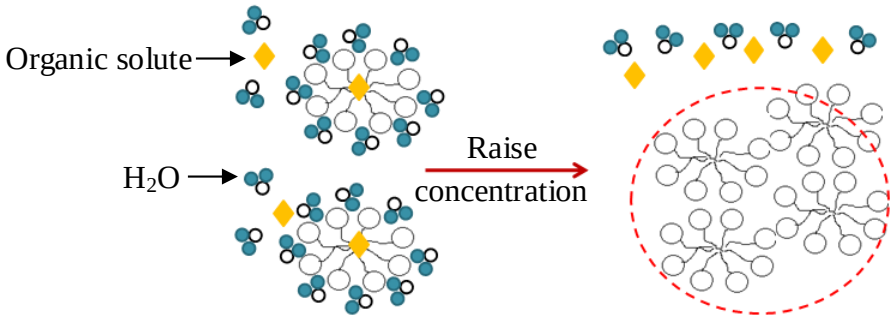

Figure 4.20 Reduction of solubilization due to the formation of micallar cluster

It was possible that large clusters formed at high Triton X-114 concentrations prevented butanol from solubilizing into surfactant-rich phase during perstraction. After 5 h of perstraction, surfactant-rich and surfactant-lean phases were separated by allowing the receiving solution to settle. Analysis of butanol mass in each phase clearly showed that, for the low surfactant concentrations, butanol mainly resided in the surfactant-lean phase as shown in Figure 4.21. Butanol mass in the surfactant-rich phases was approximately 0.2 g, which was about the same as the difference between the mass in the receiving solutions containing low surfactant concentrations and those containing high surfactant concentrations at the 5^{th} h of perstraction. Although mass of butanol in the surfactant-rich phase increased with the increase of the surfactant concentration, the

enhancement of butanol flux was not observed. This implied that butanol was solubilized into the surfactant-rich phase during the settlement of receiving solutions.

There was a strong possibility that the surfactant was also capable of capturing acetone and ethanol. Fluxes of acetone and ethanol as a function of Triton X-114 concentration are shown in Figures 4.22 and 4.23. The maximum fluxes were found from the perstraction using low surfactant concentrations.

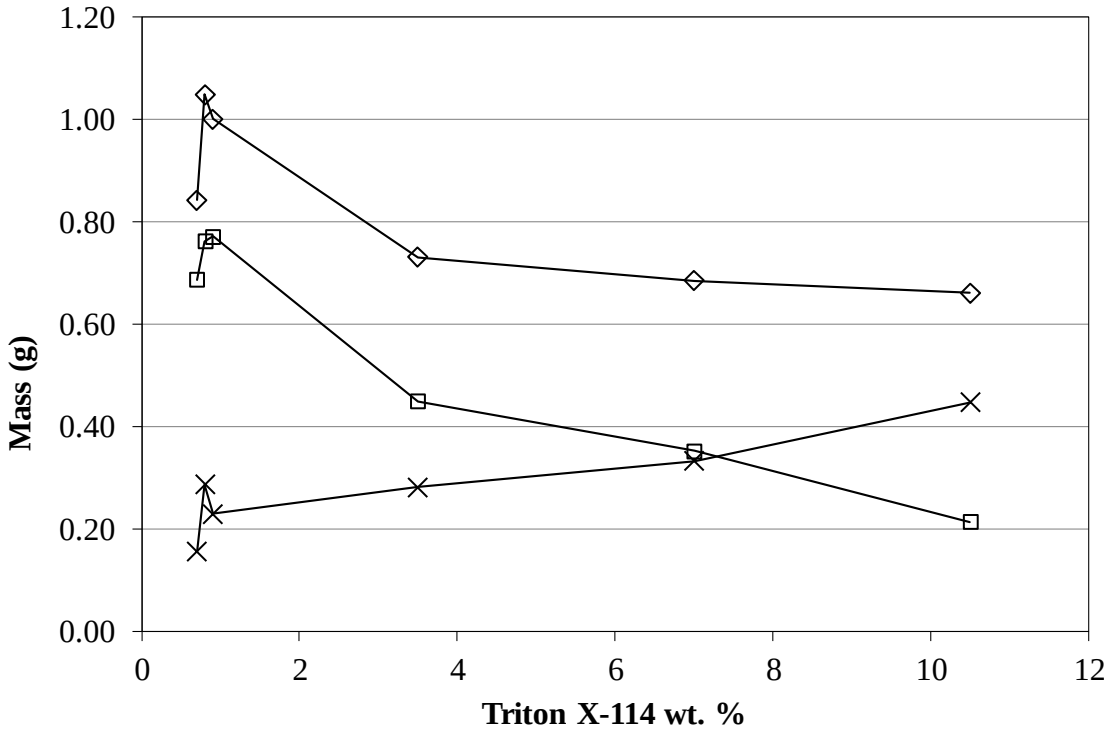

Figure 4.21 Mass of butanol after 5 h of perstraction: in the surfactant-rich phase (×), mass of butanol in the surfactant-lean phase (□), total mass of butanol in the solution (◊)

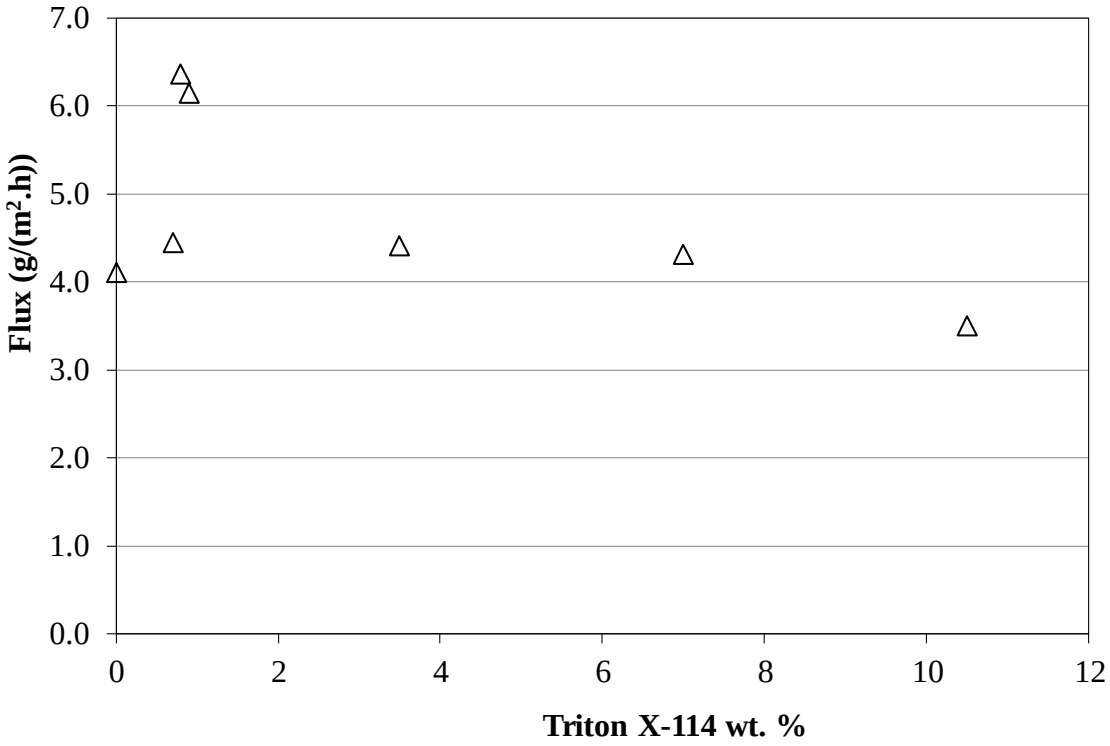

Figure 4.22 Flux of acetone as a function of Triton X-114 wt. % from perstraction using ABE solution as a feed

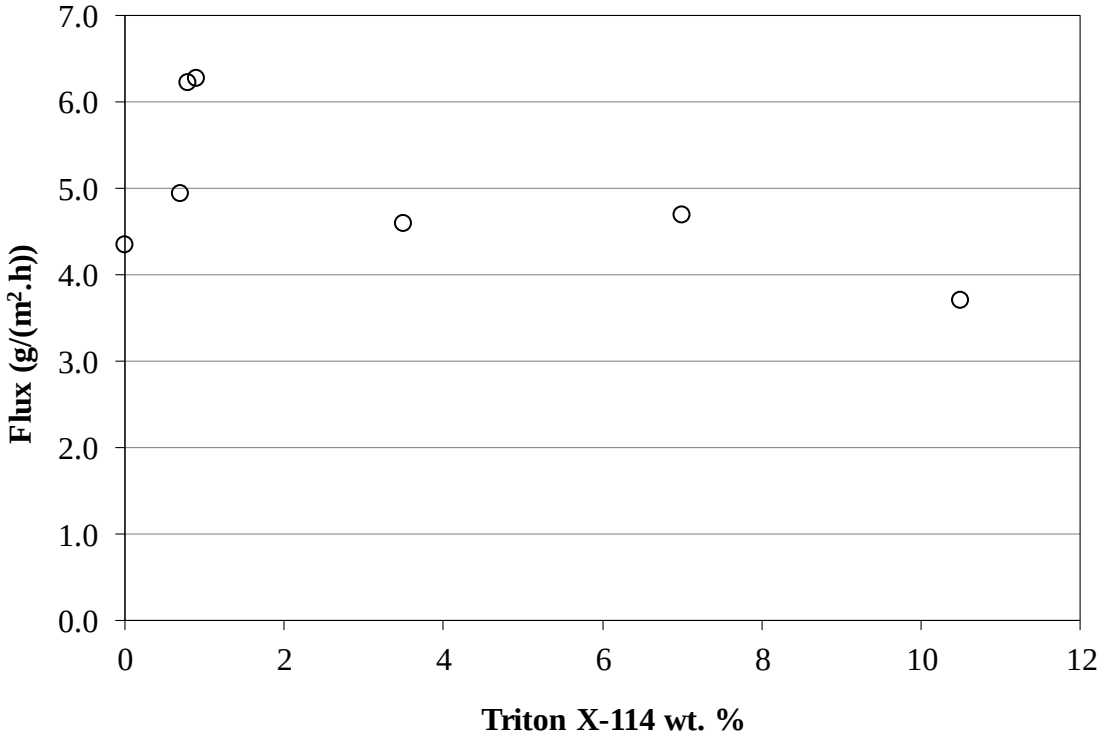

Figure 4.23 Flux of ethanol as a function of Triton X-114 wt. % from perstraction using ABE solution as a feed

The distribution coefficients obtained after 5 h of perstraction related to Triton X-114 concentrations in the same way that was found from the experiments carried out by the direct mixing of ABE and the surfactant. The distribution coefficient of butanol as a function of Triton X-114 concentration is shown in Figure 4.24. The highest distribution coefficient of butanol was 27.7, which was obtained when 0.8 wt. % Triton X-114 solution was used as a receiving solution. The coefficient decreased when a higher concentration of surfactant was used. The results implied that the ability of the surfactant to enhance butanol flux was related to the solubilization of butanol in a surfactant-rich phase. The concentration of butanol in the surfactant-rich phase was 143.3 g/L when a 0.8 wt. % Triton X-114 solution was used as a receiving phase. The butanol concentrations decreased to 11.3 - 5.3 g/L as the surfactant concentrations were increased to 3.5 - 10.5 wt. %. In contrast, butanol concentrations in the surfactant-lean phases did not significantly decreased, ranging from 3.40 to 2.96 g/L, suggesting that the distribution coefficient was controlled by the ability of butanol to dissolve into the surfactant-rich phase.

The distribution coefficients of butanol determined after five hours of perstraction using 0.7 to 0.9 wt. % Triton X-114 were higher than those observed in section 4.2. This was because butanol could be transferred into micelles by vigorous stirring during perstraction. However, at the high surfactant concentrations, the distribution coefficients of butanol were still low due to the high resistance caused by strong micelle-micelle interactions.

It was worth pointing out that the higher butanol recovery could be achieved with the use of a high Triton X-114 concentration. However, it had two main drawbacks. First, the flux or recovery rate would be low. Second, the energy required to separate butanol from the surfactant would be high due to a low capturing capacity as shown in Figure 4.25.

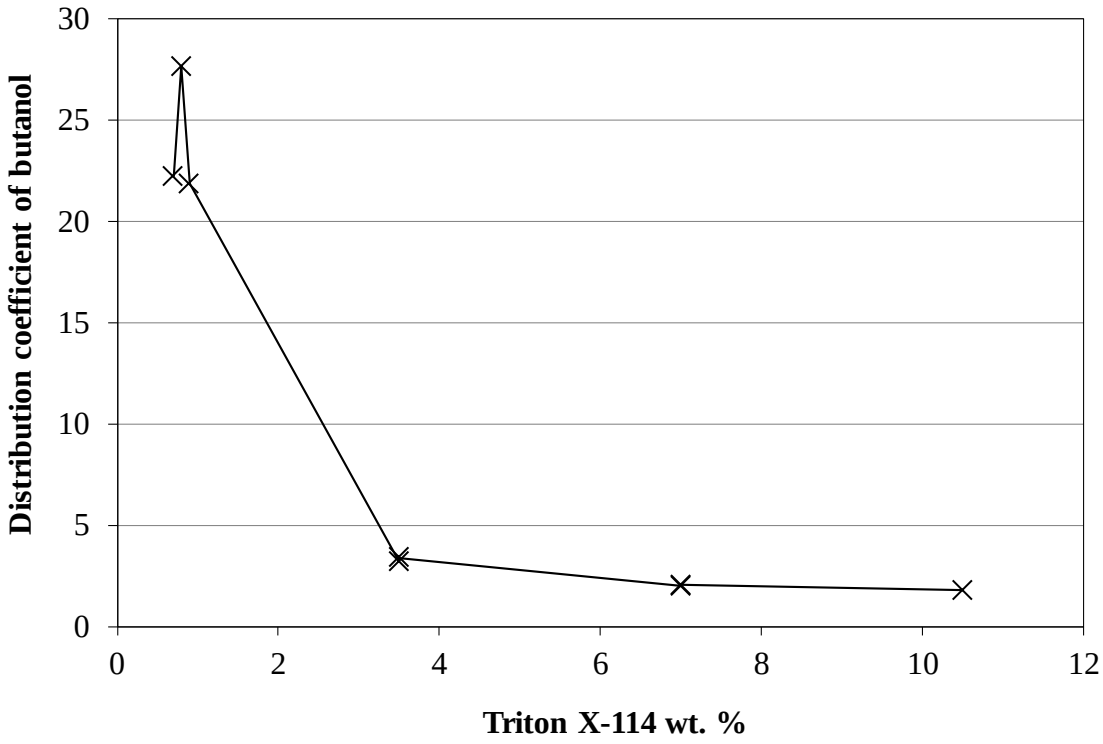

Figure 4.24 Distribution coefficient of butanol after 5 h of perstraction

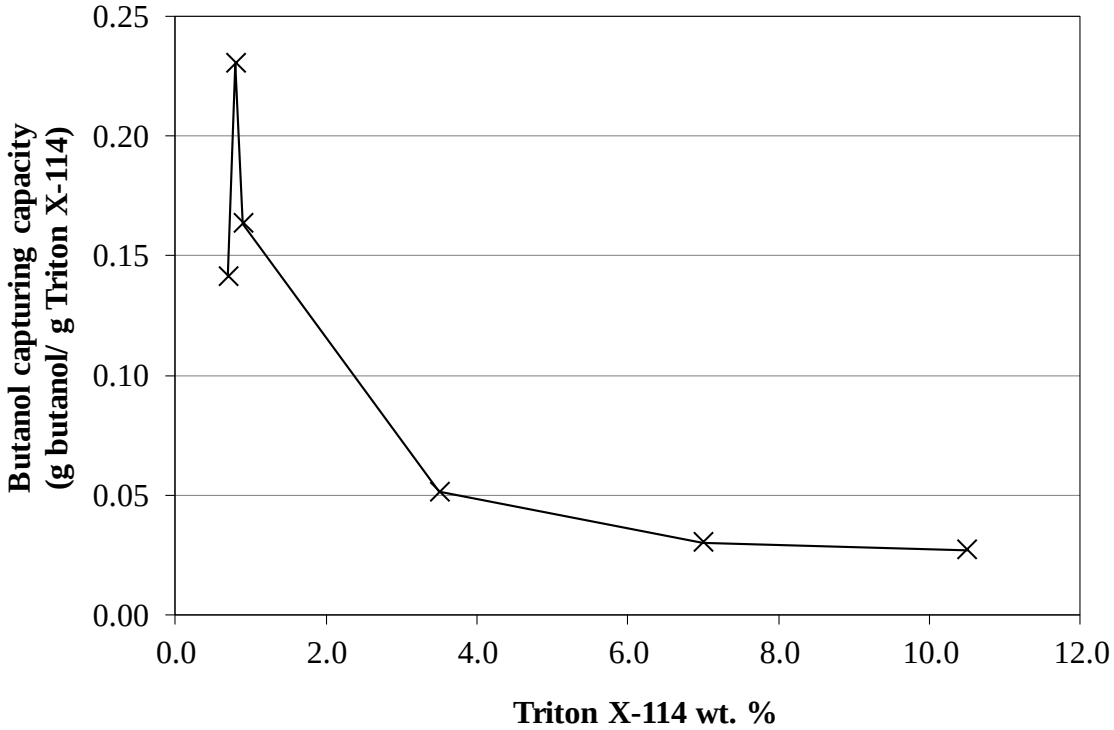

Figure 4.25 Capturing capacity of butanol after 5 h of perstraction

The distribution coefficients of acetone and ethanol were also at maximums at the low Triton X-114 concentrations as shown in Figures 4.26 and 4.27. Increase in the surfactant concentration caused the coefficients to drop.

The maximum distribution coefficient of butanol was similar to those of acetone and ethanol. This was possibly because the surfactant micelles could be fully saturated with the solutes. As the mass of butanol in the receiving solution was much higher than those of acetone and ethanol, the excess butanol was not entrapped by the saturated micelles.

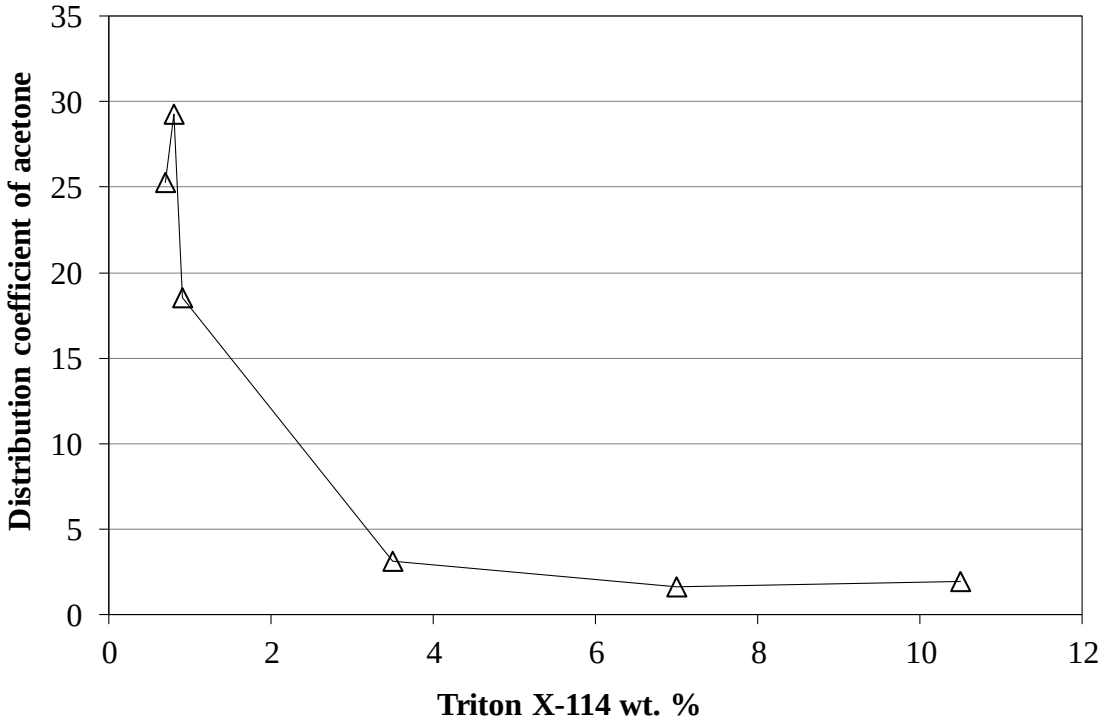

Figure 4.26 Distribution coefficient of acetone after 5 h of perstraction

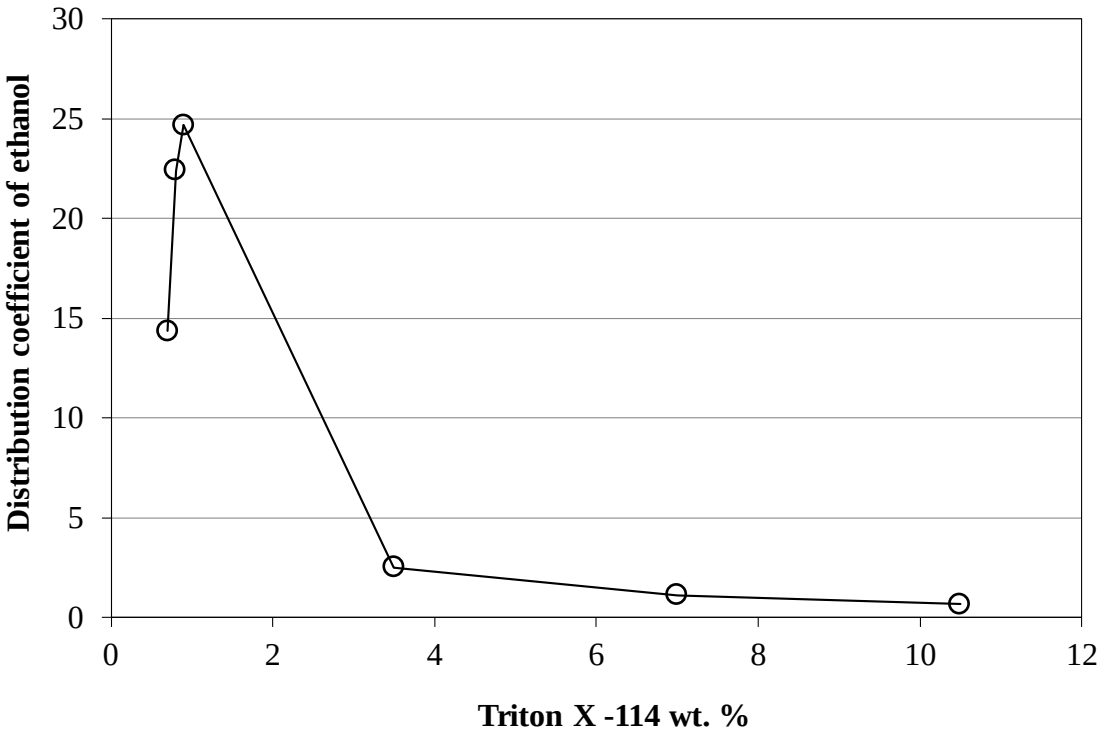

Figure 4.27 Distribution coefficient of ethanol after 5 h of perstraction

4.4 Perstraction using Receiving Solution below the Cloud Point of Triton X-114

To investigate whether the formation of clusters and consequential water-surfactant phase separation was a possible cause of the ineffectiveness of surfactant, an experiment was performed using a receiving side temperature of 6 ^{o}C. By reducing the temperature below the cloud point of surfactant, the 3.5 wt. % Triton X-114 solutions was homogenous and clear. Mass of butanol in the receiving solution containing the surfactant was significantly higher than that in the pure water as shown in Figure 4.28. Butanol flux was 95.3 g/(m^2.h) in the presence of surfactant and was only 11.9 g/(m^2.h) when pure water was used in the receiving side. Flux of butanol was enhanced by Triton X-114 because butanol solubilization was increased by a small micellar size and the higher solubility of surfactant in water [37]. These findings suggested that the phase separation at a temperature above the cloud point could be the cause of the negligible flux enhancement by the surfactant.

Although the presence of Triton X-114 could increase the permeation rate of butanol through the membrane, operation at the low temperature caused a negative effect on the magnitude of flux. Furthermore, use of the low temperature receiving solution would require more energy compared to the butanol recovery at temperature of 37 ^{o}C.

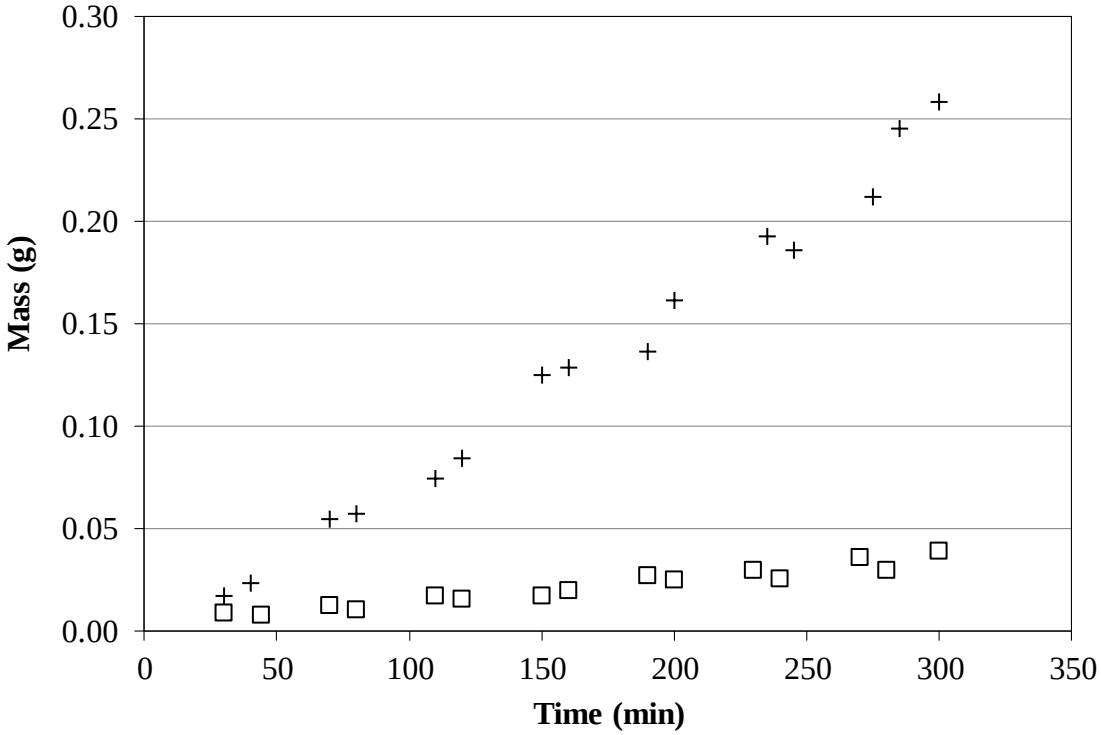

Figure 4.28 Mass of butanol in 6 ^{o}C receiving solutions as a function of time: Water as the receiving solution (□), 3.5 wt. % Triton X 114 as the receiving solution (+).

4.5 Perstraction of Single-Component Feed

Experiments were carried out using a dense PEBA membrane. Concentrations of acetone, butanol, and ethanol in feed were 1, 19.2, and 1.7 g/L respectively. A receiving phase was 3.5 wt. % Triton X-114 at 37 ^{o}C. Relationships between mass of butanol, acetone, and ethanol as a function of time are presented by Figures 4.29, 4.30, and 4.31, respectively. Butanol, acetone, and ethanol fluxes obtained from single-component feeds were 247.6, 1.9, and 2.7 g/(m^2.h), respectively. They all were lower than those of the synthetic fermentation broth feed, 274.3, 4.4, and 4.6 g/(m^2.h), for butanol, acetone, and ethanol, respectively. The membrane gave the higher fluxes because it was more swollen by the feed.

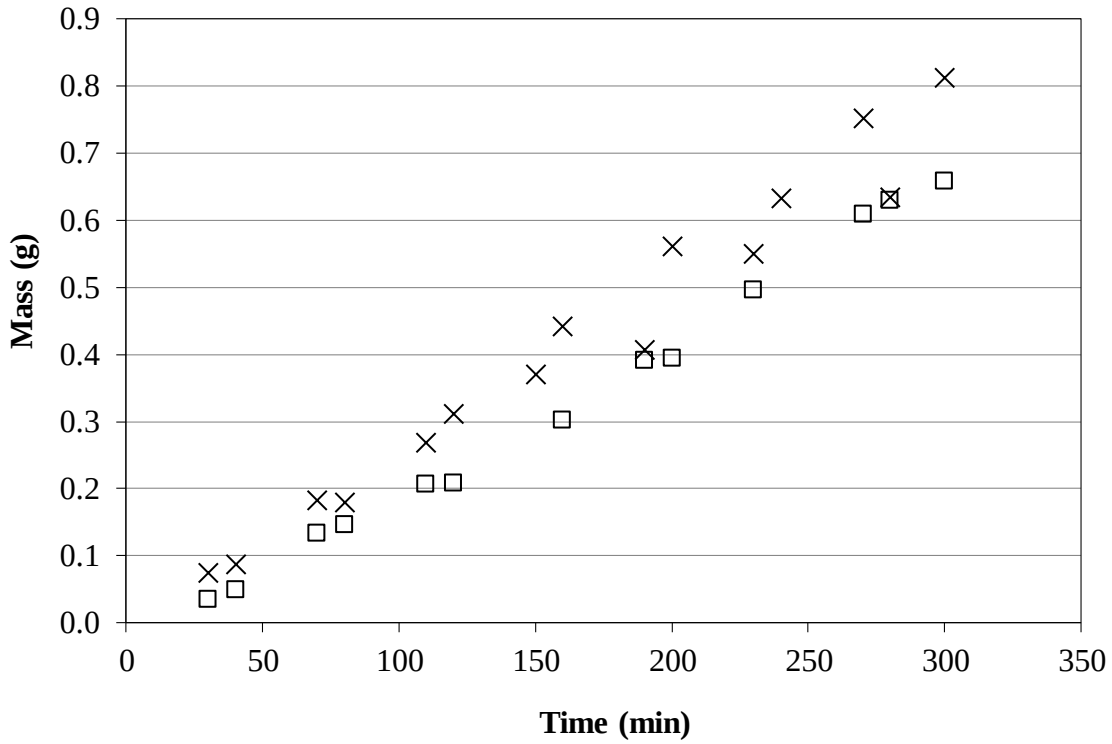

Figure 4.29 Butanol mass as a function of time: 19.2 g/L butanol feed (□), ABE feed (×)

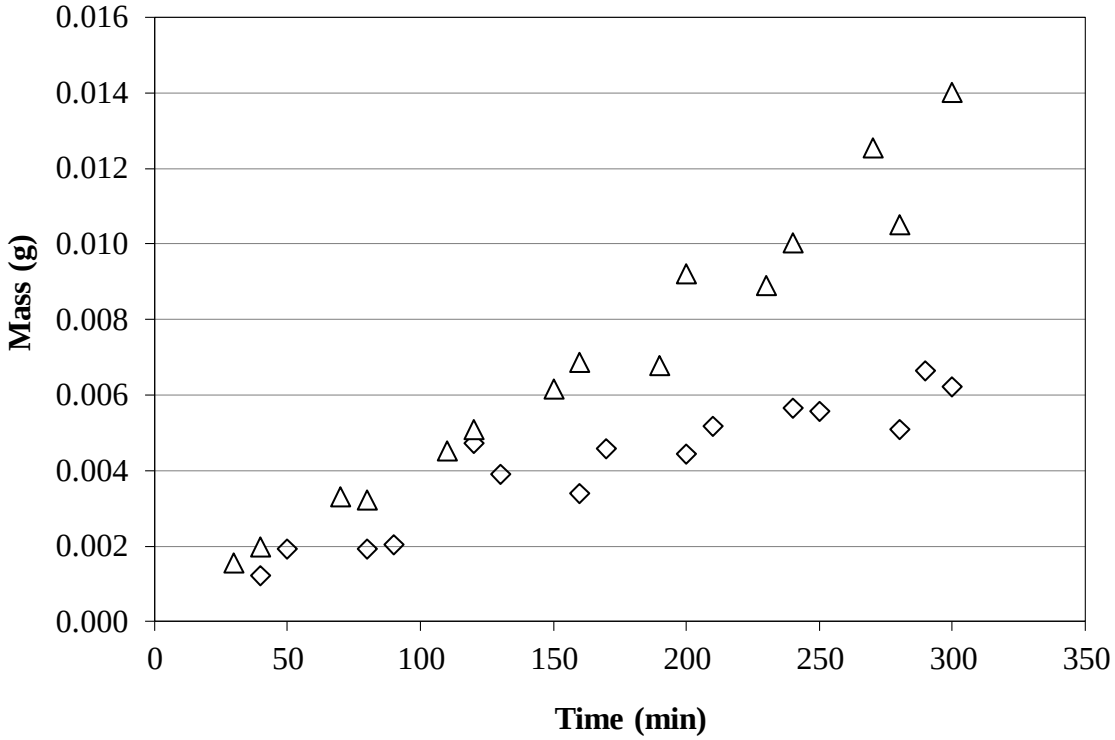

Figure 4.30 Acetone mass as a function of time: 1 g/L acetone feed (◊), ABE feed (△)

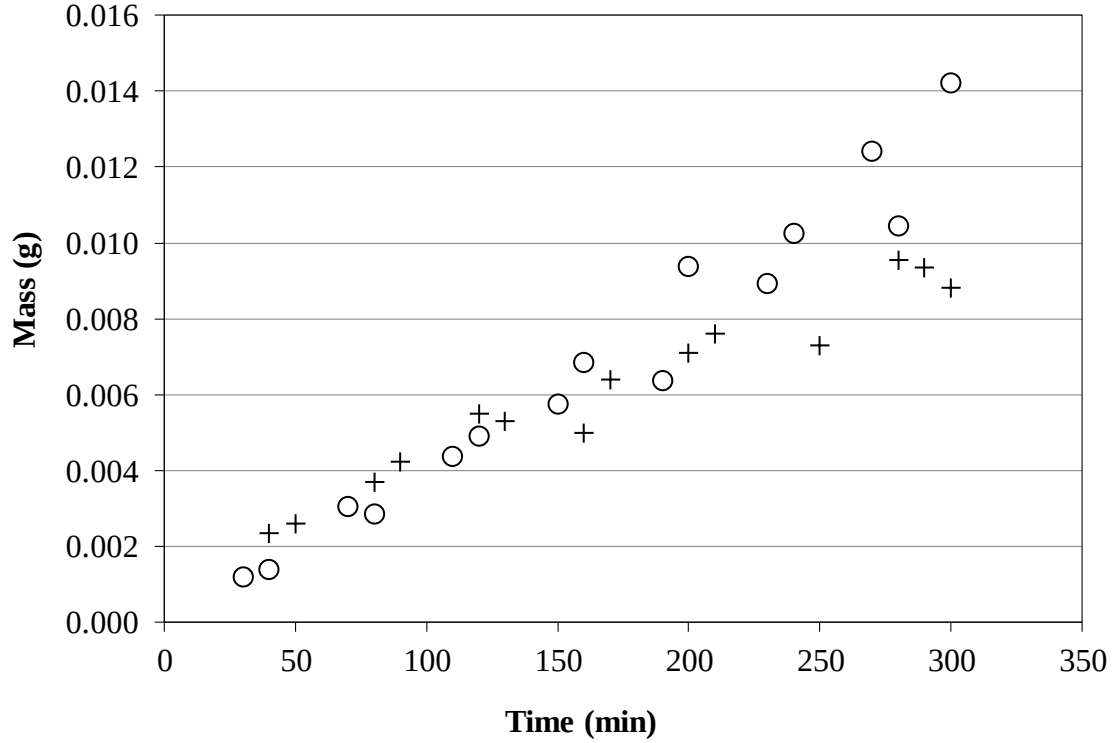

Figure 4.31 Ethanol mass as a function of time: 1.7 g/L ethanol feed (+), ABE feed (○)

4.6 Effect of initial butanol concentration in receiving phase

In a batch operation, concentration of butanol in a receiving solution would be accumulated with time. Experiments were done to observe the effect of butanol concentration in a receiving solution on fluxes. Initial concentrations of butanol in the receiving phases were 6 and 12 g/L. A feed of all experiments was an aqueous solution of 1, 19.2, 1.7 (g/L) of acetone, butanol, and ethanol, respectively.

Figure 4.32 indicates that after a long period of perstraction, butanol flux would be decreased linearly with the accumulated concentration. For example, for a receiving phase containing 12 g/L of butanol, butanol flux was 70.8 g/(m^2.h), which about 74 % reduction from the flux was obtained when there was no butanol in an initial receiving phase. A simple explanation of the flux decline was the reduction in the driving force or concentration gradient.

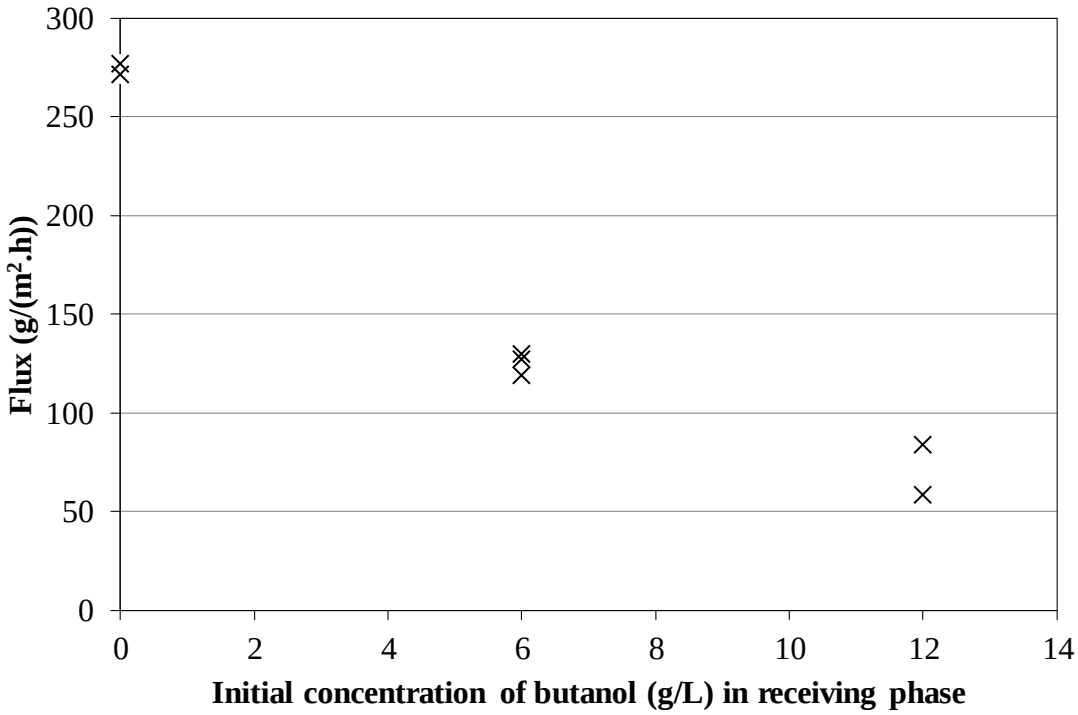

Figure 4.32 Effect of initial butanol concentration in receiving phase on butanol flux

4.7 Perstraction of ABE using asymmetric poly(ether block amide) membrane

The structure of asymmetric PEBA membrane is shown in Figure 4.33 (9-20-3(54.1µm)). It had a porous upper layer and a dense bottom layer. The thicknesses of the porous and dense layers were 35.0 and 19.1 µm. However, these two regions were not distinctly separated, probably because of the inhomogeneity of casting solution.

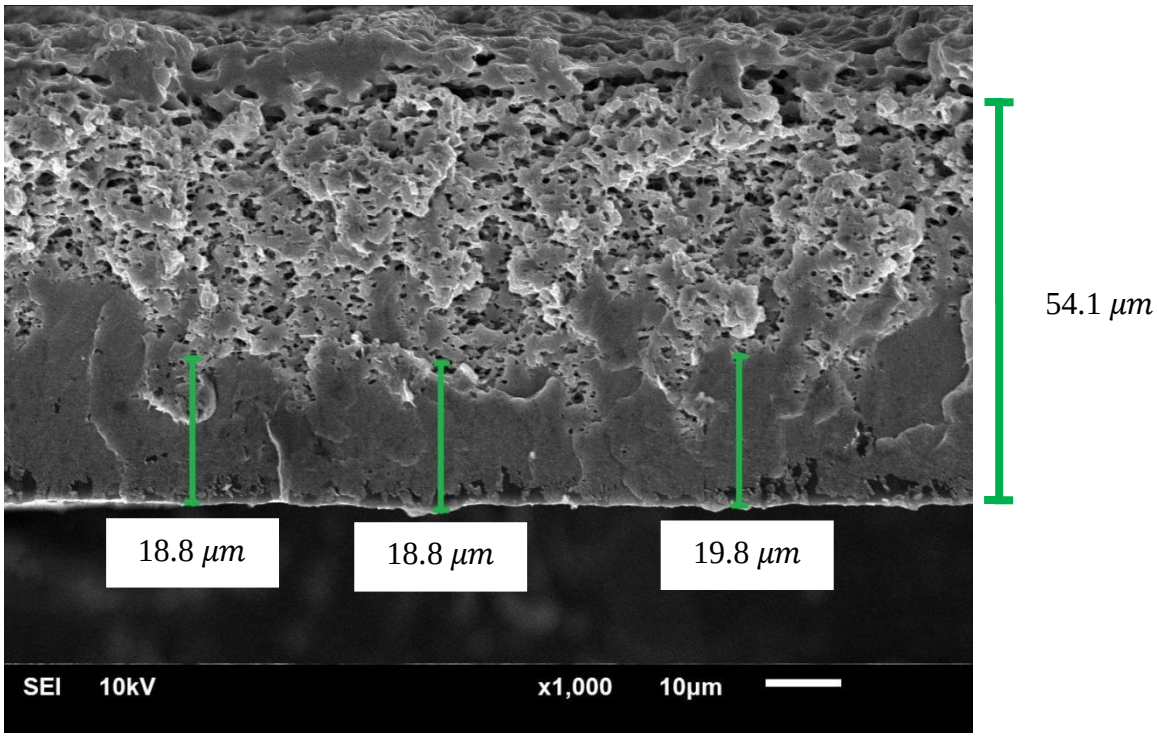

Figure 4.33 Scanning electron micrograph showing a cross section of PEBA membrane using 9 wt. % PEBA – 20 wt % methanol – 71 wt. % butanol as a casting solution and pure methanol as a coagulant

Concentrations of acetone, butanol, and ethanol in a feed were 1, 19.2, and 1.7 g/L, respectively. Pure water at 37 ^{o}C was used a receiving phase. The mass of organic solutes in the receiving solution as a function of time is presented in Figure 4.34. Fluxes of acetone, butanol, and ethanol were 3.4, 193.9, and 3.4 g/(m^2.h). These fluxes were lower than those obtained from a dense film at the same experimental conditions. A plausible explanation was that water was unable to penetrate into the hydrophobic porous layer. This created mass transfer resistance because the solutes had to permeate through the pores.

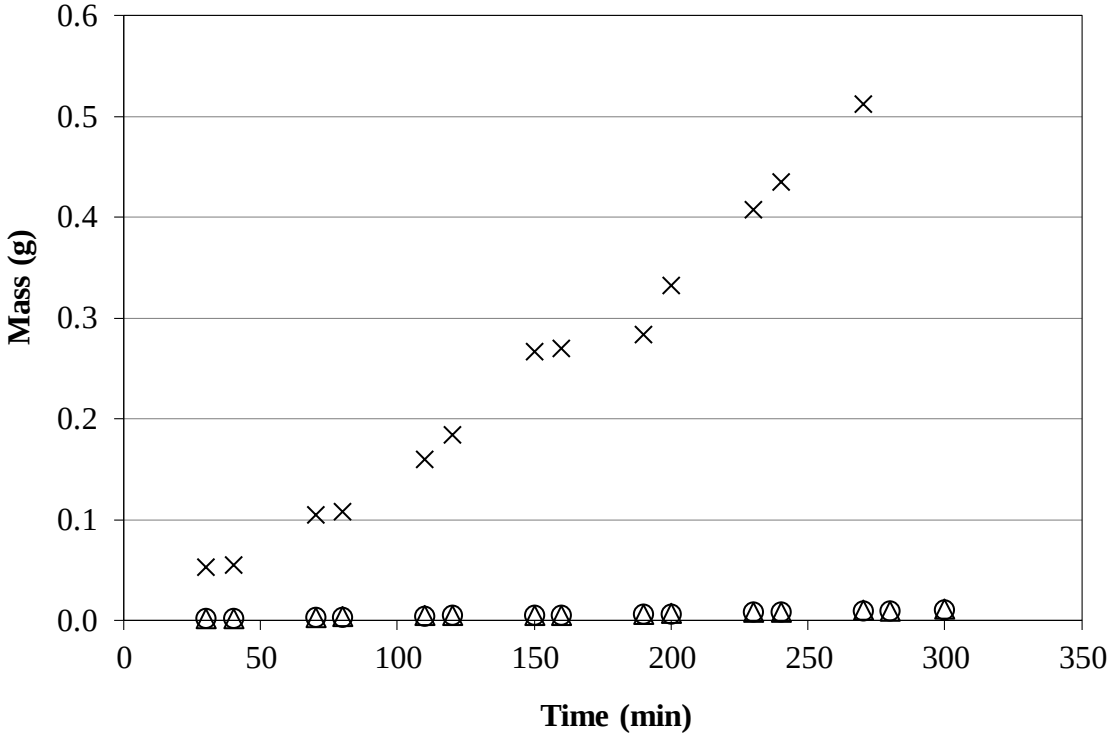

Figure 4.34 Mass of acetone (△), butanol (×), and ethanol (○) as a function time obtained from perstraction using an asymmetric PEBA

It should be noted that, to obtained high purity butanol, the entrapped butanol must be separated from the surfactant-rich phase by using distillation. Acetone, the component having the lowest boiling point is first removed, probably together with ethanol as the top of the first distillation column. Water is then separated from the remaining components by another column. Finally, butanol could be separated from the surfactant by a simple evaporation.

4.8 Pervaporation of ABE through a dense PEBA

Pervaporation experiments were done using a dense PEBA membrane. Thickness of the membrane was 16.5±1.3 μm. Concentrations of acetone, butanol, and ethanol in feed were 1, 19.2, and 1.7 g/L, respectively. The experiments were carried out with a temperature of feed at 37 ^{o}C.

Fluxes of butanol, acetone, ethanol and water calculated from Figures 4.35 to 4.38 were 9.7, 0.061, 0.33, and 77.0 g/(m^2.h). Water flux obtained from pure water feed was 79.5 g/(m^2.h). The organic fluxes were much lower than those of perstraction because water was also able to permeate through the membrane. Due to a very high water concentration in the feed, free volume of the membrane was mainly occupied by water. Despite the lower fluxes, ABE concentrations in permeate were much higher than those in a receiving phase of perstraction. Nonetheless, to prevent butanol toxicity to culture, a high flux was more favorable.

The membrane was selective to the organic solutes in the order of butanol>ethanol> water>acetone. Separation factors of organic solutes relative to water were 0.77, 2.4, and 6.3 of butanol, ethanol, and acetone, respectively. This was because the membrane was hydrophobic. Because of the preferential permeation of ethanol and butanol, the concentrations of butanol and ethanol in the permeate were higher than those in the feed although fluxes of ethanol and butanol were lower than the water flux. The separation factor of acetone was lower than 1 because molecular size of acetone, 0.469 nm, was larger than water molecular size, 0.296 nm [38].

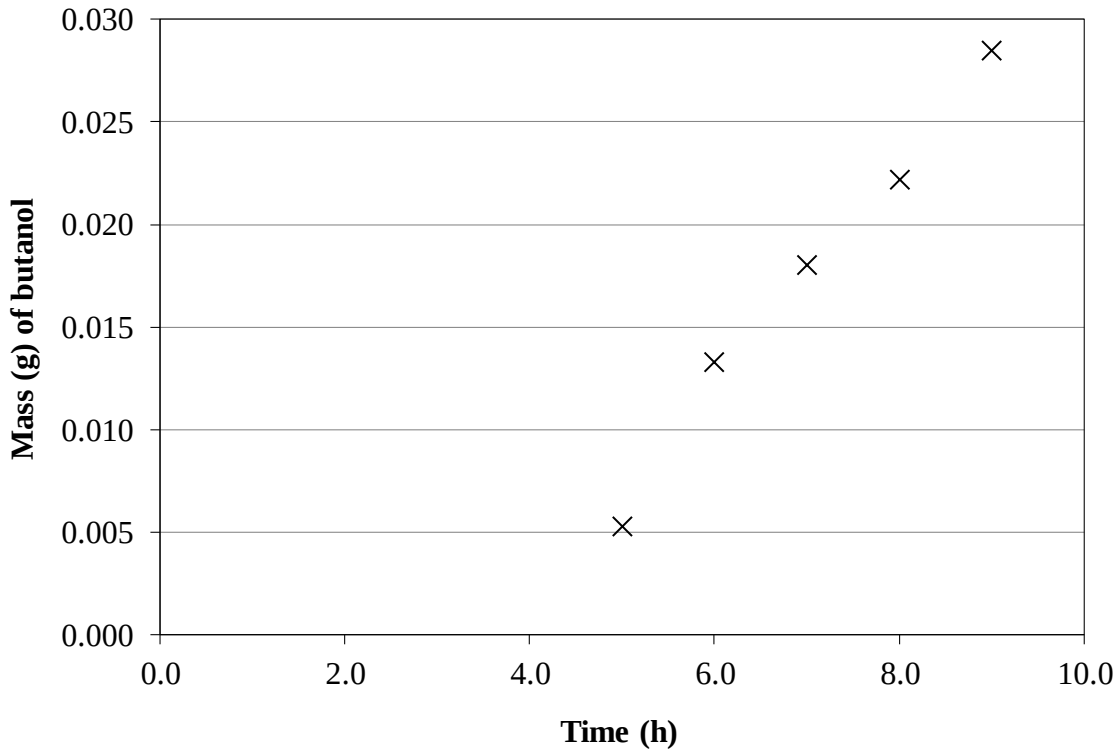

Figure 4.35 Mass of butanol as a function of time obtained from pervaporation of ABE

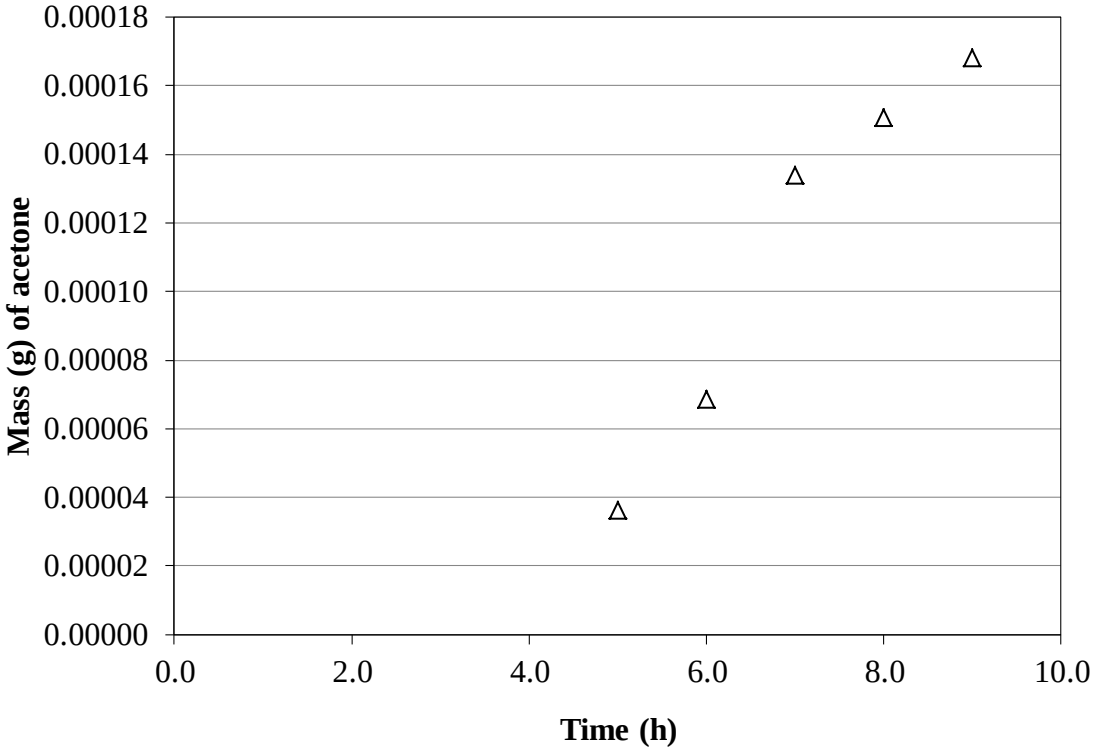

Figure 4.36 Mass of acetone as a function of time obtained from pervaporation of ABE

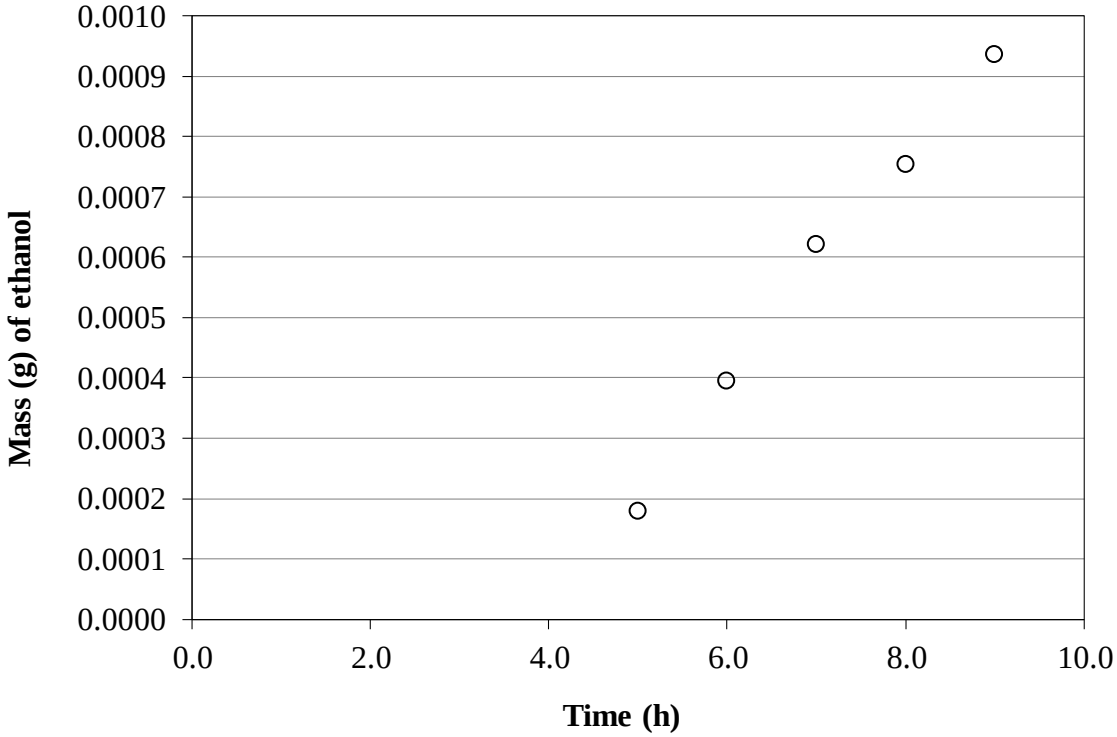

Figure 4.37 Mass of ethanol as a function of time obtained from pervaporation of ABE

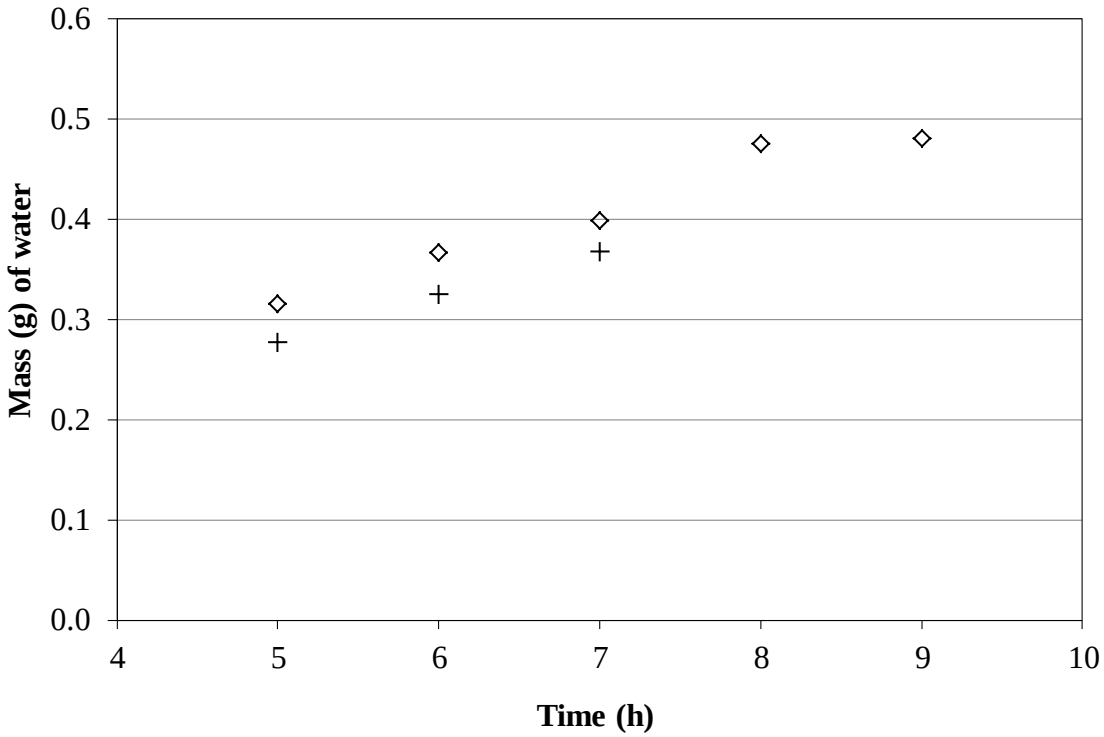

Figure 4.38 Mass of water as a function of time obtained from pervaporation of ABE: ABE feed (◊) and water feed (+)

CHAPTER 5 CONCLUSIONS AND RECOMMENDATIONS

5.1 Conclusions

The formation of asymmetric poly(ether block amide), PEBA, membranes was influenced by initial compositions of casting solution, and coagulation time. A high PEBA concentration in a casting solution generally produced a dense membrane whereas a low polymer concentration produced a totally porous membrane. Increase of coagulation time resulted in a membrane with greater porosity. Nevertheless, for a high polymer concentration, the portion of film close to the glass surface had less porosity. Addition of methanol into an initial casting solution generated films with a thicker dense layer, possibly due to partial immiscibility between the dissolved polymer and the solvent-non-solvent phases. It suggested that, the membrane having high porosity in an upper layer and a dense layer could be produced from a casting solution containing a low polymer concentration and short a coagulation time.

The increase of the organic solutes in the perstraction was done by the increase of solubility in the receiving phase. The highest butanol flux of 388.6 g/(m^2.h) was obtained from the use of 0.8 wt. % Triton X-114 solution. At higher concentrations of the surfactant, 3.5 to 10.5 wt. %, the butanol fluxes were comparable to the flux obtained from the perstraction using water as a receiving solution. This was because the micelle-micelle interaction increased with the surfactant concentration. On the contrary, at a temperature below the cloud point, organic flux enhancement was observed even in the presence of 3.5 wt. % Triton X-114 in the receiving solution. This phenomenon was supported by the increase of organic solubility in the surfactant because of the decrease in micellar size. By using 6 and 12 g butanol per liter as the initial receiving solutions, butanol flux decreased by 54.4 and 74.1 %, respectively. Finally, the organic fluxes from pervaporation were lower than those from perstraction. This was an advantage of perstraction because butanol concentration in fermentation broth could be reduced at a higher rate.

5.2 Recommendations

1. As it was found in this work that the increase of Triton X-114 concentration retarded the mass transfer of butanol from water into micelles. Although an operating temperature of 6 ^{o}C resolved the mass transfer resistance, the permeation flux of butanol through the membrane was must lower than that obtained at 37 ^{o}C. Therefore, the operating temperature should be only slightly less than the cloud point of Triton X-114, 25 ^{o}C. In addition, the prevention of mass transfer resistance could also be achieved at a relatively higher temperature by using other surfactants. The surfactants have a cloud point temperature of slightly higher than 37 ^{o}C.

2. Due to a high boiling point of Triton X-114, it stuck to a GC column. Therefore, in order to remove the surfactant, butanol should be injected into the column that was not connected to a detector, while using a low flow rate of carrier gas. In addition, the column temperature should be high.

REFERENCES

1. Demirbas, A., 2008, "Biofuels Sources, Biofuel Policy, Biofuel Economy and Global Biofuel Projections", **Energy Conversion and Management**, Vol. 49, No. 8, pp. 2106–2116.

2. Qureshi, N. and Ezeji, T.C., 2008, "Butanol, 'a superior biofuel' Production from Agricultural Residues (Renewable Biomass): Recent Progress in Technology. Biofuels", **Bioproducts and Biorefining**, Vol. 2, No. 4, pp. 319-330.

3. Ranjan, A. and Moholkar, V.S., 2012, "Biobutanol: Science, Engineering, and Economics", **International Journal of Energy Research**, Vol. 36, No. 3, pp. 277-324.

4. Abdehagh, N., Tezel, F.H. and Thibault, J., 2014, "Separation Techniques in Butanol Production: Challenges and Developments", **Biomass and Bioenergy**, Vol. 60, pp. 222-246.

5. Oudshoorn, A., van der Wielen, L.A.M. and Straathof, A.J.J., 2009, "Assessment of Options for Selective 1-Butanol Recovery from Aqueous Solution", **Industrial and Engineering Chemistry Research**, Vol. 48, No. 15, pp. 7325–7336.

6. Qureshi, N., Maddox, I.S. and Friedlt, A., 1992, "Application of Continuous Substrate Feeding to the ABE Fermentation: Relief of Product Inhibition Using Extraction, Perstraction, Stripping, and Pervaporation", **Biotechnology Progress**, Vol. 8, No. 5, pp. 382-390.

7. Liu, F., Liu, L. and Feng, X., 2005, "Separation of acetone–butanol–ethanol (ABE) from dilute aqueous solutions by pervaporation", **Separation and Purification Technology**, Vol. 42, No. 3, pp. 273–282.

8. Qureshi, N. and Maddox, I.S., 2005, "Reduction in Butanol Inhibition by Perstraction: Utilization of Concentrated Lactose/Whey Permeate by *Clostridium acetobutylicum* to Enhance Butanol Fermentation Economics", **Food and Bioproducts Processing**, Vol. 83, pp. 43-52.

9. Kraemer, K., Harwardt, A., Bronneberg, R. and Marquardt, W., 2010, "Separation of Butanol from Acetone-Butanol-Ethanol Fermentation by a Hybrid Extraction-Distillation Process", **Proceedings 20th European Symposium on Computer Aided Process Engineering – ESCAPE20**, Ischia, Naples, pp. 7-12.

10. Dhamole, P.B., Wang, Z., Liu, Y., Wang, B. and Feng, H., 2012, "Extractive Fermentation with Non-ionic Surfactants to Enhance Butanol Production", **Biomass and Bioenergy**, Vol. 40, pp. 112-119.

11. Fouad, E.A. and Feng, X., 2008, "Use of pervaporation to separate butanol from dilute aqueous solutions: Effects of operating conditions and concentration polarization", **Journal of Membrane Science**, Vol. 323, pp. 428–435.

12. Eustache, R.-P., 2006, "Poly(ether-b-amide) thermoplastic elastomers: structure, properties and applications", in: Fakirov, S., Editor, **Handbook of Condensation Thermoplastic Elastomers**, Wiley-VCH, (Chapter 10).

13. Boddeker, K.W., Bengtson, G. and Pingel, H., 1990, "Pervaporation of isomeric butanols", **Journal of Membrane Science**, Vol. 54, pp. 1–12.

14. Baker, R.W., 2012, "Membrane technology and application", 3rd ed., John Wiley and Sons Ltd, West Sussex, pp. 112-116.

15. Strathmann, H. and Kock, K., 1977, "The formation of mechanism of phase inversion membranes", **Desalination**, Vol. 21, pp. 241- 255.

16. Strathmann, H., Scheible, P. and Baker, R.W., 1971, "A rationale for the preparation of Loeb-Sourirajan-type cellulose acetate membranes", **Journal of** A**pplied Polymer Science**, Vol. 15, pp. 811-828.

17. Qi, Z. and Cussler, E.L., 1985, "Microporous hollow fibers for gas absorption: I. Mass transfer in the liquid", **Journal of Membrane Science**, Vol. 23, p. 321.

18. Gabelman, A. and Hwang, S.T., 1999, "Hollow fiber membrane contactors", **Journal of Membrane Science**, Vol. 159, p. 61.

19. Heerema, L., Wierckx, N., Roelands, M., Henk Hanemaaijer, J., Goetheer, E. Verdoes, D. and Keurentjes, J., 2011, "In situ phenol removal from fed-batch fermentations of solvent tolerant *Pseudomonas putida* S12 by pertraction", **Biochemical Engineering Journal**, Vol.53, pp. 245–252.

20. Abedini, R. and Nezhadmoghadam, A., 2010, "Application of membrane in gas separation processes: Its suitability and mechanisms", **Petroleum and Coal**, Vol. 52, No. 2, pp. 69-80.

21. Hiemenz, P.C. and Rajagopalan, R.H., 1997, "Principles of colloid and surface chemistry", 3rd ed., New York: Marcel Dekker, Inc., p. 377.

22. Sigma-Aldrich, “Triton X product information”, 3050 spruce street, St. Louis, MO 63103 USA.

23. Qureshi, N. and Blaschek, H.P., 2001, “Evaluation of recent advances in butanol fermentation”, upstream and downstream processing, **Bioprocess and Biosystems Engineering**, Vol. 24, No. 4, pp. 219-226.

24. Awang, G.M., Jones, G.A. and Ingledew, W.M., 1988, “The acetone-butanol-ethanol fermentation”, **Critical Reviews in Microbiology**, Vol. 15, No. 1, pp. 33-67.

25. Moreira, A.R., Ulmer, D.C. and Linden, J.C., 1981, “Butanol toxicity in the butylic fermentation”. **Third Symposium on Biotechnology in energy production and Conservation: proceedings**, Gatlinburg, Tenn., May 12-15, New York (USA), Wiley, pp. 567-579.

26. Kuhn, H. and Linden, J.C., 1986, “Effects of temperature and membrane fatty acid composition on butanol tolerance of *Clostridium acetobutylicum*”, In: Scott, C.D., editor, **Biotechnology and bioengineering symposium**. Proceedings of the 8th symposium on biotechnology for fuels and chemicals, May, Gatlinburg, TN, New York (USA), John Wiley and Sons, pp. 197-207.

27. Baer, S.H., Bryant, D.L. and Blaschek, H.P., 1989, “Electron spin resonance analysis of the effect of butanol on the membrane fluidity of intact cells of *Clostridium acetobutylicum*”, **Applied and Environmental Microbiology**, Vol. 55, No. 10, pp. 2729-2731.

28. Darcovich, K. and Kutowy, O., 1988, “Surface Tension Considerations for Membrane Casting Systems”, **Journal of Applied Polymer Science**, Vol. 35, pp. 1769-1778.

29. Tanny, G.B., 1974, **Journal of Applied Polymer Science**, Vol. 18, pp. 2149-2163.

30. Bloch, R and Frommer, M.A., 1970, “The mechanism for formation of “skinned” membranes I. Structure and properties of membranes cast from binary solutions”, **Desalination**, Vol. 7, No. 2, pp. 259-264.

31. Galera-Gomez, P.A. and Gu, T., 1995, “Clouding of Triton X- 114: The effect of added electrolytes on the cloud point of Triton X- 114 in the presence of ionic surfactants”, **Colloids and Surfaces A**: **Physicochemical and Engineering Aspects**, Vol. 104, pp. 307-312.

32. Hansen, C.M., 1999, "Hansen solubility parameters: a user's handbook", CRC Press LLC, Florida, pp. 4-8.

33. Fujita, S.M. and Soane, D.S., 1988, "Preparation of Crosslinked Membranes With Controlled Pore Size Distribution", **Polymer engineering and science**, Vol. 28, No.6, pp. 341-359.

34. Young, T. and Chen, L., 1995, "Pore formation mechanism of membranes from phase inversion process", **Desalination**, Vol. 103, pp. 233-247.

35. Arunagiri, A., Priya, K., Kalaichelvi, P. and Anantharaj, R., 2014, "Extraction of Reactive Orange 107 dye from aqueous stream using Triton X-114 surfactant: Quantum chemical calculations and experiment", **Journal of Industrial and Engineering Chemistry**, Vol. 20, pp. 2409–2420.

36. Niazi, A., Momeni-Isfahani, T. and Ahmari, A., 2009, "Spectrophoto metric determination of mercury in water samples after cloud point extraction using nonionic surfactant Triton X-114, **Journal of Hazardous Materials**, Vol.165, pp. 1200–1203.

37. Appusamy, A., John, I., Ponnusamy, K. and Ramalingam, A., 2014, "Removal of crystal violet dye from aqueous solution using triton X-114 surfactant via cloud point extraction", **Engineering Science and Technology, an International Journal**, Vol. 17, pp. 137-144.

38. Leeuwen, M.E. van, 1994, "Derivation of Stockmayer potential parameters for polar fluids", **Fluid Phase Equilibria**, Vol. 99, p. 1.

APPENDIX A
Calibration Curve

A.1 Calibration Curve of Butanol solution

Table A.1 Data for calibration curve of butanol solution from 0.010 to 0.10 g/L

Concentration (g/ L)	Peak Area (µV.s)			
	1	2	3	Average
0.010	80,295.25	81,543.90	77,347.70	78,381.43
0.030	115,132.28	114,966.05	94,777.05	108,785.07
0.050	123,620.50	137,423.41	132,018.30	130,562.80
0.060	162,487.22	158,212.16	171,442.70	165,464.59
0.070	171,028.30	190,574.30	195,471.84	183,793.71
0.10	246,849.88	238,394.33	252,266.38	245,836.86

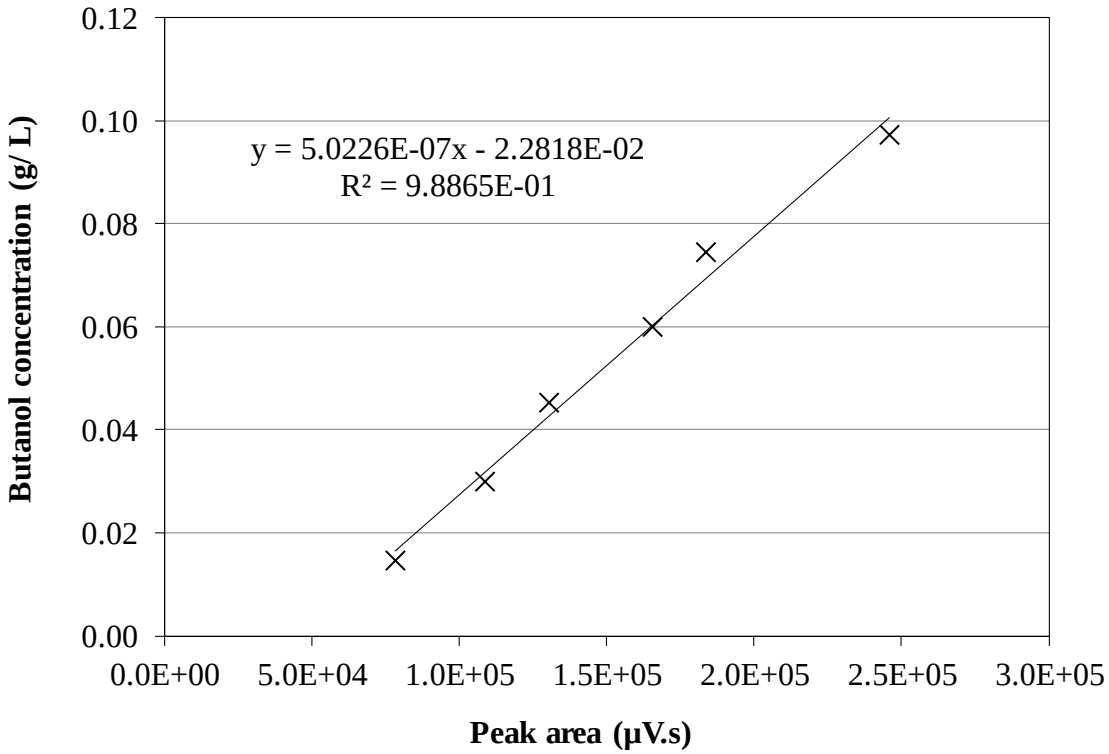

Figure A.1 Butanol concentration from 0.010 to 0.10 g/L versus peak area (µV.s)

Table A.2 Data for calibration curve of butanol solution from 0.10 to 1.0 g/L

Concentration (g/ L)	Peak Area (µV.s)			
	1	2	3	Average
0.10	246,849.88	238,394.33	252,266.38	245,836.86
0.20	422,165.56	443,251.50	475,718.41	447,045.16
0.40	828,758.88	914,060.38	892,070.19	878,296.48
0.60	1,125,460.38	1,185,357.00	1,139,516.25	1,150,111.21
0.80	1,591,607.00	1,654,429.25	1,531,170.25	1,592,402.17
1.0	2,318,850.50	2,323,745.25	2,280,471.50	2,307,689.08

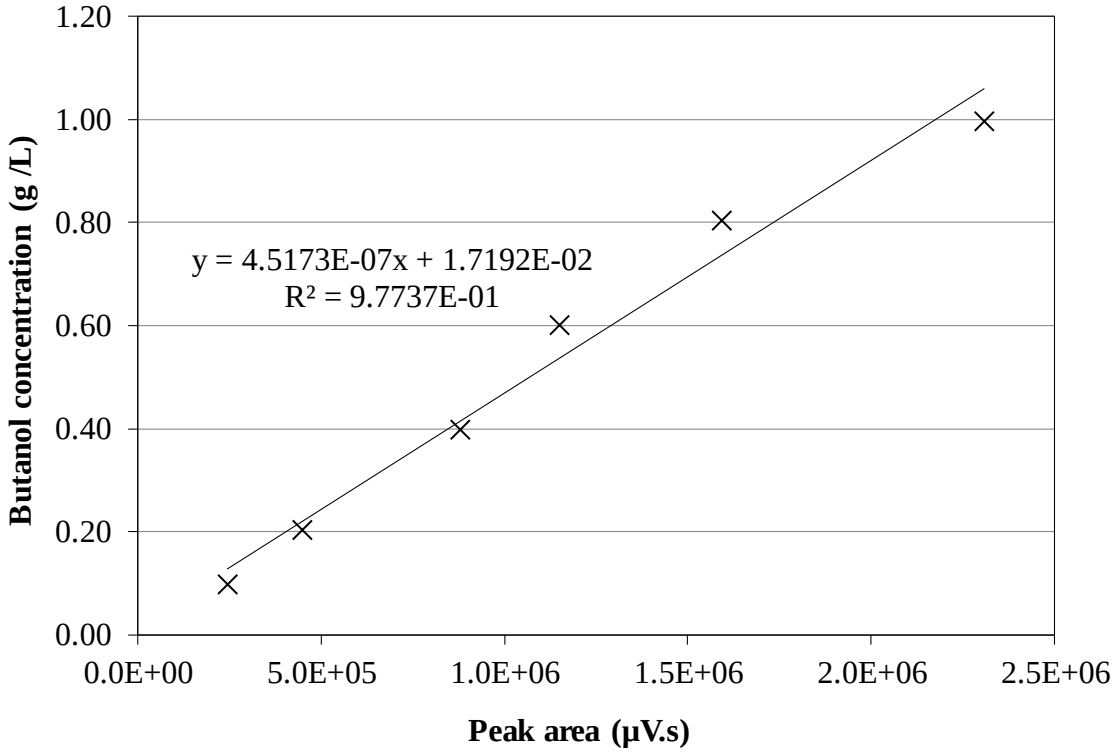

Figure A.2 Butanol concentration from 0.10 to 1.0 g/L versus peak area (µV.s)

Table A.3 Data for calibration curve of butanol solution from 2.0 to 9.0 g/L

Concentration (g/ L)	Peak Area (µV.s)			
	1	2	3	Average
2.0	3,405,328.25	3,793,262.75	4,046,968.25	3,743,481.60
3.0	5,370,519.50	5,208,093.00	5,284,892.00	5,166,962.00
4.0	7,029,929.00	6,684,290.00	7,482,658.50	7,083,191.10
5.0	9,021,549.00	8,614,942.00	8,558,445.00	8,712,105.40
6.0	10,551,593.00	10,167,825.00	10,755,663.00	10,436,674.60
7.0	12,509,558.00	12,483,231.00	11,667,038.00	12,101,092.00
8.0	15,175,874.00	13,446,813.00	14,859,772.00	14,455,818.40
9.0	16,349,281.00	17,171,808.00	16,608,603.00	16,811,290.00

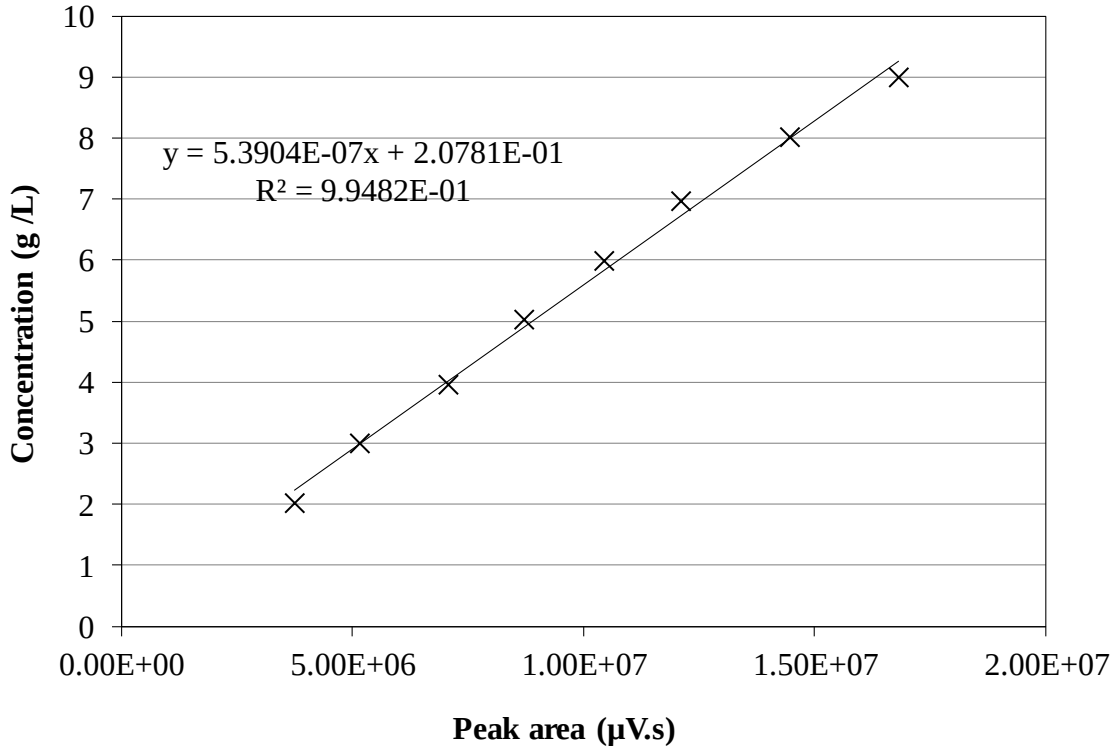

Figure A.3 Butanol concentration from 2.0 to 9.0 g/L versus peak area (µV.s)

Table A.4 Data for calibration curve of butanol solution from 1.0 to 19.2 g/L

Concentration (g/ L)	Peak Area (µV.s)			
	1	2	3	Average
1.0	2,318,850.50	2,323,745.25	2,280,471.50	2,307,689.08
1.0	2,090,054.44	2,045,225.09	2,057,148.34	2,068,873.63
1.5	3,430,155.91	3,297,886.44	3,260,815.06	3,339,426.98
2.0	4,350,829.10	4,345,405.80	4,192,531.11	4,289,072.91
2.0	3,405,328.25	4,088,924.75	3,793,262.75	3,743,481.60
2.5	5,015,839.89	5,559,754.91	5,322,448.63	5,307,131.08
3.0	5,370,519.50	4,519,194.00	5,208,093.00	5,166,962.00
3.5	7,670,028.19	7,339,360.19	7,424,851.50	7,420,407.61
4.0	7,029,929.00	6,684,290.00	7,482,658.50	7,083,191.10
5.0	9,021,549.00	8,614,942.00	8,558,445.00	8,712,105.40
5.0	9,909,080.38	10,081,060.83	9,761,951.75	9,909,235.11
6.0	10,919,039.00	10,551,593.00	9,789,253.00	10,436,674.60
6.0	11,844,233.88	11,868,522.75	12,065,353.00	11,926,036.54
7.0	12,555,994.00	12,509,558.00	11,289,639.00	12,101,092.00
7.0	13,939,155.75	14,291,933.25	13,897,694.25	14,042,927.75
8.0	13,153,214.00	14,389,661.00	12,656,567.00	13,399,814.00
8.0	13,153,214.00	14,389,661.00	12,656,567.00	14,455,818.40
9.0	16,349,281.00	16,353,560.00	16,608,603.00	16,437,148.00
10.0	16,478,104.00	17,593,624.00	16,902,444.00	16,991,390.67
12.0	20,260,272.00	19,844,706.00	19,915,218.00	20,006,732.00
14.0	24,247,608.00	21,961,104.00	22,142,154.00	22,783,622.00
16.0	29,095,184.00	28,685,366.00	28,611,734.00	28,797,428.00
17.2	33,884,384.00	33,353,322.00	33,827,736.00	33,688,480.67
19.2	35,448,320.00	35,758,760.00	33,720,800.00	35,187,089.60

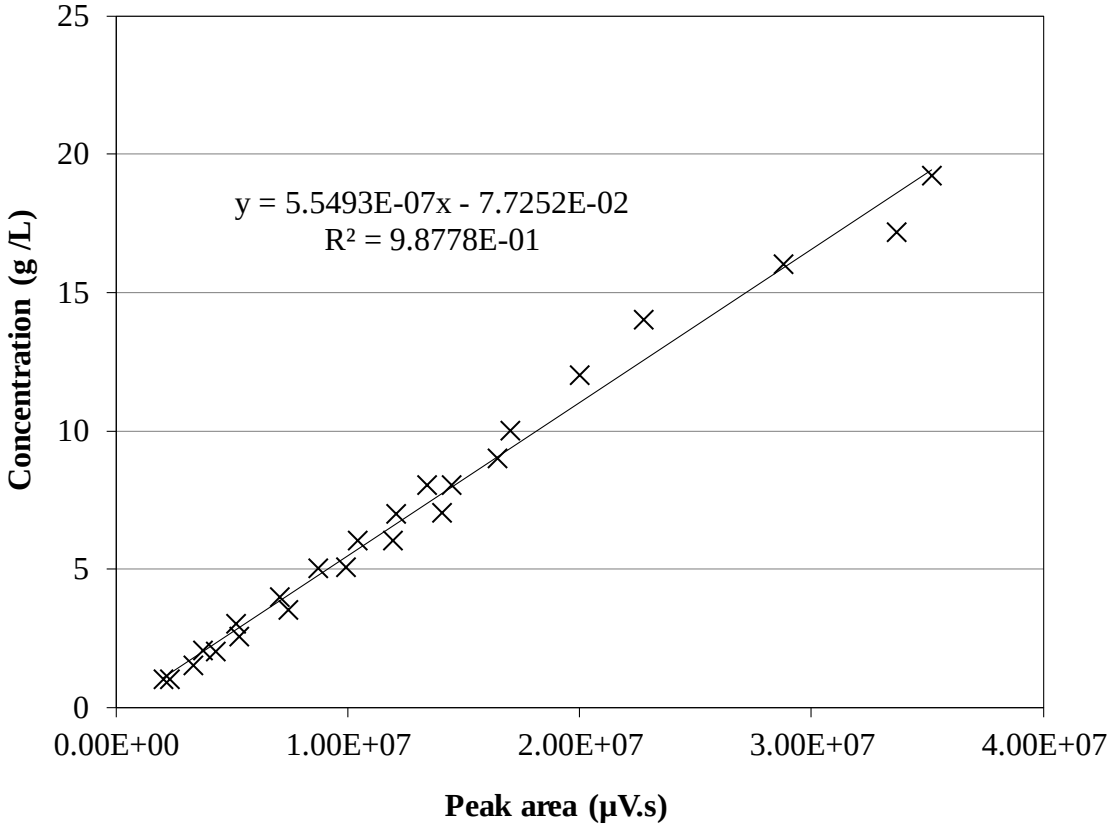

Figure A.4 Butanol concentration from 1.0 to 19.2 g/L versus peak area (µV.s)

Table A.5 Data for calibration curve of mass fraction of butanol from 0.017 to 0.066

Mass fraction	Peak Area (µV.s)			Average
	1	2	3	
0.017	33,353,322.00	33,827,736.00	32,936,672.00	33,322,009.60
0.026	41,833,440.00	43,222,964.00	41,710,636.00	42,085,072.80
0.038	48,753,620.00	48,289,024.00	49,106,864.00	48,943,992.80
0.051	55,663,384.00	53,974,248.00	56,092,272.00	55,147,952.00
0.066	60,582,224.00	61,741,860.00	62,042,412.00	61,544,212.80

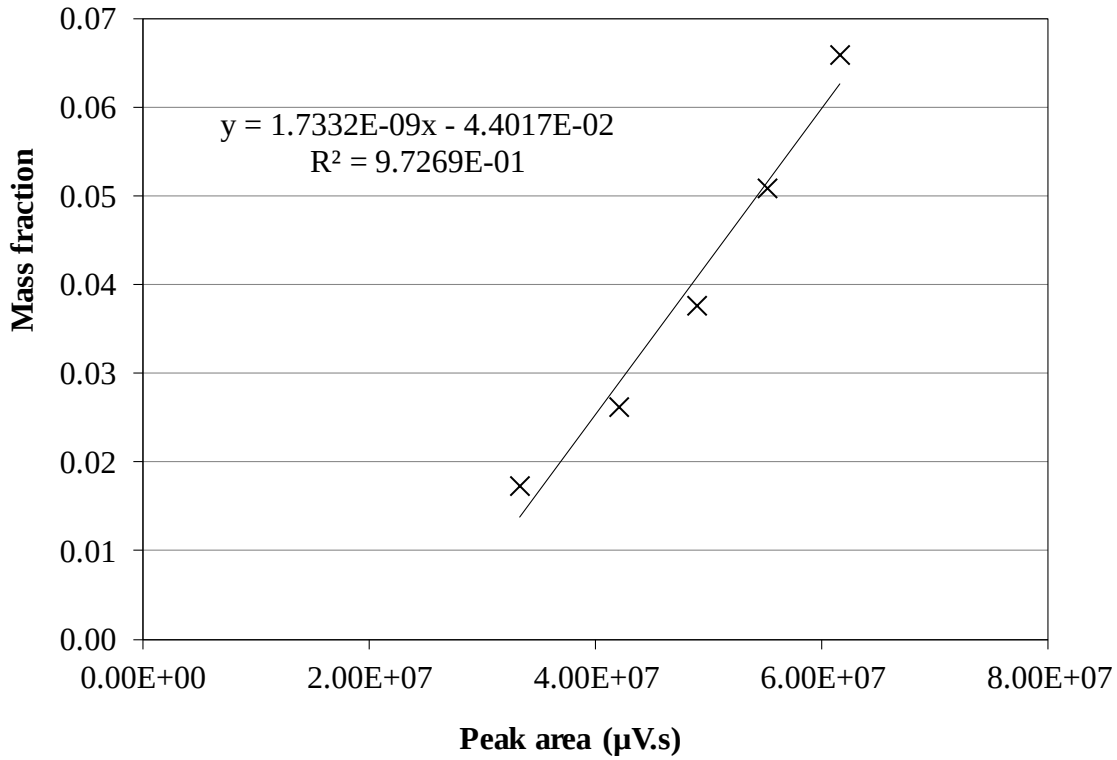

Figure A.5 Mass fraction of butanol from 0.017 to 0.066 versus peak area (µV.s)

A.2 Calibration Curve of Acetone solution

Table A.6 Data for calibration curve of acetone solution from 0.0015 to 0.010 g/L

Concentration (g/ L)	Peak Area (µV.s)			
	1	2	3	Average
0.0015	3,224.35	2,571.16	2,408.81	2,850.23
0.0030	3,864.57	4,155.63	3,731.57	3,914.76
0.0045	4,885.06	5,344.76	5,300.89	5,137.79
0.0060	6,619.04	6,862.72	7,045.96	6,824.68
0.0075	8,247.95	8,165.59	9,034.14	8,485.49
0.0090	10,390.23	10,774.56	11,068.60	10,648.42
0.010	13,263.33	11,946.54	12,425.55	12,545.14

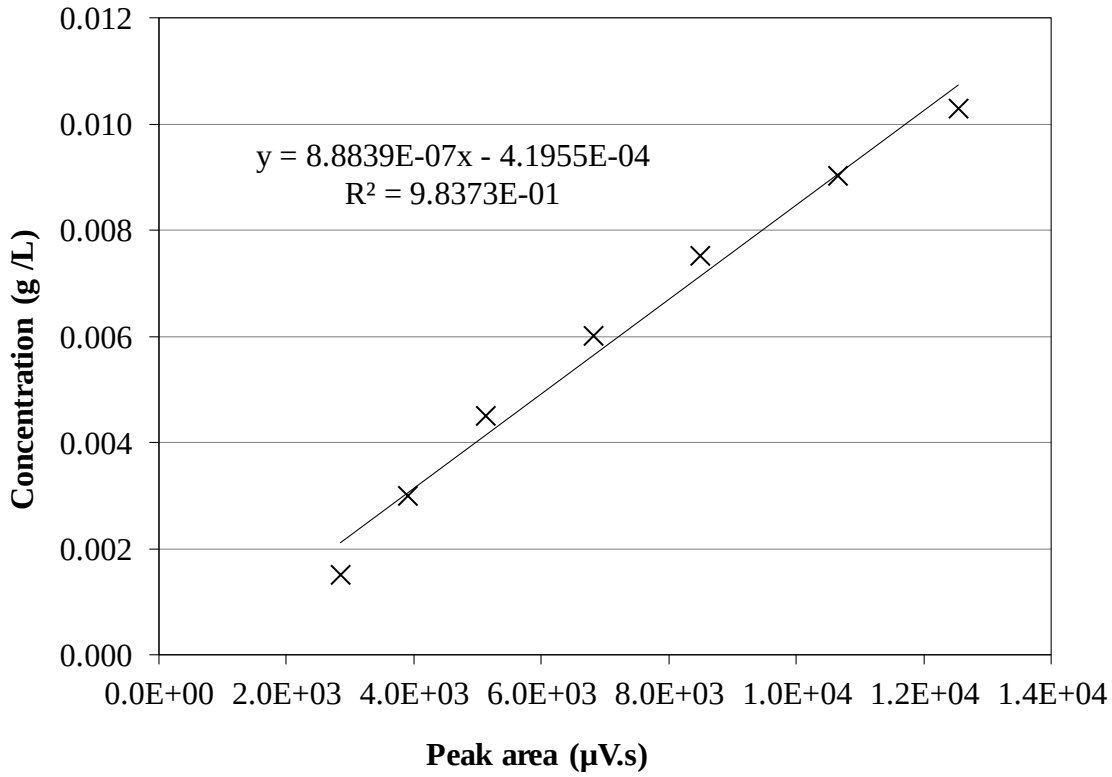

Figure A.6 Acetone concentration from 0.0015 to 0.010 g/L versus peak area (µV.s)

Table A.7 Data for calibration curve of acetone solution from 0.010 to 0.10 g/L

Concentration (g/ L)	Peak Area (µV.s)			
	1	2	3	Average
0.010	13,263.33	11,946.54	12,425.55	12,604.93
0.020	21,430.50	23,194.32	24,736.11	22,312.41
0.040	48,668.68	52,433.65	50,462.97	50,551.16
0.060	63,429.82	68,331.45	63,919.85	65,880.63
0.080	91,501.00	99,212.56	92,171.75	95,356.78
0.10	128,497.70	129,023.13	123,748.91	128,760.41

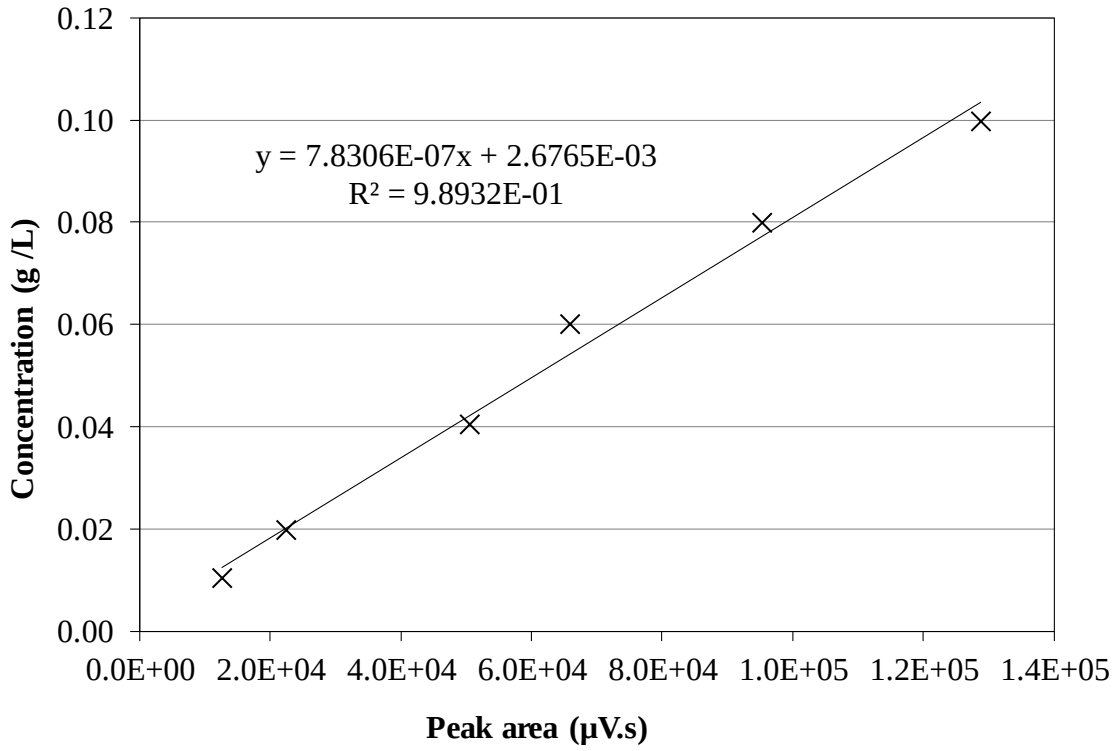

Figure A.7 Acetone concentration from 0.010 to 0.10 g/L versus peak area (µV.s)

Table A.8 Data for calibration curve of mass fraction of acetone from 0.000079 to 0.00079

Mass fraction	Peak Area (µV.s)			Average
	1	2	3	
0.000079	92,720.91	91,751.98	94,553.44	93,499.15
0.00024	271,268.56	301,779.63	294,151.28	292,746.71
0.00040	501,278.41	461,439.38	493,827.53	487,918.28
0.00064	776,011.38	751,019.25	826,915.25	780,586.55
0.00079	1,071,156.38	1,054,556.50	983,572.13	1,059,532.45

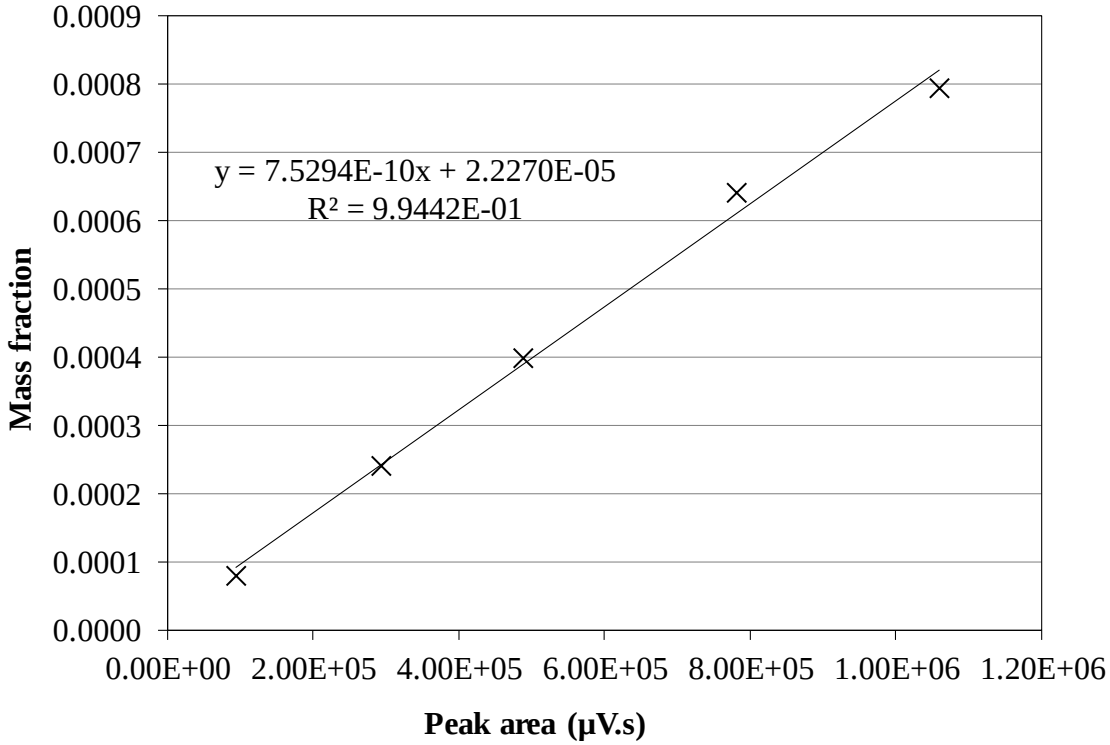

Figure A.8 Mass fraction of acetone from 0.000079 to 0.00079 versus peak area (µV.s)

A.3 Calibration Curve of Ethanol solution

Table A.9 Data for calibration curve of ethanol solution from 0.0015 to 0.0090 g/L

Concentration (g/ L)	Peak Area (µV.s)			
	1	2	3	Average
0.0015	2,353.09	2,285.99	2,743.65	2,304.13
0.0030	4,448.88	6,164.69	3,993.33	4,581.49
0.0045	6,957.94	6,838.91	6,294.79	6,780.19
0.0060	7,300.23	7,721.24	8,071.96	7,526.04
0.0075	9,818.95	9,551.85	11,282.47	10,543.79
0.0090	12,866.54	10,941.67	11,638.23	12,644.84

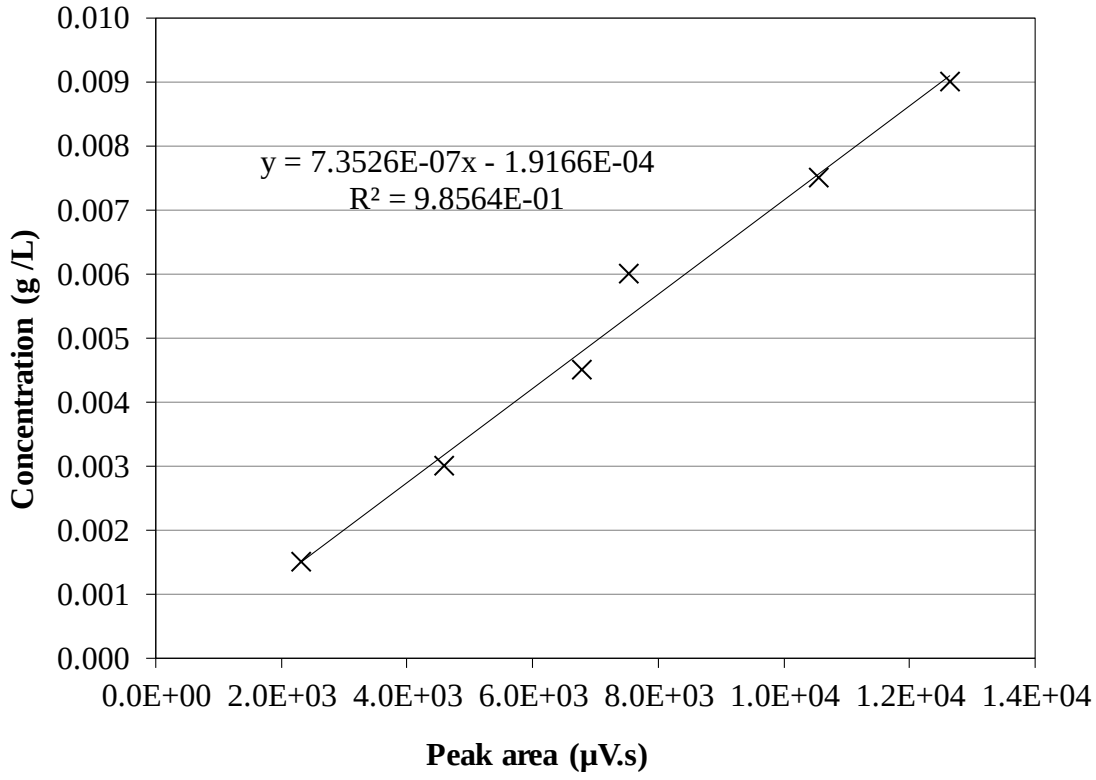

Figure A.9 Ethanol concentration from 0.0015 to 0.0090 g/L versus peak area (µV.s)

Table A.10 Data for calibration curve of ethanol solution from 0.010 to 0.10 g/L

Concentration (g/ L)	Peak Area (µV.s)			
	1	2	3	Average
0.010	22,144.80	17,770.43	18,362.18	19,425.81
0.020	28,720.65	26,687.18	31,711.08	29,039.64
0.040	56,951.72	67,791.35	68,307.44	64,350.17
0.060	76,258.78	79,886.25	76,162.15	77,435.73
0.080	124,170.23	122,037.69	115,505.84	120,571.26
0.10	156,546.41	157,390.78	154,164.39	156,033.86

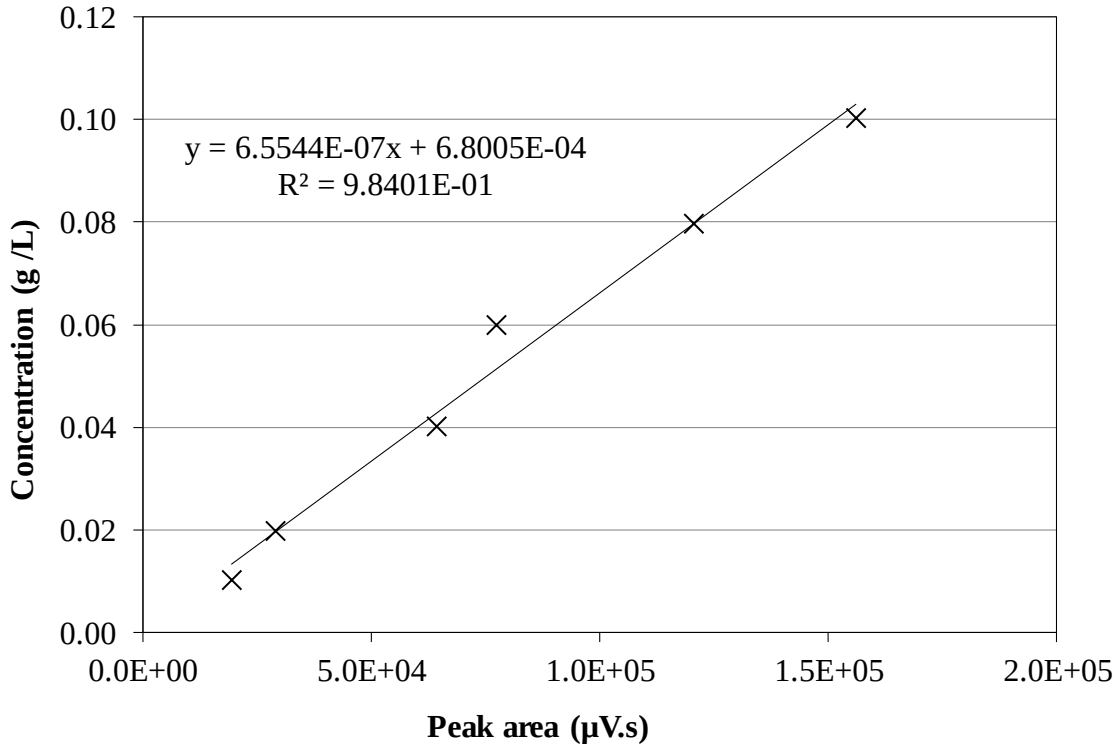

Figure A.10 Ethanol concentration from 0.010 to 0.10 g/L versus peak area (µV.s)

Table A.11 Data for calibration curve of mass fraction of ethanol from 0.00051 to 0.0026

Mass fraction	Peak Area (µV.s)			Average
	1	2	3	
0.00051	892,389.31	870,921.38	841,465.06	874,712.86
0.0010	1,249,216.00	1,370,716.00	1,276,276.00	1,273,064.00
0.0015	2,221,634.00	2,372,752.00	2,340,627.75	2,324,835.40
0.0020	3,085,962.50	2,950,985.00	3,055,349.50	3,030,024.30
0.0026	3,858,520.25	3,715,082.00	3,986,842.25	3,836,881.30

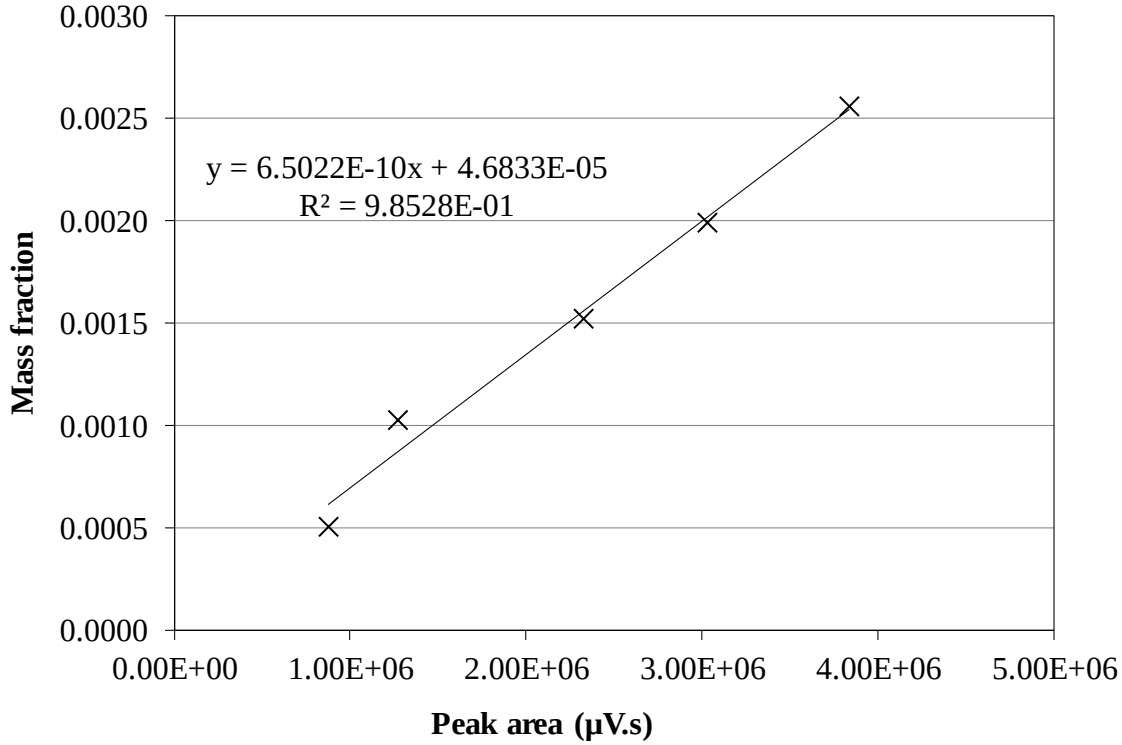

Figure A.11 Mass fraction of ethanol from 0.00051 to 0.0026 versus peak area (µV.s)

APPENDIX B
GC Conditions

B.1 GC Conditions for the Analysis of acetone, ethanol and butanol Concentrations

Column: Optima wax$^{@}$
Temperature program

OVEN 80^{o}C
INT TEMP 80^{o}C
INT TIME 0 min
RATE 8.0 ml/min
FINAL TEMP 120^{o}C

FRONT INLET (PP) TEMP 180^{o}C

COLUMN 1 (He)
Dim 30.0 m 530 mm
Flow 10 ml/min
Mode Constant flow

FRONT DET (FID) TEMP 240^{o}C
H_2 flow 7.7 psi
Air flow 350 psi
Mk up (N_2) 1.0 psi

SIGNAL 1
Range 0
Attn 0

APPENDIX C
Analysis of organic compound concentration and Calculations

C.1 Feed and Receiving Solution Preparation

C.1.1 Feed preparation

To prepare a feed containing 1, 19.2, and 1.7 g/L of acetone, butanol, and ethanol, respectively, a mixture was prepared according to Table C.1.

Table C.1 Data of the feed solution

Property	Component				
	Acetone	**Butanol**	**Ethanol**	**Water**	**Total**
Density (g/cm^3)	0.791	0.810	0.789	1.000	
Concentration (g/L)	1	19.2	1.7		
Volume (cm^3) in 350 cm^3	0.44	8.30	0.75	340.51	350.00
Mass (g)	0.35	6.72	0.60	340.51	348.17

C.1.2 Receiving preparation

For example, to prepare a receiving solution consisting of 10.5 wt. % Triton X-114, a solution was prepared according to Table C.2.

Table C.2 Data of the receiving solution

Component	Density (g/cm^3)	Volume (cm^3)	Mass (g)	Concentration (wt. %)
Triton	1.055	15.81	16.68	10.50
Water	1	142.19	142.19	89.50
Total		158.00	158.87	100.00

C.2 Calculation of Organic Concentrations

For example, to calculate a concentration of butanol in a receiving phase, a peak area reported by a GC was 12,036,874.00 (µV.s). The concentration of butanol was calculated by using the equation in Appendix A,

$$y = 5.3904\times10^{-07}x + 0.20781 \qquad (C.1)$$

where y is the butanol concentration (g/L)
x is the peak area (µV.s)

$$y = [(5.3904\times10^{-07}) \times (12{,}036{,}874.00)] + 0.20781 = 6.7 \text{ g/ L}$$

C.3 Flux Calculation

Permeate flux (J) (g/(m^2.h)) is calculated by

$$J_i = \frac{M_i}{A.t} \times \frac{16.5\ \mu m}{T} \quad \text{(C.2)}$$

where M_i is the mass of i species in a permeate, (g)
A is the membrane area, (m^2)
t is the time of the experiment, (h)
T is the membrane thickness, (μm)
16.5 is the average membrane thickness, (μm)

For example, from an experiment with the following conditions and results:
Feed concentration: acetone: butanol: ethanol: 1: 19.2: 1.7 (g/L)
Receiving solution: 0.8 wt. % Triton X-114
Perstraction time: 300 min
Effective membrane area = 5.72 ×10^{-4} m^2
Membrane thickness: 16.8 μm
Average membrane thickness: 16.5 μm
Slope of graph (mass vs time) = 3.6384×10^{-3} (g/min)

$$J_{butanol} = \frac{3.6384\times10^{-3}\ g/min}{5.72\times10^{-4} m^2} \times \frac{60\ min}{1\ h} \times \frac{16.8\ \mu m}{16.5\ \mu m}$$

$$J_{butanol} = 388.6\ g/(m^2.h)$$

C.4 Calculation of Separation factor (α)

Separation factor (α) is defined as

$$\alpha = \frac{(y_i/y_j)}{(x_i/x_j)} \quad \text{(C.3)}$$

where y_i is the weight fraction of i species in a permeate
y_j is the weight fraction of water in a permeate
x_i is the weight fraction of i species in a feed
x_j is the weight fraction of water in a feed

For example, from an experiment with the following conditions and results:
Feed concentration: acetone: butanol: ethanol: 1: 19.2: 1.7 (g/L)
Feed volume: 300 mL
Temperature of pervaporation: 37 ^{o}C
Pervaporation time: 5 h
Flux of acetone: ethanol: butanol: water: 0.061: 0.33: 9.7: 77 (g/(m^2.h))

Mass of each component in the permeate was calculated from the flux.
For example, the calculation of butanol mass in the permeate afther 5 h pervaporation.

Butanol mass (g) = Flux (g/(m^2.h)) × Area (m^2) × Time (h)

$= 9.7 \times (5.72 \times 10^{-4}) \times 5$

$= 0.02774$ g

Mass of the others was calculated in the same way. Mass of each component in the permeate is shown in Table C.3.

Table C.3 Mass of each component in the permeate

Component	**Flux (g/(m^2.h))**	**Mass in the permeate (g)**				
		5 h	**6 h**	**7 h**	**8 h**	**9 h**
Acetone	0.061	0.00017	0.00021	0.00024	0.00028	0.00031
Ethanol	0.33	0.00094	0.00113	0.00132	0.00151	0.00170
Butanol	9.7	0.02774	0.03329	0.03884	0.04439	0.04994
Water	77	0.22022	0.26426	0.30831	0.35235	0.39640
Total	87	0.24908	0.29890	0.34871	0.39853	0.44834

Table C.4 Mass of each component in the feed

Pervaporation time (h)	**Mass (g) in a feed**				
	Acetone	**Ethanol**	**Butanol**	**Water**	**Total**
5 to 9	0.30	0.51	5.76	289.91	296.48

Weight factor of butanol in the feed: $x_i = \frac{5.76}{296.48} = 0.019$

Weight factor of water in the feed: $x_j = \frac{289.91}{296.48} = 0.98$

Weight factor of butanol in the permeate: $y_i = \frac{0.02774}{0.24908} = 0.11$

Weight factor of water in the permeate: $y_j = \frac{0.22022}{0.24908} = 0.88$

Separation factor of butanol:

$$\alpha_{butanol} = \frac{(0.11/0.88)}{(0.019/0.98)}$$

$$\alpha_{butanol} = 6.3$$

C.5 Calculation of Distribution coefficient

Distribution coefficient of component is defined as

$$\text{Distribution coefficient of component i} = \frac{C_{i,RP}}{C_{i,LP}} \qquad \text{(C.4)}$$

where $C_{i,RP}$ is the Concentration of i species in the surfactant-rich phase, (g/L)

$C_{i,LP}$ is the concentration of i species in the surfactant-lean phase, (g/L)

Example

Concentration of butanol in the surfactant-rich phase: 143.3 g/L
Concentration of butanol in the surfactant-lean phase: 5.2 g/L

$$\text{Distribution coefficient of butanol} = \frac{143.3}{5.2} = 27.6$$

C.6 Calculation of capturing capacity of organic solutes

The capturing capacity of component iis defined as

$$\text{Capturing capacity of i} = \frac{m_{i,RP}}{m_{\text{Triton X}-114}} \qquad \text{(C.5)}$$

where $m_{i,RP}$ is the mass of i species in the surfactant-rich phase, (g)

$m_{\text{Triton X-114}}$ is the mass of Triton X-114 in the solution, (g)

Example

Receiving solution: 0.8 wt. % Triton X-114
Mass of butanol in the surfactant-rich phase: 0.287 g
Mass of Triton X-114: 1.24 g

$$\text{Capturing capacity of butanol} = \frac{0.287}{1.24} = 0.23 \text{ g butanol/g Triton X-114}$$

APPENDIX D
Experimental Results

D.1 The results of perstraction experiment using water as the receiving phase

D.1.1 First perstraction experiment using water

Feed solution: 1: 19.2: 1.7 (g/L) Acetone: Butanol: Ethanol
Receiving phase: Pure water
Membrane thickness: 16.8 µm
Feed volume: 300 mL
Receiving volume: 157 mL
Feed and receiving temperature: 37 ^{o}C

Table D.1 Peak areas of acetone, ethanol, and butanol concentrations in water receiving phase, first experiments

Time (min)	Receiving composition					
	Peak area of Acetone (µV.s)	Peak area of Ethanol (µV.s)	Peak area of Butanol (µV.s)	Acetone (g/l)	Ethanol (g/l)	Butanol (g/l)
30	8,418.965	8,852.585	930,726.922	0.0083	0.0068	0.44
40	11,583.273	13,707.564	1,233,526.032	0.0104	0.0097	0.58
70	18,712.311	21,402.055	2,191,890.219	0.0152	0.0144	1.04
80	24,471.266	26,155.834	2,490,817.688	0.0190	0.0173	1.11
120	43,790.875	46,056.727	4,314,729.125	0.0319	0.0294	2.05
150	49,481.070	53,423.230	4,701,012.625	0.0357	0.0339	2.24
160	52,511.426	58,660.672	5,124,981.000	0.0377	0.0370	2.46
190	70,062.070	78,927.352	6,468,277.125	0.0495	0.0494	3.15
200	70,643.633	78,553.969	6,783,624.000	0.0498	0.0492	3.32
240	84,011.258	93,419.141	7,813,703.875	0.0588	0.0582	3.85
270	96,435.883	109,736.867	8,811,334.000	0.0671	0.0681	4.36
280	98,908.156	110,136.547	8,897,643.625	0.0687	0.0684	4.40
300	105,163.234	120,516.570	9,447,328.375	0.0729	0.0747	4.69

D.1.2 Second perstraction experiments using water

Feed solution: 1: 19.2: 1.7 (g/L) Acetone: Butanol: Ethanol
Receiving phase: Pure water
Membrane thickness: 17.5 µm
Feed volume: 300 mL
Receiving volume: 157 mL
Feed and receiving temperature: 37 ^{o}C

Table D.2 Peak areas of acetone, ethanol, and butanol concentrations in water receiving phase, second experiments

Time (min)	Receiving composition					
	Peak area of Acetone (µV.s)	Peak area of Ethanol (µV.s)	Peak area of Butanol (µV.s)	Acetone (g/l)	Ethanol (g/l)	Butanol (g/l)
30	9,811.582	10,538.519	1,086,747.594	0.0093	0.0078	0.51
40	10,068.529	10,368.621	1,074,804.592	0.0094	0.0077	0.51
70	21,589.125	22,804.676	2,315,866.375	0.0171	0.0152	1.10
80	26,436.506	28,112.246	2,766,887.375	0.0203	0.0185	1.25
110	32,038.414	36,329.086	3,243,360.875	0.0241	0.0235	1.49
120	40,007.820	43,051.832	3,909,831.125	0.0294	0.0276	1.84
150	47,988.746	53,944.352	4,639,498.250	0.0347	0.0342	2.21
160	60,539.793	65,996.805	5,844,424.500	0.0431	0.0415	2.83
190	56,912.152	64,450.648	5,375,935.750	0.0407	0.0406	2.59
200	56,912.152	79,068.477	6,448,639.125	0.0407	0.0495	3.14
240	85,866.992	98,389.563	7,833,460.500	0.0600	0.0612	3.86
270	94,972.633	111,248.016	8,481,533.500	0.0661	0.0690	4.19
300	101,921.516	117,006.188	9,519,759.000	0.0707	0.0725	4.72

D.1.3 Third perstraction experiments using water

Feed solution: 1: 19.2: 1.7 (g/L) Acetone: Butanol: Ethanol
Receiving phase: Pure water
Membrane thickness: 16.8 µm
Feed volume: 300 mL
Receiving volume: 157 mL
Feed and receiving temperature: 37 ^{o}C

Table D.3 Peak areas of acetone, ethanol, and butanol concentrations in water receiving phase, third experiments

Time (min)	Receiving composition					
	Peak area of Acetone (µV.s)	Peak area of Ethanol (µV.s)	Peak area of Butanol (µV.s)	Acetone (g/l)	Ethanol (g/l)	Butanol (g/l)
30	6,397.89	8,820.56	764,473.94	0.0051	0.0060	0.36
40	8,388.03	11,027.40	933,016.38	0.0064	0.0071	0.44
70	16,110.44	18,653.39	1,851,866.00	0.0151	0.0131	0.85
80	16,492.26	20,164.77	1,811,700.75	0.0154	0.0140	0.83
110	28,068.00	29,177.40	3,074,311.50	0.0246	0.0199	1.80
120	29,290.78	32,955.34	3,114,309.00	0.0256	0.0224	1.83
150	38,186.58	41,272.42	4,174,997.25	0.0326	0.0278	2.40
160	39,931.51	42,591.25	4,176,231.50	0.0340	0.0287	2.40
190	48,073.39	57,243.80	4,940,224.00	0.0405	0.0383	2.82
200	52,141.98	56,243.72	5,333,619.00	0.0437	0.0376	3.03
230	61,259.46	72,214.13	6,118,016.00	0.0510	0.0480	3.46
240	64,879.72	70,588.94	6,410,611.50	0.0539	0.0470	3.62
270	80,144.10	84,261.20	7,868,872.00	0.0660	0.0559	4.41
280	77,805.56	84,508.60	7,835,097.25	0.0641	0.0560	4.39
300	83,840.42	90,861.54	8,441,268.65	0.0689	0.0602	4.72

D.2 The result of perstraction experiment using 0.7 wt. % Triton X-114 solution as the receiving phase

Feed solution: 1: 19.2: 1.7 (g/L) Acetone: Butanol: Ethanol
Receiving phase: 0.7 wt. % Triton X-114 solution
Membrane thickness: 16.2 µm
Feed volume: 300 mL
Receiving volume: 157 mL
Feed and receiving temperature: 37 ^{o}C

Table D.4 Peak areas of acetone, ethanol, and butanol concentrations in 0.7 wt. % Triton X-114 receiving solution

Time (min)	Receiving composition					
	Peak area of Acetone (µV.s)	Peak area of Ethanol (µV.s)	Peak area of Butanol (µV.s)	Acetone (g/l)	Ethanol (g/l)	Butanol (g/l)
30	6,188.10	8,398.52	870,982.13	0.00499	0.00574	0.41
40	8,875.78	12,329.42	1,184,549.88	0.00677	0.00780	0.55
70	16,161.59	24,218.42	2,231,226.25	0.01512	0.01669	1.35
80	19,962.81	29,126.49	2,631,927.75	0.01815	0.01989	1.56
110	27,875.49	39,274.51	3,674,650.00	0.02444	0.02652	2.13
120	33,994.21	50,403.88	4,217,700.00	0.02930	0.03379	2.43
150	48,162.20	67,076.63	5,340,150.50	0.04057	0.04467	3.04
160	53,606.68	73,239.32	6,287,373.50	0.04490	0.04870	3.55
190	56,050.50	78,835.40	6,333,894.00	0.04684	0.05235	3.58
200	65,593.22	90,085.38	7,361,617.00	0.05443	0.05969	4.14
230	69,060.60	100,677.06	7,535,030.00	0.05719	0.06661	4.23
240	80,176.10	112,913.30	8,188,386.00	0.06603	0.07460	4.58
270	83,577.79	120,318.39	8,826,570.00	0.06873	0.07943	4.93
280	86,787.11	119,523.79	9,023,893.00	0.07128	0.07892	5.04
300	96,676.48	128,095.92	9,621,173.00	0.07915	0.08451	5.36

D.3 The result of perstraction experiment using 0.8 wt. % Triton X-114 solution as the receiving phase

Feed solution: 1: 19.2: 1.7 (g/L) Acetone: Butanol: Ethanol
Receiving phase: 0.8 wt. % Triton X-114 solution
Membrane thickness: 16.8 µm
Feed volume: 300 mL
Receiving volume: 157 mL
Feed and receiving temperature: 37 ^{o}C

Table D.5 Peak areas of acetone, ethanol, and butanol concentrations in 0.8 wt. % Triton X-114 receiving solution

Time (min)	Receiving composition					
	Peak area of Acetone (µV.s)	Peak area of Ethanol (µV.s)	Peak area of Butanol (µV.s)	Acetone (g/l)	Ethanol (g/l)	Butanol (g/l)
30	10,789.24	14,096.90	1,142,198.25	0.0080	0.0087	0.53
40	15,820.88	16,667.10	1,637,352.50	0.0149	0.0101	0.76
70	23,696.43	28,113.48	2,318,309.25	0.0211	0.0192	1.06
80	33,190.73	35,221.77	3,280,122.75	0.0287	0.0239	1.50
110	44,144.75	53,102.66	4,248,674.00	0.0374	0.0355	2.44
120	51,495.55	56,144.45	4,940,823.50	0.0432	0.0375	2.82
150	65,800.47	72,266.43	6,135,715.50	0.0546	0.0481	3.47
160	66,475.96	73,948.14	6,280,923.50	0.0551	0.0492	3.55
190	85,373.40	96,015.85	7,799,878.00	0.0702	0.0636	4.37
200	89,694.96	108,454.59	8,080,289.50	0.0736	0.0717	4.53
230	106,230.95	122,556.14	9,432,943.00	0.0867	0.0809	5.26
240	105,629.34	122,836.47	9,381,195.00	0.0863	0.0811	5.23
270	117,908.60	137,631.41	10,790,190.00	0.0960	0.0907	6.00
280	127,334.89	152,983.48	11,164,795.00	0.1035	0.1008	6.20
300	139,145.70	166,087.45	12,036,874.00	0.1129	0.1093	6.68

D.4 The result of perstraction experiment using 0.9 wt. % Triton X-114 solution as the receiving phase

Feed solution: 1: 19.2: 1.7 (g/L) Acetone: Butanol: Ethanol
Receiving phase: 0.9 wt. % Triton X-114 solution
Membrane thickness: 16.7 µm
Feed volume: 300 mL
Receiving volume: 157 mL
Feed and receiving temperature: 37 ^{o}C

Table D.6 Peak areas of acetone, ethanol, and butanol concentrations in 0.9 wt. % Triton X-114 receiving solution

Time (min)	Receiving composition					
	Peak area of Acetone (µV.s)	Peak area of Ethanol (µV.s)	Peak area of Butanol (µV.s)	Acetone (g/l)	Ethanol (g/l)	Butanol (g/l)
30	15,573.50	12,201.23	1,213,137.13	0.0147	0.0077	0.57
40	16,988.21	16,670.59	1,506,733.63	0.0158	0.0101	0.70
70	27,053.60	28,795.05	2,529,497.25	0.0238	0.0197	1.51
80	35,215.21	37,898.40	3,037,749.75	0.0303	0.0256	1.78
110	51,323.05	55,538.91	4,778,751.50	0.0431	0.0371	2.73
120	49,108.32	55,691.18	4,601,360.50	0.0413	0.0372	2.63
150	61,715.13	67,375.67	5,836,626.00	0.0513	0.0449	3.31
160	71,523.66	81,472.48	6,471,387.50	0.0591	0.0541	3.65
190	90,719.39	103,132.36	7,852,993.50	0.0744	0.0682	4.40
200	86,327.88	98,566.32	7,654,270.50	0.0709	0.0652	4.29
230	115,469.65	132,437.75	9,939,127.00	0.0941	0.0873	5.54
240	98,776.43	113,023.52	8,543,983.00	0.0808	0.0747	4.78
270	132,349.09	156,509.59	11,244,740.00	0.1075	0.1031	6.25
280	111,438.74	132,838.36	9,343,306.00	0.0909	0.0876	5.21
300	144,785.55	177,825.41	11,478,554.70	0.1174	0.1170	6.37

D.5 The result of perstraction experiment using 3.5 wt. % Triton X-114 solution as the receiving phase

Feed solution: 1: 19.2: 1.7 (g/L) Acetone: Butanol: Ethanol
Receiving phase: 3.5 wt. % Triton X-114 solution
Membrane thickness: 15.2 µm
Feed volume: 300 mL
Receiving volume: 157 mL
Feed and receiving temperature: 37 ^{o}C

Table D.7 Peak areas of acetone, ethanol, and butanol concentrations in 3.5 wt. % Triton X-114 receiving solution

Time (min)	Receiving composition					
	Peak area of Acetone (µV.s)	Peak area of Ethanol (µV.s)	Peak area of Butanol (µV.s)	Acetone (g/l)	Ethanol (g/l)	Butanol (g/l)
30	11,943.02	11,017.57	1,070,225.41	0.0107	0.0081	0.51
40	16,304.71	13,383.15	1,261,567.38	0.0136	0.0095	0.60
70	30,130.15	32,218.99	2,770,146.94	0.0228	0.0210	1.25
80	29,105.23	30,200.70	2,733,191.06	0.0221	0.0197	1.23
110	42,645.33	47,368.67	3,940,925.25	0.0312	0.0302	1.85
120	48,378.92	53,326.06	4,518,685.25	0.0350	0.0338	2.15
150	59,541.84	63,078.05	5,298,394.00	0.0424	0.0397	2.55
160	67,009.75	75,373.98	6,255,378.50	0.0474	0.0472	3.04
190	66,127.13	70,036.79	5,783,247.25	0.0468	0.0440	2.80
200	91,238.65	104,363.89	7,865,569.25	0.0636	0.0649	3.87
230	87,948.23	99,229.76	7,706,151.75	0.0614	0.0617	3.79
240	99,658.32	114,285.48	8,837,259.50	0.0692	0.0709	4.37
270	125,687.97	138,619.03	10,430,485.25	0.0866	0.0857	5.19
280	104,536.23	116,465.13	8,844,239.50	0.0725	0.0722	4.38
300	141,083.75	159,381.63	11,247,720.75	0.0969	0.0983	5.61

D.6 the result of perstraction experiment using 7.0 wt. % Triton X-114 solution as the receiving phase

Feed solution: 1: 19.2: 1.7 (g/L) Acetone: Butanol: Ethanol
Receiving phase: 7.0 wt. % Triton X-114 solution
Membrane thickness: 17.5 µm
Feed volume: 300 mL
Receiving volume: 157 mL
Feed and receiving temperature: 37 ^{o}C

Table D.8 Peak areas of acetone, ethanol, and butanol concentrations in 7.0 wt. % Triton X-114 receiving solution

Time (min)	Receiving composition					
	Peak area of Acetone (µV.s)	Peak area of Ethanol (µV.s)	Peak area of Butanol (µV.s)	Acetone (g/l)	Ethanol (g/l)	Butanol (g/l)
40	16,006.99	12,639.92	1,030,403.53	0.0134	0.0091	0.49
70	25,429.64	20,052.59	1,997,263.44	0.0197	0.0136	0.95
80	29,759.85	25,473.37	2,414,426.19	0.0226	0.0169	1.07
150	51,613.08	50,507.82	4,297,159.75	0.0371	0.0321	2.04
190	71,735.64	74,602.75	6,206,352.75	0.0506	0.0467	3.02
200	73,277.17	77,242.71	6,202,196.75	0.0516	0.0484	3.02
230	83,878.90	92,131.62	7,013,202.75	0.0587	0.0574	3.43
240	89,422.77	95,148.56	7,274,176.25	0.0624	0.0592	3.57
270	108,030.62	122,573.93	8,771,930.00	0.0748	0.0759	4.34
290	105,583.13	114,549.43	8,741,385.00	0.0732	0.0710	4.32
300	108,732.66	119,131.84	8,946,950.25	0.0753	0.0738	4.43

D.7 The result of perstraction experiment using 10.5 wt. % Triton X-114 solution as the receiving phase

Feed solution: 1: 19.2: 1.7 (g/L) Acetone: Butanol: Ethanol
Receiving phase: 10.5 wt. % Triton X-114 solution
Membrane thickness: 15.7 µm
Feed volume: 300 mL
Receiving volume: 157 mL
Feed and receiving temperature: 37 ^{o}C

Table D.9 Peak areas of acetone, ethanol, and butanol concentrations in 10.5 wt. % Triton X-114 receiving solution

Time (min)	Receiving composition					
	Peak area of Acetone (µV.s)	Peak area of Ethanol (µV.s)	Peak area of Butanol (µV.s)	Acetone (g/l)	Ethanol (g/l)	Butanol (g/l)
30	13,692.18	10,910.46	1,050,029.63	0.0118	0.0080	0.50
44	20,944.18	15,840.00	1,352,980.50	0.0167	0.0110	0.64
75	34,355.88	32,047.43	2,739,871.25	0.0256	0.0209	1.24
85	37,762.24	32,441.83	3,298,296.00	0.0279	0.0211	1.52
110	46,398.51	43,330.18	4,078,907.50	0.0337	0.0277	1.92
120	61,509.29	64,631.61	5,499,975.38	0.0438	0.0407	2.66
150	65,471.09	65,346.53	6,166,785.50	0.0464	0.0411	3.00
160	71,078.21	73,465.94	6,604,905.00	0.0501	0.0461	3.22
190	69,150.23	71,074.95	6,269,433.00	0.0489	0.0446	3.05
203	77,907.24	82,243.88	7,215,723.00	0.0547	0.0514	3.54
240	87,339.07	94,534.03	8,240,111.25	0.0610	0.0589	4.07
280	97,003.70	107,520.67	9,216,873.00	0.0674	0.0668	4.57
300	109,460.97	119,644.42	10,350,945.57	0.0758	0.0741	5.15

D.8 The result of experiment using the feed containing only 1 g/L acetone

Feed solution: 1 g/L Acetone
Receiving phase: 3.5 wt. % Triton X-114 solution
Membrane thickness: 17.6 µm
Feed volume: 300 mL
Receiving volume: 157 mL
Feed and receiving temperature: 37 ^{o}C

Table D.10 Peak areas of acetone concentrations in 3.5 wt. % Triton X-114 solution by using only 1.0 g/L acetone in the feed

Time (min)	Peak area of Acetone (µV.s)	Acetone (g/l)
40	1,893.64	0.00708
50	5,530.17	0.01141
80	5,530.23	0.01141
90	6,005.29	0.01198
120	19,496.72	0.02804
130	15,351.47	0.02311
160	12,856.05	0.02014
170	18,854.19	0.02728
200	18,109.31	0.02639
210	21,724.32	0.03070
240	24,167.81	0.03360
250	23,690.24	0.03304
280	21,286.96	0.03017
290	29,092.80	0.03947
300	27,075.20	0.03707

D.9 The result of experiment using the feed containing only 1.7 g/L ethanol

Feed solution: 1.7 g/L Ethanol
Receiving phase: 3.5 wt. % Triton X-114 solution
Membrane thickness: 16.0 µm
Feed volume: 300 mL
Receiving volume: 157 mL
Feed and receiving temperature: 37 ^{o}C

Table D.11 Peak areas of ethanol concentrations in 3.5 wt. % Triton X-114 solution by using only 1.7 g/L in the feed

Time (min)	Peak area of Ethanol (µV.s)	Ethanol (g/l)
40	3,649.90	0.015
50	5,201.40	0.017
80	11,241.75	0.024
90	14,290.50	0.028
120	21,321.60	0.036
130	20,291.75	0.035
160	18,462.20	0.033
170	26,468.50	0.042
200	30,350.40	0.047
210	33,180.90	0.050
250	31,446.90	0.048
280	44,071.10	0.063
290	42,946.27	0.061
300	39,953.60	0.058

D.10 The result of experiment using the feed containing only 19.2 g/L butanol

Feed solution: 19.2 g/L Butanol
Receiving phase: 3.5 wt. % Triton X-114 solution
Membrane thickness: 17.2 µm
Feed volume: 300 mL
Receiving volume: 157 mL
Feed and receiving temperature: 37 ^{o}C

Table D.12 Peak areas of butanol concentrations in 3.5 wt. % Triton X-114 solution by using only 19.2 g/L butanol in the Feed

Time (min)	Peak area of Butanol (µV.s)	Butanol (g/l)
30	439,088.91	0.21
40	618,399.88	0.29
70	1,717,521.00	0.81
80	1,871,862.69	0.89
110	2,781,965.69	1.26
120	2,791,579.81	1.26
160	3,910,111.56	1.84
190	4,962,398.25	2.38
200	5,000,298.00	2.40
230	6,220,830.75	3.03
270	7,558,976.50	3.71
280	7,806,357.50	3.84
300	8,817,158.60	4.36

D.11 The results of perstraction experiment using a temperature of receiving phase below the cloud point of Triton X-114

D.11.1 Perstraction experiments using pure water as the receiving phase

Feed solution: 1: 19.2: 1.7 (g/L) Acetone: Butanol: Ethanol
Receiving phase: Pure water
Membrane thickness: 17.3 µm
Feed volume: 300 mL
Receiving volume: 157 mL
Feed temperature: 37 ^{o}C
Receiving temperature: 6 ^{o}C

Table D.13 Peak areas of acetone, ethanol, and butanol concentrations in 6 ^{o}C water receiving phase

Time (min)	Receiving composition					
	Peak area of Acetone (µV.s)	Peak area of Ethanol (µV.s)	Peak area of Butanol (µV.s)	Acetone (g/l)	Ethanol (g/l)	Butanol (g/l)
30	638.80	869.75	109,042.20	0.00015	0.00045	0.0319
44	781.45	549.95	101,289.60	0.00027	0.00021	0.0281
70	1,382.40	1,420.50	158,426.40	0.00081	0.00085	0.0568
80	656.85	428.70	128,968.40	0.00016	0.00012	0.0420
110	2,299.17	2,673.18	220,214.81	0.00162	0.00177	0.0878
120	1,892.30	1,315.05	201,189.20	0.00126	0.00078	0.0782
150	2,405.02	1,714.28	221,411.35	0.00172	0.00107	0.0884
160	2,909.51	1,882.60	250,731.91	0.00217	0.00119	0.1031
190	3,780.39	2,993.36	342,450.70	0.00294	0.00201	0.1492
200	3,382.90	2,678.40	320,994.90	0.00259	0.00178	0.1384
230	4,429.44	3,498.66	375,786.11	0.00352	0.00238	0.1659
240	3,557.06	3,042.33	323,677.30	0.00274	0.00205	0.1398
270	5,285.73	4,159.02	456,356.59	0.00428	0.00287	0.2064
280	4,361.60	3,042.34	378,400.59	0.00346	0.00205	0.1672
300	5,682.44	4,413.67	495,777.03	0.00463	0.00305	0.2262

D.11.2 Perstraction experiments using 3.5 wt. % Triton X-114 as the receiving phase

Feed solution: 1: 19.2: 1.7 (g/L) Acetone: Butanol: Ethanol
Receiving phase: 3.5 wt. % Triton X-114 solution
Membrane thickness: 17.3 µm
Feed volume: 300 mL
Receiving volume: 157 mL
Feed temperature: 37 ^{o}C
Receiving temperature: 6 ^{o}C

Table D.14 Peak areas of acetone, ethanol, and butanol concentrations in 3.5 wt. % Triton X-114 receiving solution at 6 ^{o}C

Time (min)	Receiving composition					
	Peak area of Acetone (µV.s)	Peak area of Ethanol (µV.s)	Peak area of Butanol (µV.s)	Acetone (g/l)	Ethanol (g/l)	Butanol (g/l)
30	2,182.50	6,763.99	219,165.65	0.00152	0.00478	0.09
40	3,965.39	9,971.19	297,031.70	0.00310	0.00714	0.13
70	6,648.67	11,105.63	696,065.38	0.00549	0.00797	0.33
80	7,128.88	11,125.03	731,651.72	0.00591	0.00799	0.34
110	9,257.07	12,780.49	948,779.27	0.00780	0.00921	0.45
120	10,965.15	12,987.42	1,076,204.50	0.00932	0.00936	0.52
150	15,020.49	19,430.96	1,595,660.88	0.01422	0.01152	0.78
160	15,730.58	20,016.55	1,642,436.30	0.01478	0.01183	0.80
190	16,688.79	19,229.09	1,744,970.50	0.01554	0.01142	0.85
200	21,122.31	27,618.23	2,064,853.56	0.01907	0.01581	1.01
235	23,757.73	28,580.90	2,460,141.31	0.02116	0.01632	1.21
245	23,192.76	26,843.80	2,374,419.75	0.02071	0.01541	1.17
275	26,627.74	32,858.41	2,705,688.75	0.02345	0.01856	1.34
285	28,884.97	33,380.73	3,133,334.00	0.02524	0.01883	1.55
300	33,562.43	37,250.77	3,303,250.27	0.02896	0.02086	1.64

D.12 The results of perstraction experiment using 6 g/L butanol concentration as the receiving phase

D.12.1 First perstraction experiments using 6 g/L butanol

Feed solution: 1: 19.2: 1.7 (g/L) Acetone: Butanol: Ethanol
Receiving phase: 6 g/L Butanol
Membrane thickness: 17.8 µm
Feed volume: 300 mL
Receiving volume: 157 mL
Feed and receiving temperature: 37 ^{o}C

Table D.15 Peak areas of acetone, ethanol, and butanol concentrations in the receiving phase containing the initial concentration of butanol as 6 g/L, first experiments

Time (min)	Receiving composition					
	Peak area of Acetone (µV.s)	Peak area of Ethanol (µV.s)	Peak area of Butanol (µV.s)	Acetone (g/l)	Ethanol (g/l)	Butanol (g/l)
30	3,055.98	2,130.12	8,995,176.50	0.00470	0.00227	5.0
40	4,390.50	2,771.30	8,265,209.50	0.00576	0.00269	4.6
70	13,168.67	9,558.43	11,132,124.00	0.01274	0.00712	6.2
80	12,268.52	9,368.89	9,642,394.25	0.01203	0.00699	5.4
110	22,048.00	18,547.74	11,771,142.00	0.01980	0.01299	6.5
120	26,228.22	20,727.98	12,702,702.00	0.02313	0.01441	7.0
150	30,907.10	24,924.10	12,031,624.75	0.02685	0.01715	6.7
160	36,162.06	29,860.05	13,024,149.50	0.03103	0.02037	7.2
190	36,500.63	30,104.97	11,698,063.75	0.03130	0.02053	6.5
200	42,120.78	33,644.02	12,666,638.25	0.03577	0.02284	7.0
230	55,605.71	47,686.69	14,305,098.50	0.04649	0.03201	7.9
240	56,517.13	49,268.80	14,185,773.50	0.04721	0.03304	7.8
270	47,305.78	39,765.60	10,763,751.25	0.03989	0.02684	6.0
280	58,168.67	55,433.58	12,603,409.50	0.04853	0.03707	7.0
300	66,161.33	59,163.02	12,936,443.50	0.05488	0.03950	7.2

D.12.2 Second perstraction experiments using 6 g/L butanol

Feed solution: 1: 19.2: 1.7 (g/L) Acetone: Butanol: Ethanol
Receiving phase: 6 g/L Butanol
Membrane thickness: 16.9 µm
Feed volume: 300 mL
Receiving volume: 157 mL
Feed and receiving temperature: 37 ^{o}C

Table D.16 Peak areas of acetone, ethanol, and butanol concentrations in the receiving phase containing the initial concentration of butanol as 6 g/L, second experiments

Time (min)	Receiving composition					
	Peak area of Acetone (µV.s)	Peak area of Ethanol (µV.s)	Peak area of Butanol (µV.s)	Acetone (g/l)	Ethanol (g/l)	Butanol (g/l)
30	8,660.40	10,880.40	10,913,438.00	0.0066	0.0070	6.1
40	10,632.73	11,139.48	12,469,587.00	0.0079	0.0072	6.9
70	18,043.23	20,216.32	13,128,633.00	0.0166	0.0141	7.3
80	21,110.03	23,110.03	13,536,955.00	0.0191	0.0160	7.5
110	31,008.41	33,480.39	13,841,587.00	0.0269	0.0227	7.7
120	32,302.26	34,660.95	13,639,248.00	0.0280	0.0235	7.5
150	40,682.81	44,745.20	13,992,589.00	0.0346	0.0301	7.7
160	37,486.05	43,154.45	12,005,602.25	0.0321	0.0291	6.7
190	53,378.50	57,936.15	14,697,322.00	0.0447	0.0387	8.1
200	49,949.00	56,560.75	13,145,588.00	0.0420	0.0378	7.3
230	62,069.17	70,039.23	14,980,199.00	0.0516	0.0466	8.3
240	64,391.14	72,604.31	14,924,870.00	0.0535	0.0483	8.2
270	75,379.41	84,387.06	15,868,044.00	0.0622	0.0560	8.8
280	68,497.20	79,012.34	14,299,874.00	0.0567	0.0525	7.9
300	82,547.72	92,880.28	16,273,205.00	0.0679	0.0615	9.0

D.12.3 Third perstraction experiments using 6 g/L butanol

Feed solution: 1: 19.2: 1.7 (g/L) Acetone: Butanol: Ethanol
Receiving phase: 6 g/L Butanol
Membrane thickness: 16.6 µm
Feed volume: 300 mL
Receiving volume: 157 mL
Feed and receiving temperature: 37 ^{o}C

Table D.17 Peak areas of acetone, ethanol, and butanol concentrations in the receiving phase containing the initial concentration of butanol as 6 g/L, third experiments

Time (min)	Receiving composition					
	Peak area of Acetone (µV.s)	Peak area of Ethanol (µV.s)	Peak area of Butanol (µV.s)	Acetone (g/l)	Ethanol (g/l)	Butanol (g/l)
30	7,194.17	8,723.48	12,944,782.00	0.0057	0.0059	7.17
40	9,361.24	10,632.56	13,285,382.00	0.0071	0.0069	7.36
70	18,331.15	18,989.00	13,872,427.00	0.0130	0.0113	7.68
80	21,529.33	22,645.82	14,213,564.00	0.0194	0.0157	7.86
110	30,455.47	31,867.03	14,539,207.00	0.0265	0.0217	8.04
120	32,231.92	33,286.18	14,520,411.00	0.0279	0.0226	8.03
150	44,070.83	45,422.67	15,315,769.00	0.0373	0.0305	8.46
160	47,288.47	50,049.03	15,335,920.00	0.0399	0.0336	8.47
190	56,782.69	59,878.71	16,058,737.00	0.0474	0.0400	8.86
200	39,544.91	48,191.24	11,275,183.00	0.0337	0.0323	6.26
230	69,297.43	73,850.16	17,029,464.00	0.0574	0.0491	9.39
240	73,518.15	78,789.80	17,096,496.00	0.0607	0.0523	9.43
270	82,803.35	88,910.15	17,119,946.00	0.0681	0.0589	9.44
280	78,727.14	87,191.16	16,461,497.00	0.0649	0.0578	9.08
300	80,963.63	89,948.73	15,968,764.00	0.0667	0.0596	8.82

D.13 The results of perstraction experiment using 12 g/L butanol concentration as a receiving phase

D.13.1 First perstraction experiments using 12 g/L butanol

Feed solution: 1: 19.2: 1.7 (g/L) Acetone: Butanol: Ethanol
Receiving phase: 12 g/L Butanol
Membrane thickness: 16.5 µm
Feed volume: 300 mL
Receiving volume: 157 mL
Feed and receiving temperature: 37 ^{o}C

Table D.18 Peak areas of acetone, ethanol, and butanol concentrations in the receiving phase containing the initial concentration of butanol as 12 g/L, first experiments

Time (min)	Receiving composition					
	Peak area of Acetone (µV.s)	Peak area of Ethanol (µV.s)	Peak area of Butanol (µV.s)	Acetone (g/l)	Ethanol (g/l)	Butanol (g/l)
30	8,967.66	6,630.20	20,390,594.50	0.0068	0.0048	11.2
40	12,131.00	9,903.40	20,207,654.50	0.0089	0.0065	11.1
70	19,578.30	17,084.60	18,746,522.00	0.0178	0.0103	10.3
80	24,011.59	18,592.89	19,551,026.00	0.0214	0.0111	10.8
110	34,470.68	29,833.48	19,710,541.50	0.0297	0.0204	10.9
120	32,449.16	27,476.44	17,036,708.00	0.0281	0.0188	9.4
150	47,159.70	41,881.41	20,211,045.00	0.0398	0.0282	11.1
160	48,239.65	43,606.16	18,697,318.50	0.0406	0.0293	10.3
190	55,920.22	50,642.48	18,462,243.00	0.0467	0.0339	10.2
200	61,821.70	54,608.30	20,072,516.50	0.0514	0.0365	11.1
230	68,105.31	62,198.14	19,452,457.00	0.0564	0.0415	10.7
240	73,922.98	62,787.81	19,202,265.50	0.0611	0.0419	10.6
270	92,882.98	83,276.72	22,600,121.50	0.0761	0.0552	12.5
280	94,664.30	87,246.41	23,159,932.00	0.0775	0.0578	12.8
300	99,256.02	89,252.88	21,974,688.50	0.0812	0.0592	12.1

D.13.2 Second perstraction experiments using 12 g/L butanol

Feed solution: 1: 19.2: 1.7 (g/L) Acetone: Butanol: Ethanol
Receiving phase: 12 g/L Butanol
Membrane thickness: 17.0 µm
Feed volume: 300 mL
Receiving volume: 157 mL
Feed and receiving temperature: 37 ^{o}C

Table D.19 Peak areas of acetone, ethanol, and butanol concentrations in the receiving phase containing the initial concentration of butanol as 12 g/L, second experiments

Time (min)	Receiving composition					
	Peak area of Acetone (µV.s)	Peak area of Ethanol (µV.s)	Peak area of Butanol (µV.s)	Acetone (g/l)	Ethanol (g/l)	Butanol (g/l)
30	5,666.93	9,375.27	17,934,108.00	0.0047	0.0063	9.9
40	7,030.56	11,306.34	16,461,080.00	0.0055	0.0073	9.1
70	19,695.07	24,641.78	24,391,850.00	0.0179	0.0143	13.5
80	21,821.05	27,353.35	23,259,778.00	0.0196	0.0157	12.8
110	30,338.26	37,559.09	23,046,534.00	0.0264	0.0254	12.7
120	27,864.83	35,965.82	20,478,962.00	0.0244	0.0244	11.3
150	33,737.66	43,818.83	18,791,428.00	0.0291	0.0295	10.4
160	35,283.38	45,546.92	18,816,696.00	0.0303	0.0306	10.4
190	52,008.62	62,299.73	21,910,264.00	0.0436	0.0416	12.1
200	45,262.28	59,152.02	18,713,810.00	0.0383	0.0395	10.3
230	77,225.16	89,265.19	27,077,104.00	0.0637	0.0592	14.9
240	49,216.70	65,834.49	17,476,948.00	0.0414	0.0439	9.6
270	56,007.75	75,552.41	18,374,474.00	0.0468	0.0502	10.1
280	59,914.80	80,433.95	18,189,610.00	0.0499	0.0534	10.0
300	63,603.04	85,699.61	18,273,046.00	0.0528	0.0568	10.1

D.14 The results of distribution coefficient experiment: first experiment

Total mass of Acetone in the surfactant solution: 0.0125 g
Total mass of Ethanol in the surfactant solution: 0.0123 g
Total mass of Butanol in the surfactant solution: 0.750 g
Volume of solution: 157 ml
Temperature of experiment: 37 ^{o}C

Table D.20 Volume of surfactant-rich phase and surfactant-lean phase from using Triton X-114 solution at 37 ^{o}C, first experiments

Triton (wt. %)	Mass of Triton X- 114 (g)	Volume of Surfactant - rich phase (ml)	Volume of Surfactant - lean phase (ml)
0.50	0.78	4.0	153.0
0.60	0.94	3.5	153.5
0.74	1.16	5.0	152.0
0.80	1.24	5.5	151.5
0.90	1.40	6.5	150.5
1.00	1.56	8.0	149.0
1.10	1.72	8.5	148.5
1.20	1.88	9.0	148.0
1.30	2.03	10.5	146.5
1.42	2.22	11.5	145.5
1.50	2.34	12.0	145.0

Table D.21 Peak areas of acetone concentrations in the surfactant-lean phase, first experiments

Triton (wt. %)	Peak area (µV.s) of Acetone				Acetone (g/L) in aqueous phase
	1	2	3	Average	
0.50	56,771.70	52,295.91	46,474.07	51,847.23	0.0433
0.60	75,478.13	69,579.77	66,922.49	70,660.13	0.0580
0.74	64,479.40	69,304.04		66,891.72	0.0551
0.80	79,575.59	77,521.81		78,548.70	0.0642
0.90	73,409.45	72,496.29		72,952.87	0.0598
1.00	79,462.54	73,584.83		76,523.68	0.0626
1.10	73,619.28	65,091.60		69,355.44	0.0570
1.20	58,736.11	62,877.21	58,398.73	60,004.01	0.0497
1.30	67,737.20	64,072.77	67,538.36	66,449.44	0.0547
1.42	66,741.04	66,215.68		66,478.36	0.0547
1.50	56,480.76	57,172.37	56,926.15	56,859.76	0.0472

Table D.22 Peak areas of ethanol concentrations in the surfactant-lean phase, first experiments

Triton (wt. %)	Peak area (µV.s) of Ethanol				Ethanol (g/L) in aqueous phase
	1	2	3	Average	
0.50	84,941.59	77,479.48	68,601.93	77,007.67	0.0512
0.60	92,503.02	83,074.06	79,762.38	85,113.15	0.0565
0.74	80,431.50	80,829.69		80,630.59	0.0535
0.80	81,336.81	84,138.22		82,737.52	0.0549
0.90	80,754.75	80,276.86		80,515.80	0.0535
1.00	84,185.66	82,089.21		83,137.44	0.0552
1.10	82,004.92	73,520.90		77,762.91	0.0516
1.20	73,859.09	79,205.89	74,663.72	75,909.57	0.0504
1.30	80,300.49	78,032.09	80,661.54	79,664.71	0.0529
1.42	71,754.91	78,000.81		74,877.86	0.0498
1.50	79,036.89	77,076.65	76,840.73	77,651.42	0.0516

Table D.23 Peak areas of butanol concentrations in the surfactant-lean phase, first experiments

Triton (wt. %)	Peak area (µV.s) of Butanol				Butanol (g/L) in aqueous phase
	1	2	3	Average	
0.50	10,457,452.00	10,008,820.00	9,307,886.00	9,924,719.33	4.93
0.60	11,277,808.00	10,283,801.00	9,110,019.00	10,223,876.00	5.09
0.74	9,108,257.00	9,834,987.00		9,471,622.00	4.70
0.80	8,562,958.00	7,982,499.00		8,272,728.50	4.08
0.90	9,682,323.00	9,561,937.00		9,622,130.00	4.78
1.00	10,333,356.00	9,838,523.00		10,085,939.50	5.01
1.10	10,039,324.00	9,300,807.00		9,670,065.50	4.80
1.20	8,464,128.00	9,183,263.00	8,779,825.00	8,809,072.00	4.36
1.30	9,308,771.00	9,325,434.00	9,552,372.00	9,395,525.67	4.66
1.42	8,189,471.00	8,798,735.00		8,494,103.00	4.20
1.50	8,491,392.00	8,947,817.00	9,066,923.00	8,835,377.33	4.37

Table D.24 Mass of organic solutes in the surfactant-rich phase and the surfactant-lean phase, first experiments

Triton (wt. %)	Mass of Acetone (g) in aqueous phase	Mass of Ethanol (g) in aqueous phase	Mass of Butanol (g) in aqueous phase	Mass of Acetone (g) in Organic phase	Mass of Ethanol (g) in Organic phase	Mass of Butanol (g) in Organic phase
0.50	0.00662	0.00783	0.75453	0.00588	0.00447	
0.60	0.00890	0.00867	0.78062	0.00360	0.00363	
0.74	0.00837	0.00814	0.71417	0.00413	0.00416	0.03583
0.80	0.00972	0.00832	0.61840	0.00278	0.00398	0.13160
0.90	0.00900	0.00804	0.71878	0.00350	0.00426	0.03122
1.00	0.00933	0.00822	0.74716	0.00317	0.00408	0.00284
1.10	0.00846	0.00767	0.71289	0.00404	0.00463	0.03711
1.20	0.00735	0.00746	0.64494	0.00515	0.00484	0.10506
1.30	0.00802	0.00775	0.68260	0.00448	0.00455	0.06740
1.42	0.00796	0.00724	0.61047	0.00454	0.00506	0.13953
1.50	0.00684	0.00748	0.63383	0.00566	0.00482	0.11617

Table D.25 Organic concentrations in the surfactant-rich phase and distribution coefficients, first experiments

Triton (wt. %)	Acetone (g/L) in Organic phase	Ethanol (g/L) in Organic phase	Butanol (g/L) in Organic phase	Distribution coefficient of Acetone	Distribution coefficient of Ethanol	Distribution coefficient of Butanol
0.50	1.47	1.12		34.0	21.9	
0.60	1.03	1.04		17.7	18.4	
0.74	0.83	0.83	7.17	15.0	15.6	1.5
0.80	0.50	0.72	23.93	7.9	13.2	5.9
0.90	0.54	0.65	4.80	9.0	12.2	1.0
1.00	0.40	0.51	0.35	6.3	9.2	0.1
1.10	0.48	0.54	4.37	8.3	10.5	0.9
1.20	0.57	0.54	11.67	11.5	10.7	2.7
1.30	0.43	0.43	6.42	7.8	8.2	1.4
1.42	0.39	0.44	12.13	7.2	8.8	2.9
1.50	0.47	0.40	9.68	10.0	7.8	2.2

Table D.26 Capturing capacity of organic solutes, first experiments

Triton (wt. %)	**Acetone capturing capacity (g acetone/ g Triton X-114)**	**Ethanol capturing capacity (g ethanol/ g Triton X-114)**	**Butanol capturing capacity (g butanol/ g Triton X-114)**
0.50	0.00753	0.00573	
0.60	0.00383	0.00387	
0.74	0.00356	0.00359	0.03087
0.80	0.00223	0.00320	0.10571
0.90	0.00249	0.00303	0.02225
1.00	0.00203	0.00261	0.00182
1.10	0.00235	0.00269	0.02158
1.20	0.00274	0.00258	0.05595
1.30	0.00221	0.00225	0.03327
1.42	0.00205	0.00228	0.06298
1.50	0.00241	0.00206	0.04960

D.15 The results of distribution coefficient experiment: second experiments

Total mass of Acetone in the surfactant solution: 0.0125 g
Total mass of Ethanol in the surfactant solution: 0.0123 g
Total mass of Butanol in the surfactant solution: 0.750 g
Volume of solution: 157 ml
Temperature of experiment: 37 ^{o}C

Table D.27 Volume of surfactant-rich phase and surfactant-lean phase from using Triton X-114 solutions at temperature of 37 ^{o}C, second experiments

Triton (wt. %)	Mass of Triton X - 114 (g)	Volume of Surfactant - rich phase (ml)	Volume of Surfactant - lean phase (ml)
0.50	0.78	4.0	153.0
0.60	0.94	4.0	153.0
0.70	1.16	7.0	150.0
0.80	1.24	3.5	153.5
0.90	1.40	4.5	152.5
1.00	1.56	5.0	152.0
1.30	2.03	10.0	147.0
1.50	2.34	12.0	145.0
3.50	5.46	26.0	131.0
7.00	10.96	48.5	108.5

Table D.28 Peak areas of acetone concentrations in the surfactant-lean phase, second experiments

Triton (wt. %)	Peak area (µV.s) of Acetone				Acetone (g/L) in aqueous phase
	1	2	3	Average	
0.50	40,523.74	41,949.13	41,490.07	41,320.98	0.0350
0.60	77,569.44	72,713.28	72,382.24	74,221.65	0.0608
0.70	66,118.11	73,330.18	103,088.95	80,845.74	0.0660
0.80	71,920.92	62,074.56	53,016.46	62,337.32	0.0515
0.90	70,319.42	111,049.58	63,547.37	81,638.79	0.0666
1.00	63,862.59	88,645.48	120,594.45	91,034.17	0.0740
1.30	60,858.81	65,955.60	65,122.52	63,978.98	0.0528
1.50	55,100.39	75,560.19	52,176.05	60,945.54	0.0504
3.50	89,281.40	62,637.77	63,294.75	71,737.98	0.0589
7.00	147,159.53	106,735.80	95,304.11	116,399.82	0.0938

Table D.29 Peak areas of ethanol concentrations in the surfactant-lean phase, second experiments

Triton (wt. %)	Peak area (µV.s) of Ethanol				Ethanol (g/L) in aqueous phase
	1	2	3	Average	
0.50	80,793.82	76,861.22	75,955.63	77,870.22	0.0517
0.60	88,647.68	82,687.96	82,796.03	84,710.56	0.0562
0.70	82,165.84	85,887.46	80,074.85	82,709.38	0.0549
0.80	80,056.70	69,534.11	62,744.74	70,778.52	0.0471
0.90	97,377.50	102,194.96	92,164.90	97,245.79	0.0644
1.00	73,834.73	77,166.22	87,373.74	79,458.23	0.0528
1.30	79,387.40	85,183.81	83,914.90	82,828.71	0.0550
1.50	76,635.42	77,228.78	73,092.06	75,652.09	0.0503
3.50	83,576.76	72,662.93	73,948.74	76,729.48	0.0510
7.00	138,804.22	131,431.17	121,113.26	130,449.55	0.0862

Table D.30 Peak areas of butanol concentrations in the surfactant-lean phase, second experiments

Triton (wt. %)	Peak area (µV.s) of Butanol				Butanol (g/L) in aqueous phase
	1	2	3	Average	
0.50	9,326,636	9,529,807	9,319,057	9,391,833	4.66
0.60	10,743,890	9,881,805	9,923,998	10,183,231	5.06
0.70	9,312,040	10,213,451	8,441,921	9,322,471	4.62
0.80	10,222,484	8,711,130	7,894,057	8,942,557	4.43
0.90	10,467,732	10,018,372	10,134,372	10,206,826	5.08
1.00	9,741,163	8,611,650	9,903,263	9,418,692	4.67
1.30	8,952,984	9,627,086	9,479,221	9,353,097	4.64
1.50	9,159,718	9,088,950	8,796,217	9,014,962	4.46
3.50	8,928,657	7,772,681	8,483,406	8,394,915	4.14
7.00	8,812,242	9,009,104	8,044,189	8,621,845	4.26

Table D.31 Mass of organic solutes in the surfactant-rich and the surfactant-lean phase, second experiments

Triton (wt. %)	Mass of Acetone (g) in aqueous phase	Mass of Ethanol (g) in aqueous phase	Mass of Butanol (g) in aqueous phase	Mass of Acetone (g) in Organic phase	Mass of Ethanol (g) in Organic phase	Mass of Butanol (g) in Organic phase
0.50	0.00536	0.00791	0.713	0.00714	0.00439	0.0374
0.60	0.00930	0.00860	0.775	0.00320	0.00370	
0.70	0.00990	0.00823	0.693	0.00260	0.00407	0.0567
0.80	0.00790	0.00723	0.679	0.00460	0.00507	0.0706
0.90	0.01016	0.00982	0.774	0.00234	0.00248	
1.00	0.01124	0.00802	0.710	0.00126	0.00428	0.0400
1.30	0.00776	0.00808	0.682	0.00474	0.00422	0.0683
1.50	0.00731	0.00729	0.647	0.00519	0.00501	0.1028
3.50	0.00771	0.00668	0.543	0.00479	0.00562	0.2070
7.00	0.01018	0.00935	0.462	0.00232	0.00295	0.2876

Table D.32 Organic concentrations in the surfactant-rich and distribution coefficient, second experiments

Triton (wt. %)	Acetone (g/L) in Organic phase	Ethanol (g/L) in Organic phase	Butanol (g/L) in Organic phase	Distribution coefficient of Acetone	Distribution coefficient of Ethanol	Distribution coefficient of Butanol
0.50	1.785	1.097	9.35	51.0	21.2	2.0
0.60	0.800	0.925		13.2	16.5	
0.70	0.372	0.581	8.10	5.6	10.6	1.8
0.80	1.313	1.450	20.16	25.5	30.8	4.6
0.90	0.521	0.550		7.8	8.5	
1.00	0.252	0.856	7.99	3.4	16.2	1.7
1.30	0.474	0.422	6.83	9.0	7.7	1.5
1.50	0.433	0.418	8.56	8.6	8.3	1.9
3.50	0.184	0.216	7.96	3.1	4.2	1.9
7.00	0.048	0.061	5.93	0.5	0.7	1.4

Table D.33 Capturing capacity of organic solutes, second experiments

Triton (wt. %)	**Acetone capturing capacity (g acetone/ g Triton X-114)**	**Ethanol capturing capacity (g ethanol/ g Triton X-114)**	**Butanol capturing capacity (g butanol/ g Triton X-114)**
0.50	0.009146	0.005619	0.04791
0.60	0.003406	0.003942	
0.70	0.002243	0.003504	0.04888
0.80	0.003692	0.004076	0.05667
0.90	0.001670	0.001765	
1.00	0.000806	0.002741	0.02559
1.30	0.002341	0.002083	0.03371
1.50	0.002217	0.002140	0.04388
3.50	0.000877	0.001029	0.03789
7.00	0.000212	0.000269	0.02624

D.16 The results of distribution coefficient experiment after the end of perstraction

The distribution coefficient of organic solutes was determined after perstraction experiment was finished.

Table D.34 Peak areas of acetone concentrations in the surfactant-lean phase after the end of perstraction

Triton (wt. %)	Peak area (µV.s) of Acetone					Acetone (g/L) in aqueous phase
	1	2	3	4	Average	
0.7	75,231.44	83,778.03	85,256.11		81,421.86	0.067016
0.8	119,649.16	99,162.53	97,937.64		105,583.11	0.086229
0.9	155,701.30	106,553.15	106,893.54		123,049.33	0.100117
3.5	78,060.63	92,500.74	103,577.40	78,217.64	88,089.10	0.046345
3.5	94,660.23	81,192.45			87,926.34	0.064456
7.0	67,694.49	65,665.20	62,816.99		65,392.23	0.061492
7.0	87,493.26	97,567.00			92,530.13	0.061383
10.5	69,688.89	52,020.03			60,854.46	0.043316

Table D.35 Peak areas of ethanol concentrations in the surfactant-lean phase after the end of perstraction

Triton (wt. %)	Peak area (µV.s) of Ethanol					Ethanol (g/L) in aqueous phase
	1	2	3	4	Average	
0.7	110,583.27	120,662.54	125,428.40		118,891.40	0.0785
0.8	149,472.53	129,446.82	128,198.87		135,706.07	0.0895
0.9	148,497.70	137,656.34	139,596.75		141,916.93	0.0935
3.5	84,607.66	85,205.29	77,270.74		82,361.23	0.0515
3.5	112,707.54	126,540.40			119,623.97	0.0741
7.0	95,935.17	109,042.86	124,137.19	102,125.87	107,810.27	0.0669
7.0	115,364.47	112,754.05			114,059.26	0.0707
10.5	126,552.91	125,819.77			126,186.34	0.0781

Table D.36 Peak areas of butanol concentrations in the surfactant-lean phase after the end of perstraction

Triton (wt. %)	Peak area (µV.s) of Butanol				Butanol (g/L) in aqueous phase
	1	2	3	Average	
0.7	7,767,625.5	8,343,683.5	8,853,076.0	8,321,461.7	4.66
0.8	10,315,235.0	8,645,967.0	8,897,763.0	9,286,321.7	5.18
0.9	9,431,787.0	9,346,972.0	9,438,874.0	9,405,877.7	5.25
3.5	6,124,786.5	6,193,512.1	5,814,234.1	6,044,177.6	2.94
3.5	7,339,852.5	8,389,640.0		7,864,746.3	3.87
7.0	5,658,177.5	6,670,249.5	7,536,860.0	6,501,544.3	3.17
7.0	7,231,928.8	6,743,881.0		6,987,904.9	3.42
10.5	6,082,574.5	6,102,662.0		6,092,618.3	2.96

Table D.37 Mass of organic solutes in the surfactant-rich and the surfactant-lean phase after the end of perstraction

Triton (wt. %)	Mass of Acetone (g) in aqueous phase	Mass of Ethanol (g) in aqueous phase	Mass of Butanol (g) in aqueous phase	Mass of Acetone (g) in Organic phase	Mass of Ethanol (g) in Organic phase	Mass of Butanol (g) Organic phase
0.7	0.010	0.012	0.687	0.00254	0.00169	0.155
0.8	0.013	0.013	0.762	0.00505	0.00401	0.287
0.9	0.015	0.014	0.771	0.00371	0.00462	0.229
3.5	0.006	0.007	0.387	0.00352	0.00361	0.234
3.5	0.009	0.010	0.511	0.00525	0.00412	0.329
7.0	0.007	0.007	0.339	0.00458	0.00328	0.314
7.0	0.007	0.008	0.366	0.00553	0.00437	0.350
10.5	0.003	0.006	0.213	0.00709	0.00434	0.447

Table D.38 Organic concentrations in the surfactant-rich phase and distribution coefficients after the end of perstraction

Triton (wt. %)	**Acetone (g/L) in Organic phase**	**Ethanol (g/L) in Organic phase**	**Butanol (g/L) in Organic phase**	**Distribution coefficient of Acetone**	**Distribution coefficient of Ethanol**	**Distribution coefficient of Butanol**
0.7	1.694	1.126	103.5	25.28	14.35	22.22
0.8	2.526	2.005	143.3	29.30	22.40	27.66
0.9	1.857	2.308	114.7	18.55	24.68	21.86
3.5	0.141	0.144	9.4	3.03	2.80	3.19
3.5	0.210	0.165	13.2	3.26	2.22	3.40
7.0	0.092	0.066	6.3	1.49	0.98	1.98
7.0	0.111	0.087	7.0	1.80	1.23	2.05
10.5	0.083	0.051	5.3	1.93	0.65	1.78

Table D.39 Capturing capacity of organic solutes after the end of perstraction

Triton (wt. %)	**Acetone capturing capacity (g acetone/ g Triton X-114)**	**Ethanol capturing capacity (g ethanol/ g Triton X-114)**	**Butanol capturing capacity (g butanol/ g Triton X-114)**
0.7	0.002316	0.00154	0.1414
0.8	0.004058	0.00322	0.2302
0.9	0.002647	0.00329	0.1635
3.5	0.000641	0.000657	0.0427
3.5	0.000957	0.000751	0.0600
7.0	0.000418	0.000299	0.0286
7.0	0.000504	0.000398	0.0319
10.5	0.000431	0.000264	0.0272

D.17 The results of pavaporation experiment

D.17.1 The Feed containing ABE solution

Feed solution: 1: 19.2: 1.7 (g/L) acetone: butanol: ethanol
Feed volume: 300 mL
Flow rate of dried Air: 120 mL/ min
Temperature of pervaporation: 37 ^{o}C

Table D.40 Mass fraction of acetone in the permeate

Time (hr)	Peak area of Acetone (µV.s)				Acetone (g/ g total mass)
	1	2	3	Average	
5	132,259.94	109,124.01	117,339.46	119,574.47	0.000112302
6	229,997.33	208,647.39	187,951.80	208,865.51	0.000179533
7	427,201.50	400,149.16	360,946.16	396,098.94	0.000320509
8	388,971.09	367,774.57	358,833.22	371,859.63	0.000302258
9	439,612.75	398,849.84	385,416.28	407,959.63	0.000329439

Table D.41 Mass fraction of ethanol in the permeate

Time (hr)	Peak area of Ethanol (µV.s)				Ethanol (g/ g total mass)
	1	2	3	Average	
5	812,153.33	731,421.63	805,500.00	783,024.99	0.000555972
6	1,530,602.88	1,438,419.25	1,602,577.88	1,523,866.67	0.001037682
7	2,197,944.50	2,196,364.50	2,254,080.75	2,216,129.92	0.001487805
8	2,207,476.75	2,281,573.00	2,275,261.50	2,254,770.42	0.001512930
9	2,836,586.75	2,728,329.50	2,681,557.50	2,748,824.58	0.001834174

Table D.42 Mass fraction of butanol in the permeate

Time (hr)	Peak area of Butanol (µV.s)				Butanol (g/ g total mass)
	1	2	3	Average	
5	36,202,624	32,466,682	36,027,400	34,898,902	0.016469777
6	45,966,148	45,048,768	45,542,036	45,518,984	0.034876503
7	50,070,256	50,924,896	49,988,984	50,328,045	0.043211568
8	50,889,188	50,793,372	51,468,464	51,050,341	0.044463452
9	58,612,648	57,155,636	57,078,824	57,615,703	0.055842536

Table D.43 Mass of organic solutes in the permeate

Time (hr)	Membrane Thickness (µm)	Total mass (g)	Acetone (g)	Ethanol (g)	Butanol (g)
5	17.8	0.320	0.0000359	0.0001779	0.005270
6	16.5	0.380	0.0000682	0.0003943	0.013253
7	17.4	0.417	0.0001337	0.0006204	0.018019
8	17.8	0.498	0.0001505	0.0007534	0.022143
9	17.3	0.510	0.0001680	0.0009354	0.028480

D.17.2 The Feed containing pure water

Feed solution: pure water
Feed volume: 300 mL
Flow rate of dried Air: 120 mL/ min
Temperature of pervaporation: 37 ^{o}C

Table D.44 Mass of water in the permeate

Time	Membrane Thickness (µm)	Mass of Water (g)
5	16.7	0.280
6	16.7	0.329
7	16.7	0.372

CURRICULUM VITAE

NAME Mr. Pheerapong Chanachod

DATE OF BIRTH 19 January 1989

EDUCATIONAL RECORD

HIGH SCHOOL	High School Graduation Princess Chulabhorn's College Lopburi, 2006
BACHELOR'S DEGREE	Bachelor of Science (Biotechnology) Silpakorn University, 2011
MASTER'S DEGREE	Master of Engineering (Chemical Engineering) King Mongkut's University of Technology Thonburi, 2014

PUBLICATION Pheerapong Chanachod and Anawat Sungpet, 2014, **"**Perstraction of Synthetic Bio-butanol Fermentation Broth by Dense Poly (ether-block-amide) Membranes", **The 4th TIChE International Conference,** December 18-19, 2014, Chiang Mai, Thailand.